Characterization of the viscoelastic and flow properties of High Density Polyethylene Resins for Pipes in the Solid and Melt State

Juan Antonio Pretelt Caceres

Dissertation submitted to the faculty of Virginia Polytechnic Institute and State University in partial fulfillment of the requirements for the degree of

Doctor of Philosophy

In

Chemical Engineering

Donald G. Baird, Chair

Scott W. Case

Richey M. Davis

Stephen M. Martin

11/20/2019

Blacksburg, VA

Keywords: High Density Polyethylene, Pipes, Rheology, Dynamic Mechanical Analysis, Creep

Characterization of the viscoelastic and flow properties of High Density Polyethylene Resins for Pipes in the Solid and Melt State

Juan Antonio Pretelt Caceres

Abstract

The frequent use of high-density polyethylene pipes over the last decades has been possible because these pipes are lightweight, corrosion resistant, unlikely to have leaks, and are low cost. The chain structure of the polymer, the extrusion and cooling conditions, the resulting morphology and the ambient conditions all play an important role in the pipe's performance. A new generation of high density polyethylene resins has improved the performance of pipes, but brought new challenges to their testing and characterization. There is a need to understand the rheological behavior of the resins, their processing, and their associated properties in a finished pipe.

The rheological behavior of the resins was studied to characterize the effect of high molecular weight tails in a bimodal molecular weight distribution. The use of cone-and-plate and parallel-plate geometries in a rheometer provided simple flow that characterized the steady and dynamical response of the polymer melts. The rheological measurements detected differences in the resins: the resin with higher molecular weight tail showed increased zero shear-rate viscosity, a much slower relaxation of stresses and a resin that more readily deviates from linear viscoelastic behavior. The rheology of the resins allowed modeling their flow through different extrusion dies. The flow channels for pipe dies are thick, so velocities and shear rates are low. Using a different die had a larger impact in shear rates and stresses compared to using different resins. The resin with higher molecular weight shows much higher shear stresses for the same die and temperature, which makes processing harder.

The flow of a fluid through a pipe causes constant stress, which at long enough times is one the reasons for pipe failure. Tests that characterize the service lifetime of pipes take long times and are expensive. Dynamical mechanical analysis allows characterizing the viscoelastic properties of the pipe and creep testing confirms that shift factors work for viscoelastic properties measured independently. For the characterized pipes, one hour of testing at 80 °C is equivalent to a month of testing at 25 °C. This works characterizes pipes made from two resins and two different dies. The measurements showed that the pipes were statistically the same.

Characterization of the viscoelastic and flow properties of High Density Polyethylene Resins for Pipes in the Solid and Melt State

Juan Antonio Pretelt Caceres

General Audience Abstract

The use of high-density polyethylene pipes has thrived over the last decades. This has been possible because these pipes are lightweight, corrosion resistant, unlikely to have leaks, and are low cost. The structure of the polymer and the manufacturing process both affect the pipe's performance. A new generation of high density polyethylene resins has improved the performance of the pipes, but brought new challenges to their testing and characterization. There is a need to understand the flow characteristics of the resins and their properties as a finished pipe.

The flow behavior of the polymers in simple geometries gave insights into the polymer's structure. A higher molecular weight resin showed increased resistance to flow and deviated from ideal behavior more readily. These flow characteristics let one model certain aspects of the manufacturing process. Pipe manufacturing is a slow process because of the high resistance to flow of the polymer. Changing the processing equipment, and to a minor degree changing the resins, had an important impact in the manufacturing process.

The tests that characterize the service lifetime of pipes take long times and are expensive. When pipes have fluids flowing at high pressures, it takes decades for them to fail. There are viscoelastic tests that allow much quicker characterization of pipes and help predict their long term behavior. This works characterizes pipes made from two resins and two different dies. This works characterizes pipes made from two resins and two different dies. The measurements showed that the pipes were statistically the same.

Acknowledgements

If I can see far it is because I stand on the shoulder of giants. To my advisor, Dr. Donald Baird, thank you. Your support, trust and belief in me have been invaluable. To my committee, Dr. Scott Case, Dr. Richey Davis and Dr. Stephen Martin, Thank you. Your kindness, encouragement and constructive feedback helped me understand and develop this project. Thank you to LyondellBasell for providing financial support, materials and their input to carry out this research.

To my former and current lab mates: Mark, Kevin, Chen, Hongyu, Greg, Craig, Jianger, Mubashir, Vikas, Kennedy, Jier and Tianran: working with you was a great experience. I will always appreciate the camaraderie, the discussions and all your care.

A big thank you to the chemical engineering staff: Diane, Tina, Stacey, Andrea, Jane and Riley. Your patience, support and kindness mean a lot. You were always there to make everything run smoothly.

Finally, to my family and all the friends I made in Blacksburg, you made my time in Blacksburg some of the best of my life. You helped keep me sane and happy. There are too many of you to write here, but I want to give special mentions to the people at Team Mannon and my wife Mimosa.

Original Contributions

1. This study finds distinct differences in the rheology of high density polyethylene resins used in the manufacture of pipes. The presence of more pronounced high molecular weight tails changes the rheological behavior in several ways. The zero shear rate viscosity is increased and the capacity to dissipate residual stresses decreases. The higher molecular weight tails force the resin to deviate from ideal behavior more readily as evidenced by jump strain testing.
2. This work established the degree of time shifting from changing the temperature of High Density Polyethylene pipes. Using dynamic mechanical analysis provided data that could be analyzed quickly, and the degree of time shifting was applicable to multiple viscoelastic properties. The process is applicable to semi-crystalline polymers, which are not covered by the typical time-temperature superposition procedures.

Table of Contents

List of Figures

Chapter 1. Introduction

The use of high-density polyethylene (HDPE) pipes has thrived over the last decades. They have replaced traditional materials such as copper, aluminum, iron, concrete and clay in several applications [1]. This has been possible because HDPE pipes are lightweight, corrosion resistant, unlikely to have leaks, and are low cost. Common uses for them are transporting natural gas, potable and rural water, agriculture irrigation, and sewage systems [2].

The expected service lifetime of HDPE pipes is 50–100 years. Their performance depends on several factors, which pipe manufacturers must consider to guarantee such a lifetime [3]. The most common fabrication method for pipes is extrusion. The chain structure of the HDPE, the extrusion and cooling conditions, the resulting morphology and the ambient conditions all play an important role in the pipe's performance [4]–[7].

Several standards are available and used throughout the pipe industry to qualify pipes and pipe resins. One such test is ASTM D2837, which gives detailed data on the failure of pipe. The results are the industrial standard for assessing resins [8]. This test is expensive and takes over a year to carry out. Another test is the Pennsylvania Notch Test (PENT), which relies on measuring slow crack growth in the resin. This test is often used for quality screening of resins as results are available in the order of 20–30 hours for the previous generation of HDPE pipe resins. A new generation of HDPE resins, enabled by a better understanding of molecular architecture and improvements in polymerization technology, has rendered this test unimportant as it now goes on for months [1], [9]–[11].

Creep rupture is one of the key factors that determines the expected lifetime of HDPE pipes. Some HDPE pipes are pressurized all of their service life, so the applied stress builds up plastic deformation with time. This eventually leads to large local bulging of pipes and their failure, with failure being defined as a leak in the pipe [5]. An increase in temperature or an increase in the applied load

will cause a faster failure [10]. While high temperatures provide acceleration of the tests, using a too high temperature brings the material too close to the melting point, which will affect any shifting done via Time-Temperature Superposition (TTSP).

The semi-crystalline nature of HDPE adds complexity to the shifting, making it depend on its crystallinity [12]. Popelar [13], [14] and Fukui [15], [16] found that solid HDPE needs a bidirectional shift for constructing coherent master curves. The classic horizontal shift will shift time and relates to the mobility and relaxation of the polymer molecules. The additional vertical shift will shift moduli and some authors attribute it to changes in temperature bring about changes in crystallinity, while others to uncoordinated motions of the crystalline lattice [13]–[16].

Extrusion of HDPE pellets is the method of choice to manufacture pipes. During processing, the complex flow fields generated will affect the properties of the final product. For example, if shear stresses are too high, this will cause surface defects in the final product and process instabilities [17]. When it enters the cooling chamber, the intensity of cooling and the pulling speed/orientation will affect the formation of the semi-crystalline structure [5], [18] and will cause residual stresses in the finished pipe too [19].

Rheological tests not only allow characterizing the flow characteristics of HDPE resins for pipes, but they also give insight into the molecular structure of the resins. While the tests are isothermal and have simple kinematics, they still allow measuring the flow properties needed to simulate a complex process such as extrusion. They can also be more sensitive to material differences than properties measured in the solid resin, such as modulus because of the strong dependence of viscosity on molecular weight [17].

The sections that follow review the concepts presented in further detail. Section 1.1 looks at the process of creep rupture in HDPE pipes and its relation to the performance of the pipe. Section

1.2 briefly touches on the relevance of rheology in the manufacturing stage and the nature of the resin. Section 1.3 follows with a general overview of the extrusion process for pipe and its relevance. To conclude, section 1.4 finishes this introduction with the intended objectives for the work proposed in this research plan.

1.1. Creep Rupture of HDPE pipes

Pressure from the flowing fluid in a pipe causes internal stresses in the pipe's walls. Given that cylindrical coordinates easily describe pipes, the principal stress components lay in the axial and hoop direction. Equations (1.1.1) and (1.1.2) show how to get the principal stresses for a thin-walled pipe, where P is pressure, D is diameter and t is thickness. A pipe is thin walled if its ratio of radius to thickness greater than 10.

$$\sigma_{\text{Hoop}} = \frac{PD}{2t} \tag{1.1.1}$$

$$\sigma_{\text{Axial}} = \frac{PD}{4t} \tag{1.1.2}$$

Creep describes the gradual deformation of a material subjected to sustained loading. The material will strain constantly, and at a high enough temperature or stress, it cannot resist more deformation causing it to rupture. This phenomenon is complex and dependent on the properties of the material and the environmental conditions. Specifically, creep will causes a material to fail long term at a stress much lower than its short-term rupture stress. The plastic deformation that happens at high stresses makes it so that strain changes non-linearly respect to time and stress. The long chain nature

of a polymer is responsible for the creep deformation mechanism. Constant loading causes the polymer molecules to move and disentangle from each other slowly, steadily increasing the strain accumulated [20]–[23].

To certify pipe materials and characterize long-term performance, it is common to test pipe sections at several temperatures and at various pressures. ASTM D1598 outlines the test procedure with failure criteria [24]. ASTM D2837 provides a TTSP like approach that allows extrapolating the information via linear regression [8]. This method allows one to estimate the stress levels that yield a service life of 50 to 100 years at room temperature. The stress commonly used in industry for this purpose is the hoop stress. The long-term hydrostatic strength (LTHS) is an estimated average of the hoop stress that results in pipe failure at a certain time. It allows categorizing the resistance of the material into established stress values called the Hydrostatic Design Basis (HDB). While the information obtained from the method is the industrial standard and well understood, it is expensive and takes more than a year to obtain results [22], [24]. Methods that can provide faster results are highly desirable, not just to replace the industrial standard, but to enable faster quality control and development of new materials.

The HDB of a pipe allows a pipe user to determine the maximum internal pressure of the fluid transported by using equation (1.1.1), with a safety factor that ensures the pipe does not fail during the guaranteed lifetime. Typical values of HDB for current pipe HDPE resins are 1600 psi (11.03 MPa) or 1250 psi (8.62 MPa) [8], [25]. The stresses and strains the pipe experiences during its service lifetime are enough for HDPE to show non-linear behavior [26], [27]. It is the ability of HDPE to endure large plastic deformation without failing that provides the desired toughness for pipe applications.

A non-linear viscoelastic response in creep means that compliance depends on stress or the isochronous stress-strain curve deviates from linearity [20]. An isochronous stress-strain curve measures the stress-strain response at constant times. While it would be desirable to describe a failure response in terms of linear viscoelasticity for HDPE pipes, such an extension to non-linear rate dependent problems is not possible. How the stress level impacts the time dependence of the material response is not well understood and is an area of active research [20], [28].

The composite structure of the amorphous and crystalline phases in HDPE makes for a complicated mechanical behavior. Around room temperature, most amorphous polymers are below their glass transition temperature, which makes them brittle and fracture at few percents strain. The amorphous phase of HDPE is rubbery at room temperature and allows the connected crystalline phase to deform without breaking [29]. However, even small strains will not be recoverable and will cause permanent deformation [27].

1.2. Role of Rheology

Polymeric fluids show a variety of flow properties that sets them apart from other materials. Their high molecular weight makes them structurally complex since the molecules can take on many conformations, making several properties depend on flow velocity gradients [30]. A few examples: their viscosity is shear rate dependent; normal stresses are present in simple shear flow; they show elastic effects like die swell; and flow properties that change depending on the time scale of the measurement [17], [31]. These effects do not arise in Newtonian fluids.

Rheological tests allow one to examine polymer melts in simple flows and in isothermal conditions and to get rheological material functions from the data. The material functions will then be able to describe the more complex flows present during the manufacturing/shaping operations and are relevant to the extrusion process [30].

Rheological tests also give relevant information on the molecular architecture of the polymer. For flexible chain polymers, above a critical molecular weight, viscosity (η) is proportional to the 3.4 power of molecular weight. The primary normal stress coefficient (Ψ_1) is proportional to the 6.8 power of molecular weight. Branching, which is common in polyethylene resins, has a major effect on rheological measurements, especially in the extensional behavior [17], [31].

1.3. Extrusion Processing for Pipe Manufacture and Part Morphology

Polymer extrusion is a continuous manufacturing process to make objects of a constant cross-section. In this process, a hopper sitting on top of the barrel of the extruder feeds a plasticizing screw. The polymer steadily softens and melts because of the mechanical work by the rotating screws at a temperature controlled by heaters along the barrel. The screw also generates enough pressure in order for the melt to pass through a die so it may solidify into the desired shape. In particular, the pipe extrudate enters a calibrator whereby the use of vacuum fixes the outside diameter, followed by a water bath where cooling takes place. A take-up device constantly pulls on the pipe and then cuts it to a desired length.

While HDPE pipes have been in use for decades now, the stringent requirements imposed on pipes add certain challenges to the extrusion process:

- The HDPE resins used for pipe manufacturing are of very high molecular weight, so even at low shear rates, shear stresses are high, often causing surface defects [1], [22], [32].
- The asymmetrical nature of the cooling process induces residual stresses, which may influence the performance of the pipe acting as an external pressure [19], [33].
- The thick walls required for the pipe make it so that the extruded material will usually sag as the pipe cools down [34], [35].

- The pipe is usually cooled only from the outside, which combined with thick walls makes for a slow extrusion process [36].

The morphological features of the pipe will depend on the extrusion processing and cooling conditions. The morphological structure of the polymer is of great importance to the part's performance [30]. For example, there is macromolecular orientation along the axis of the pipe, as this is the extrusion direction, resulting in higher axial strength of the pipe [23]. However, as seen in equations (1.1.1) and (1.1.2) the processing orientation is not beneficial when the stress is higher in the hoop direction than the axial direction [37], [38].

1.4. Research Objectives

This research focuses on the characterization of HDPE resins for the production of pipes. The aim is to compare the rheological and viscoelastic properties of resins and pipes provided by LyondellBasell. In the melt state, the rheological properties of two distinct resins give information of their behavior during their extrusion processing. For solid pipes, the viscoelastic properties of finished pipes as a function of the processing conditions and the resins used, give an idea of their performance. As a result, the following objectives are proposed:

1. To determine whether non-linear rheological behavior could detect differences between two resins provided by LyondellBasell. Pipes made from the resins have similar burst behavior. The relevant rheological tests include small amplitude oscillatory shear, steady shear and transient tests like startup of flow and jump strain.
2. To find the potential to accelerate viscoelastic testing using time-temperature superposition for HDPE pipes. The interest is shifting creep data at high temperatures to long times. A consistent shift would allow assessing the performance of the pipes much faster than current industry standards.

3. Assess the differences between pipes manufactured with different HDPE resins and under different processing conditions. Based on industry burst tests, the pipes behave similarly, but the interest is to compare their creep and DMA data. This also allows checking if the results are consistent with the pipes burst behavior.

References

[1] R. K. Krishnaswamy, "Analysis of ductile and brittle failures from creep rupture testing of high-density polyethylene (HDPE) pipes," *Polymer*, vol. 46, no. 25, pp. 11664–11672, Nov. 2005.

[2] A. Peacock, *Handbook of Polyethylene: Structures: Properties, and Applications*. CRC Press, 2000.

[3] *The Plastics Pipe Institute Handbook of Polyethylene Pipe*. Plastics Pipe Institute, 2008.

[4] Y. Zhang and P.-Y. B. Jar, "Comparison of Mechanical Properties Between PE80 and PE100 Pipe Materials," *J. Mater. Eng. Perform.*, vol. 25, no. 10, pp. 4326–4332, Oct. 2016.

[5] R. K. Krishnaswamy and M. J. Lamborn, "The influence of process history on the ductile failure of polyethylene pipes subject to continuous hydrostatic pressure," *Adv. Polym. Technol.*, vol. 24, no. 3, pp. 226–232, Sep. 2005.

[6] N. Sun, M. Wenzel, and A. Adams, "Morphology of high-density polyethylene pipes stored under hydrostatic pressure at elevated temperature," *Polymer*, vol. 55, no. 16, pp. 3792–3800, Aug. 2014.

[7] D. Tátraaljai, M. Vámos, Á. Orbán-Mester, P. Staniek, E. Földes, and B. Pukánszky, "Performance of PE pipes under extractive conditions: Effect of the additive package and processing," *Polym. Degrad. Stab.*, vol. 99, pp. 196–203, Jan. 2014.

[8] ASTM D2837-13e1, "Standard Test Method for Obtaining Hydrostatic Design Basis for Thermoplastic Pipe Materials or Pressure Design Basis for Thermoplastic Pipe Products," ASTM International, 2013.

[9] E. Nezbedová, P. Hutař, M. Zouhar, Z. Knésl, J. Sadílek, and L. Náhlík, "The applicability of the Pennsylvania Notch Test for a new generation of PE pipe grades," *Polym. Test.*, vol. 32, no. 1, pp. 106–114, Feb. 2013.

[10] M. J. W. Kanters, K. Remerie, and L. E. Govaert, "A new protocol for accelerated screening of long-term plasticity-controlled failure of polyethylene pipe grades," *Polym. Eng. Sci.*, vol. 56, no. 6, pp. 676–688, Jun. 2016.

[11] T. Wu, L. Yu, Y. Cao, F. Yang, and M. Xiang, "Effect of molecular weight distribution on rheological, crystallization and mechanical properties of polyethylene-100 pipe resins," *J. Polym. Res.*, vol. 20, no. 10, p. 271, Oct. 2013.

[12] B. Crist, C. J. Fisher, and P. R. Howard, "Mechanical properties of model polyethylenes: tensile elastic modulus and yield stress," *Macromolecules*, vol. 22, no. 4, pp. 1709–1718, Apr. 1989.

[13] C. F. Popelar, C. H. Popelar, and V. H. Kenner, "Viscoelastic material characterization and modeling for polyethylene," *Polym. Eng. Sci.*, vol. 30, no. 10, pp. 577–586, May 1990.

[14] C. H. Popelar, V. H. Kenner, and J. P. Wooster, "An accelerated method for establishing the long term performance of polyethylene gas pipe materials," *Polym. Eng. Sci.*, vol. 31, no. 24, pp. 1693–1700, Dec. 1991.

[15] Y. Fukui, T. Sato, M. Ushirokawa, T. Asada, and S. Onogi, "Rheo-optical studies of high polymers. XVII. Time-temperature superposition of time-dependent birefringence for high-density polyethylene," *J. Polym. Sci. Part -2 Polym. Phys.*, vol. 8, no. 7, pp. 1195–1209, 1970.

[16] S. Onogi, T. Sato, T. Asada, and Y. Fukui, "Rheo-optical studies of high polymers. XVIII. Significance of the vertical shift in the time-temperature superposition of rheo-optical and viscoelastic properties," *J. Polym. Sci. Part -2 Polym. Phys.*, vol. 8, no. 7, pp. 1211–1225, 1970.
[17] D. G. Baird and D. I. Collias, *Polymer Processing: Principles and Design*. Wiley, 2014.
[18] L. Pi, X. Hu, M. Nie, and Q. Wang, "Role of Ultrahigh Molecular Weight Polyethylene during Rotation Extrusion of Polyethylene Pipe," *Ind. Eng. Chem. Res.*, vol. 53, no. 35, pp. 13828–13832, Sep. 2014.
[19] J. Poduška *et al.*, "Residual stress in polyethylene pipes," *Polym. Test.*, vol. 54, pp. 288–295, Sep. 2016.
[20] H. F. Brinson and L. C. Brinson, *Polymer Engineering Science and Viscoelasticity: An Introduction*. Springer, 2015.
[21] F. Vakili-Tahami and M. R. Adibeig, "Using developed creep constitutive model for optimum design of HDPE pipes," *Polym. Test.*, vol. 63, no. Supplement C, pp. 392–397, Oct. 2017.
[22] T. A. Osswald and G. Menges, *Materials Science of Polymers for Engineers*. Carl Hanser Verlag GmbH & Company KG, 2012.
[23] Y. Pan, X. Gao, J. Lei, Z. Li, and K. Shen, "Effect of different morphologies on the creep behavior of high-density polyethylene," *RSC Adv.*, vol. 6, no. 5, pp. 3470–3479, 2016.
[24] ASTM D1598-15a, "Standard Test Method for Time-to-Failure of Plastic Pipe Under Constant Internal Pressure," ASTM International, 2015.
[25] AWWA, *Pe Pipe-design and Installation (M55)*. American Water Works Association, 2011.
[26] Moore Ian D. and Zhang Chuntao, "Nonlinear Predictions for HDPE Pipe Response under Parallel Plate Loading," *J. Transp. Eng.*, vol. 124, no. 3, pp. 286–292, May 1998.
[27] J. Lai and A. Bakker, "An integral constitutive equation for nonlinear plasto-viscoelastic behavior of high-density polyethylene," *Polym. Eng. Sci.*, vol. 35, no. 17, pp. 1339–1347, Sep. 1995.
[28] W. G. Knauss, "2.07 - Viscoelasticity and the Time-dependent Fracture of Polymers," in *Comprehensive Structural Integrity*, I. Milne, R. O. Ritchie, and B. Karihaloo, Eds. Oxford: Pergamon, 2003, pp. 383–428.
[29] A. J. Kinloch and R. J. Young, *Fracture Behaviour of Polymers*. Dordrecht: Springer Netherlands, 1995.
[30] Z. Tadmor and C. G. Gogos, *Principles of Polymer Processing*. John Wiley & Sons, 2013.
[31] R. B. Bird and O. Hassager, *Dynamics of Polymeric Liquids: Fluid mechanics*. Wiley, 1987.
[32] P. J. DesLauriers *et al.*, "A comparative study of multimodal vs. bimodal polyethylene pipe resins for PE-100 applications," *Polym. Eng. Sci.*, vol. 45, no. 9, pp. 1203–1213, Sep. 2005.
[33] P. Hutař, M. Ševčík, A. Frank, L. Náhlík, J. Kučera, and G. Pinter, "The effect of residual stress on polymer pipe lifetime," *Eng. Fract. Mech.*, vol. 108, pp. 98–108, Aug. 2013.
[34] C. Kolitawong, A. J. Giacomin, and U. Nontakaew, "Viscous dissipation in plastic pipe extrusion," *Polym. Eng. Sci.*, vol. 53, no. 10, pp. 2205–2218, Oct. 2013.
[35] C. Saengow, A. J. Giacomin, and C. Kolitawong, "Extruding plastic pipe from eccentric dies," *J. Non-Newton. Fluid Mech.*, vol. 223, pp. 176–199, Sep. 2015.
[36] J. F. T. Pittman, G. P. Whitham, and I. A. Farah, "Wall thickness uniformity in plastic pipes: Computer simulations of the effectiveness of die mandrel offsetting and pipe rotation in combatting sag," *Polym. Eng. Sci.*, vol. 35, no. 11, pp. 921–928, Jun. 1995.
[37] F.-Z. An, Z.-W. Wang, J. Hu, X.-Q. Gao, K.-Z. Shen, and C. Deng, "Morphology Control Technologies of Polymeric Materials During Processing," *Macromol. Mater. Eng.*, vol. 299, no. 4, pp. 400–423, Apr. 2014.
[38] M. Nie, Q. Wang, and S. Bai, "Morphology and property of polyethylene pipe extruded at the low mandrel rotation," *Polym. Eng. Sci.*, vol. 50, no. 9, pp. 1743–1750, Sep. 2010.

Chapter 2. Literature Review

2.1 General Review

This section introduces the reader to general concepts that merit a brief discussion. Section 2.1.1 reviews how industry classifies pipes and the motivation for standardizing pipes. Section 2.1.2 reviews the characteristics of HDPE resins used in the manufacture of pipe and how they have evolved in time.

2.1.1 Pipe Classification

A material's performance under stress, depending on service conditions, determines how suitable it is for pressured plastic pipe. In early generation pipes, three mechanisms were the main cause of a pipe's failure. At long times, pipe failure is brittle, as chemical degradation takes place when anti-oxidants and stabilizers stop being effective. Failure is almost independent of the stresses applied when degradation occurs [1], [2]. At intermediate times, pipes fail in a quasi-brittle manner from cracks that grow from notches, scratches and other small imperfections present in the pipe. The slow crack growth (SCG) process takes years to occur with the crazing mechanism developed over several stages [3], [4]. Through a better understanding of these failure mechanisms resin manufacturers have changed their resins so that now, these two failures mechanisms don't occur in the time scale of practical use for HDPE pipes [5]. Short term, failure is ductile, as creep causes large-scale deformation, thinning the walls and stress to become higher so the pipe eventually fails.

One of the most important measures of a pipe's performance is the hoop stress the material can withstand for 50 years at room temperature. Such extended periods of time are the convention in the industry because of the immense cost of repairing or rehabilitating pipe [2], [6]. See Figure 2.1.1 for typical creep rupture data for a pipe. Each line represents a set of pipes that failed. Creep rupture

results lie along a straight line when plotted on log stress vs log time of failure coordinates, until reaching a "knee". The failure mechanism for the pipe changes then from ductile to controlled by crack growth. The hoop stresses that cause failure at 50 and 100 years come through extrapolation.

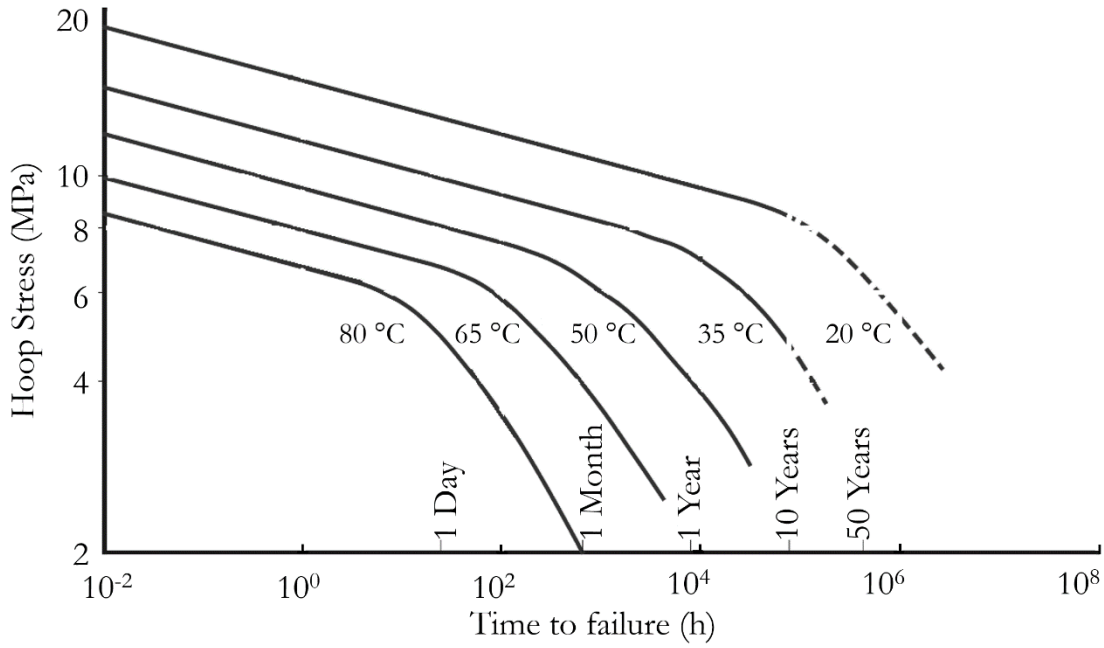

Figure 2.1.1: Typical stress to time to failure curve for an HDPE pipe resin. Modified from [7]

The extrapolation standard is based on Arrhenius relation between logarithm of time, logarithm of stress and inverse of absolute temperature, [1], [8]. The general model used is Equation (2.1.1); it allows one to fit the data and get four parameters to predict the time to failure from stress and temperature. Notice that in Equation (2.1.1), stress and temperature are the independent variables. This is for practical reasons, because even when time to failure is the observed quantity, and should be the independent variable, stress depends on fluid pressure which the user sets [6].

$$\log_{10} t = c_1 + \frac{c_2}{T} + c_3 \log_{10} \sigma + c_4 \frac{\log_{10} \sigma}{T} \tag{2.1.1}$$

The procedure stated in ASTM D1598 allows one to collect the creep rupture data and ASTM D2837 lays out how to extrapolate the data to 100,000 hours. The behavior is consistent in this time span [9]. A material's HDB is determined by categorizing the extrapolated value at 100,000 hours (the LTHS) into one of several standard values of strength. The numbers increase around 25% in values such as 800 psi, 1,000 psi, 1250 psi, 1600 psi (5.52 MPa, 6.89 MPa, 11 MPa, 13.8 MPa). These categories simplify material selection for producers and help standardize product design [10].

2.1.2 HDPE Resins for Pipe

HDPE is a thermoplastic, semi-crystalline polymer made from ethylene using titanium based Ziegler-Natta catalysts or chromium based Phillips catalysts. Polyethylene is one the lowest cost synthetic polymers and across its different families has the largest demand of common thermoplastic materials [11]. HDPE is highly versatile, finding use in many applications. This is possible because of the many ways in which the reaction processes allows tuning the material's architecture. The features of an HDPE resin that will determine its performance in a pipe application are: density, molecular weight (MW) and molecular weight distribution (MWD) all of which need to strike a certain balance [12].

Density affects the resins performance as slightly decreasing density, compared to an HDPE homopolymer, improves toughness and SCG. To decrease density, small amounts of higher order olefins add a small concentration of short chain branching. This increases the spacing between polymer molecules [13], slightly decreasing density compared to a homopolymer. While small increases in density result in higher load-bearing capability for the pipe, they do so at the expense of toughness and SCG [14].

High average MW impart better mechanical properties to the manufactured part. Additionally, high MW improves melt strength, or the tendency for the melt not to deform or sag during the cooling

stage. For HDPE pipe resins MW are usually over 100,000 g/mol [10], [15]. However, increasing MW also increases viscosity making the extrusion process considerably more difficult or costly, sometimes without significant improvement of mechanical properties [16], [17].

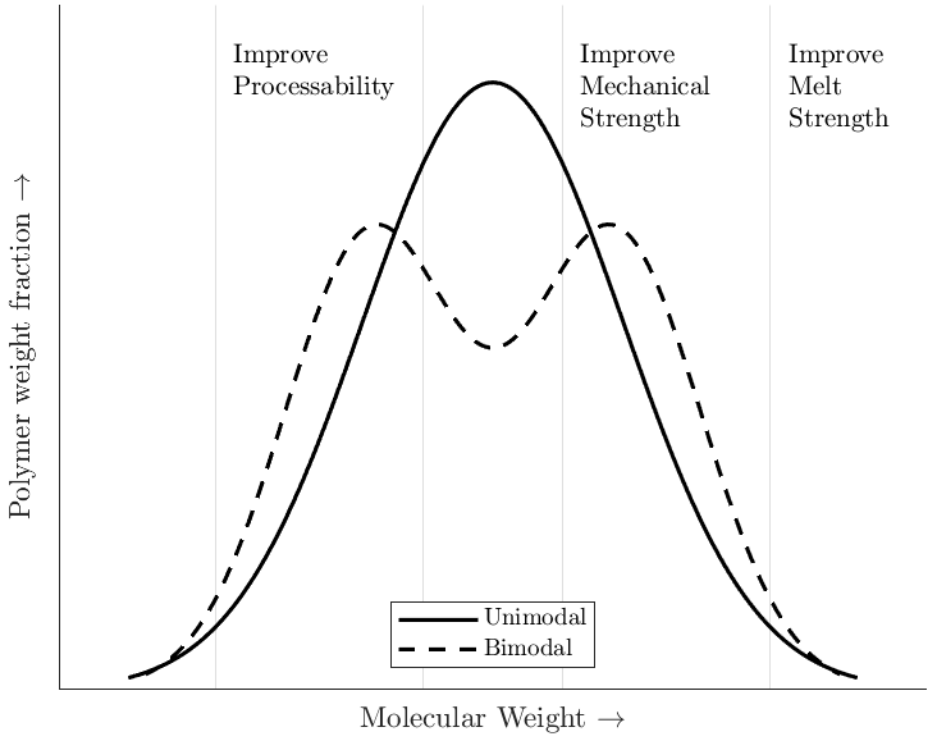

Figure 2.1.2: Concept of the role played by different chain lengths in a given MWD. Adapted from [18]

The molecules of HDPE have different chain lengths resulting in an MW that is not the same for all molecules. A broad MWD shows that the molecules differ considerably in length. The effect of a broad MWD is better processability, but at the expense of stiffness and impact strength. Important too is the modality of the resin: how many peaks show up on a graph of polymer weight fraction vs MW. If only one peak appears the resin is unimodal, but if several peaks appear it is multimodal [14]. Different lengths in a given MWD play a different role in the extrusion process and the

mechanical properties of a part [18]. Figure 2.1.2 illustrates the roles different length molecules play in pipe and how a bimodal MWD is beneficial for pipe production.

Continued advances in catalyst technology and a better understanding of the pipes failure have enabled the development of resins with improved performance. New generation catalysts make bi-modal resins in a single reactor, simplifying the resin manufacturing process [18]. New catalysts allow the preferred incorporation of co-monomers in the longer polymers chains, increasing the probability that the high MW copolymers will act as tie molecules connecting to the crystals formed by low MW homopolymers. This physical network holds the matrix together and is responsible for improved mechanical properties [19]–[21].

2.2 Viscoelastic Properties

Polymers exhibit viscoelastic behavior; they display both elastic and viscous behavior when deformed. A usual manifestation of viscoelastic behavior is that strain lags behind an applied stress. When a polymer is loaded, there will be an instantaneous elastic strain followed by gradual retarded strain. The stress required to achieve a deformation and deformation rate depends on the configuration of molecules. A new state of equilibrium materializes after the deformation, influencing the mechanical performance of the polymer during its lifetime. This makes it harder to design parts expected to be in use for long periods of time [22], [23].

Polyethylene is one of the most studied materials in polymer science. It has a simple monomer abundant in natural gas; it is low cost, easy to process, widely available and used in a wide range of applications [24]. Many researchers have studied the viscoelastic properties of HDPE solids and melts under many circumstances connecting its response to changes in properties like density, MW and

MWD chain branching and processing conditions [17], [25]–[32]. Viscoelastic tests are product specific when the applications are for long-term products, such as pipes or geo-membranes, but it is also of interest to understand how properties like MW, MWD affect the viscoelastic response.

The material properties of HDPE are wide ranging and a function of temperature. Small variations in the polymer's architeccture result in property changes that can be significant. This is part of the motivation to perform stringent quality control and investigate the creep behavior of production and development batches before they go into large-scale industrial applications [33].

2.2.1 Dynamic Mechanical Analysis

A simple definition for Dynamic Mechanical Analysis (DMA) is the application of an oscillating force to a sample and the analysis of following strain response. The sinusoidal force applied results in a sinusoidal strain. See equations (2.2.1) and (2.2.2). It is easier to implement sinusoidal stimulus in a sample, compared to the step stimulus required for creep or stress relaxation measurements [23], [34]. Material properties like modulus, viscosity and compliance are calculated from the amplitude of the deformation wave and the lag between the stress and the strain response. DMA gives a measurement each time a sine wave is applied, which allows fast measurements under different frequencies, strains or temperatures sweeps for a sample [34].

$$\tau(t) = \tau_0 \sin \omega t \tag{2.2.1}$$

$$\gamma(t) = \gamma_0 \sin(\omega t - \delta) \tag{2.2.2}$$

DMA allows direct measurement of a material's tendency to store and to dissipate energy. These two quantities are the storage (G') and loss modulus (G'') respectively. The ratio between the

moduli or the damping is $\tan\delta = \frac{G''}{G'}$. It shows how the material loses energy to the arrangement of molecules and internal friction. The extreme cases of $\tan\delta$ equal to zero and infinity represent the ideal cases of a perfectly elastic material and a perfect viscous material, respectively. The phase angle δ is a measure of the lag between the storage and loss response. See Figure 2.2.1. A viscoelastic material will fall somewhere between the extreme cases and changes in the $\tan\delta$ value signal transitions in the polymer's behavior. Such transitions reveal motions of the polymer chain and the time scale under which they occur.

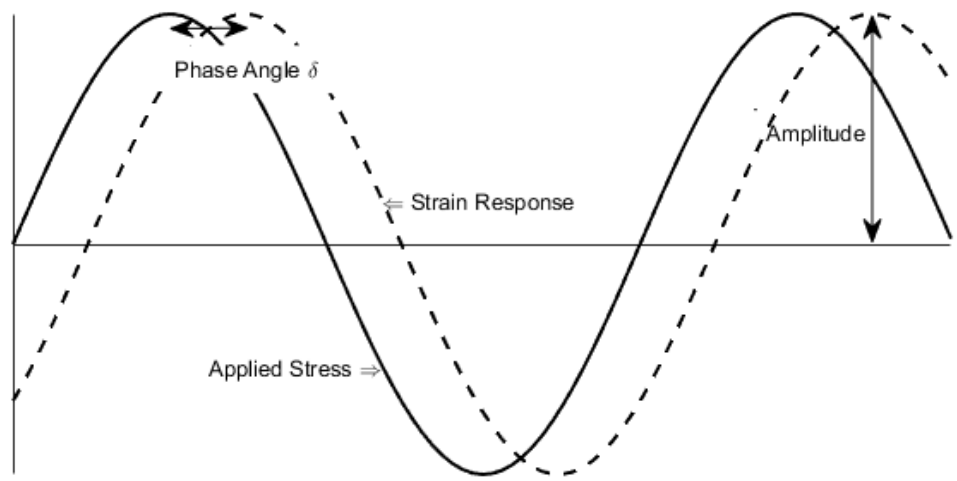

Figure 2.2.1: Representation of stress and strain curves in an oscillatory experiment.

Figure 2.2.2 shows typical DMA results for HDPE resins. The storage modulus is of the order of 1GPa in the glassy region that occurs at low temperatures and then drops two orders of magnitude as temperature increases and before it reaches the melting temperature. Such values are typical for semi-crystalline polymers. The curve in part (a) suggests that above -25 °C, the modulus values change noticeably, making the pipe's creep performance sensitive to the temperature of its surroundings [17], [34], [35].

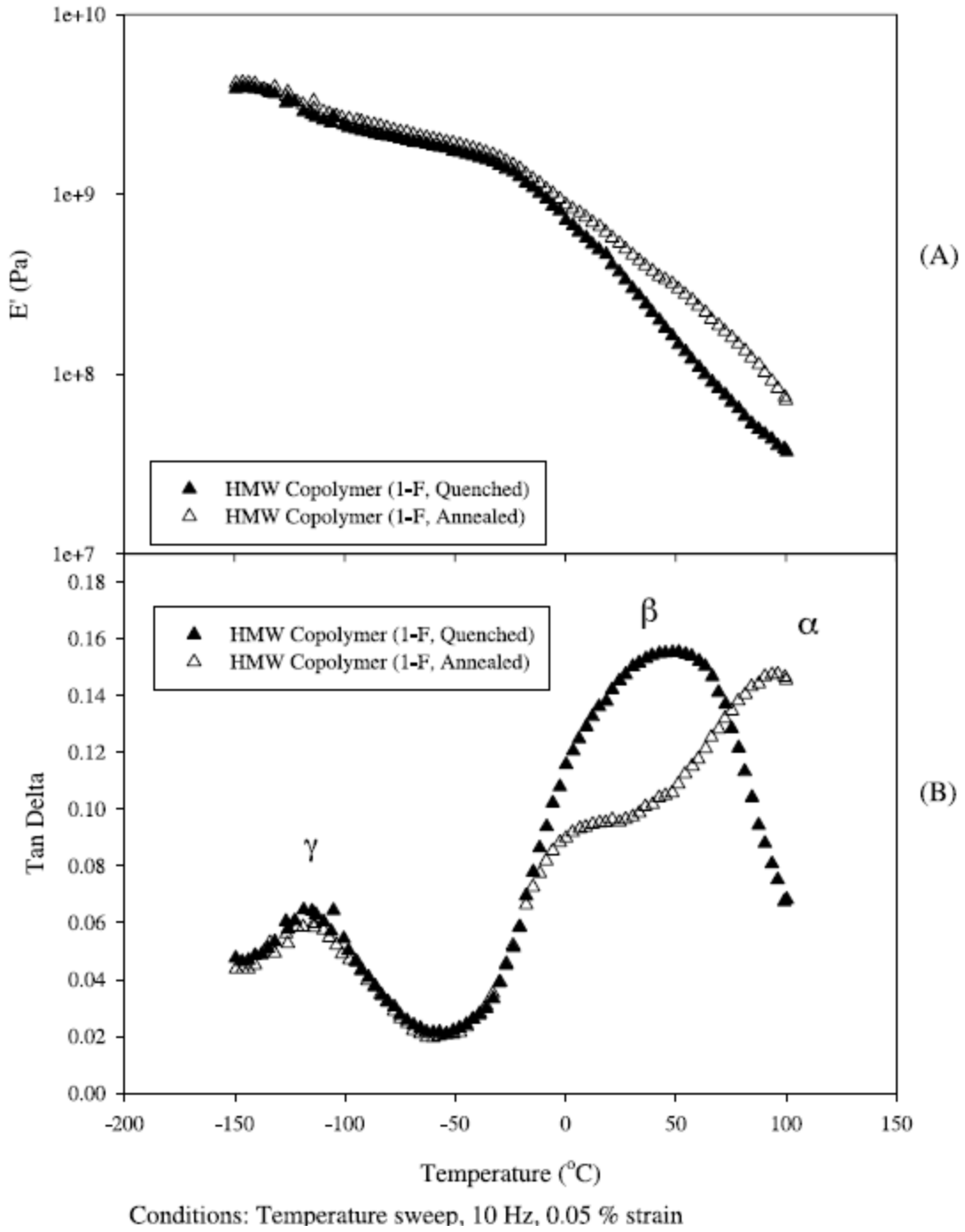

Figure 2.2.2: Typical DMA results for HDPE under different cooling conditions. (a) Storage Modulus and (b) Tan δ. Reproduced with permission from [17]

HDPE displays relaxations in the DMA spectrum below its melting temperature of 130°C. They are designated as α, β, and γ relaxations, see Figure 2.2.2 (b). The α relaxation occurs in the 30 to 120 °C range and is associated with chain motion in the crystalline region of the polymer. The β relaxation occurs in the -30 to 10 °C range and is associated with the motion of chain units in the interfacial region between the amorphous and crystalline regions. The γ relaxation occurs in the -150 to -120 °C range and while some authors associate it with the T_g , others associated with crankshaft motions in short segments of the polymer chains [35]–[37] . The α and β relaxation are visible in the DMA spectrum depending on the processing conditions of the finished, tested part.

2.2.2 Creep and Stress Relaxation

Creep describes the gradual deformation of a material subjected to sustained loading. The stresses for creep can be below the yield stress: those required to deform the material permanently in the short term. Stress relaxation is the phenomenon by which the stress to maintain a constant strain on a sample decreases with time. Both phenomena depend on short-range rearrangement of molecules. For creep, strain accumulates as the load causes molecules to slide, rotate and unwind, while in stress relaxation the molecules get to rotate and unwind as well after being initially strained, requiring less stress to keep the same strain level [38].

Figure 2.2.3 shows typical creep curves for polyethylene for several load levels. Initially, strains increase slowly with the sample deforming uniformly. After a critical time, the deformation increases quickly developing a neck where stress concentrates, followed by a region where strain remains almost constant [24]. Parts fail upon reaching the critical time where strain increases rapidly. The critical time is a function of temperature and stress applied [5].

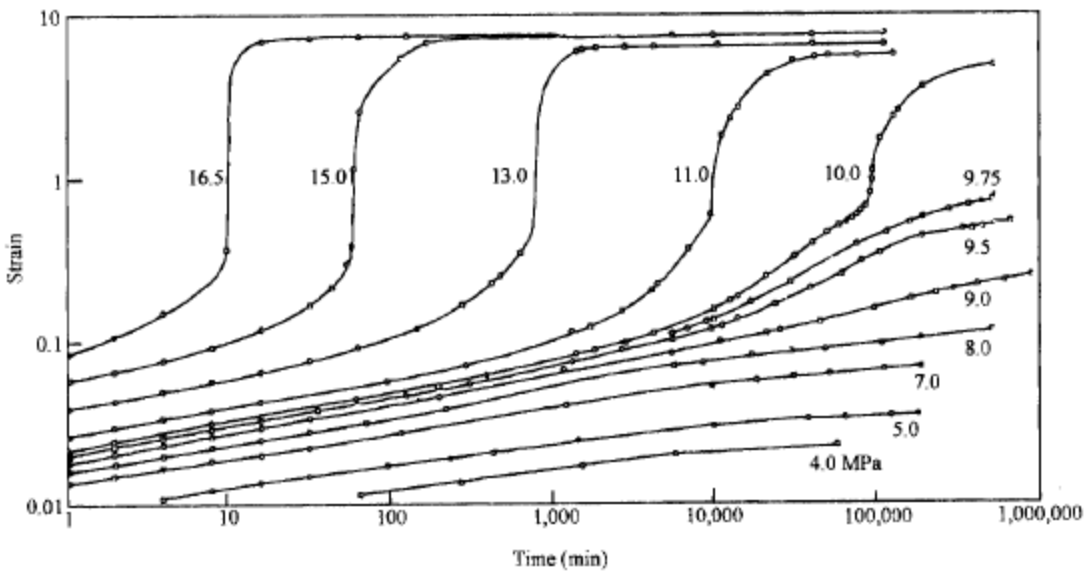

Figure 2.2.3: Strain as a function of time for polyethylene. Reproduced with permission from [24]

Both creep and stress relaxation are static experiments because they receive constant stimulation throughout the respective test. There are several challenges implementing static experiments because of not being able to generate a unit step function perfectly, meaning the initial measurements should be discarded according to the response time of the equipment performing the stimulus and measurement. With creep, an additional difficulty comes from the area of the sample reducing throughout the test, so most creep tests are constant load while true stress increases during the test [39]. This is not an inconvenience at low strain levels, but becomes relevant at the high strains HDPE deforms to during prolonged creep tests. Stress relaxation also faces additional challenges that makes the test cumbersome to perform [7].

Popelar and coworkers [40], [41] performed stress relaxations tests on HDPE to determine the shifting required to create master-curves to speed up pipe testing. Their tests did not give time to failure, but after directly testing pipes, the time to failure t_f would shift to a reference temperature according to equations (2.2.3) and (2.2.4). The terms b_T and a_T are the shift factors explained in section

2.3.2. After determining the stress and time to failure at high temperature, or sped up test conditions, the results shifted to the reference temperature allow one to establish the performance of the pipe.

$$\sigma(T_R) = \sigma(T)b_T \tag{2.2.3}$$

$$t_f(T_R) = t_f(T)/a_T \tag{2.2.4}$$

2.3 Time Temperature Superposition

As an example for TTSP, consider the data shown in Figure 2.3.1 for the amorphous polymer polyisobuthylene. The results show that relaxation modulus depends on temperature and duration of the measurement. This is usually the case for viscoelastic properties. For any polymer, a high temperature leads to a small relaxation time, while a low one gives a long relaxation time. Though TTSP was first derived empirically, it also comes from kinetic theory for diluted and undiluted polymers [42].

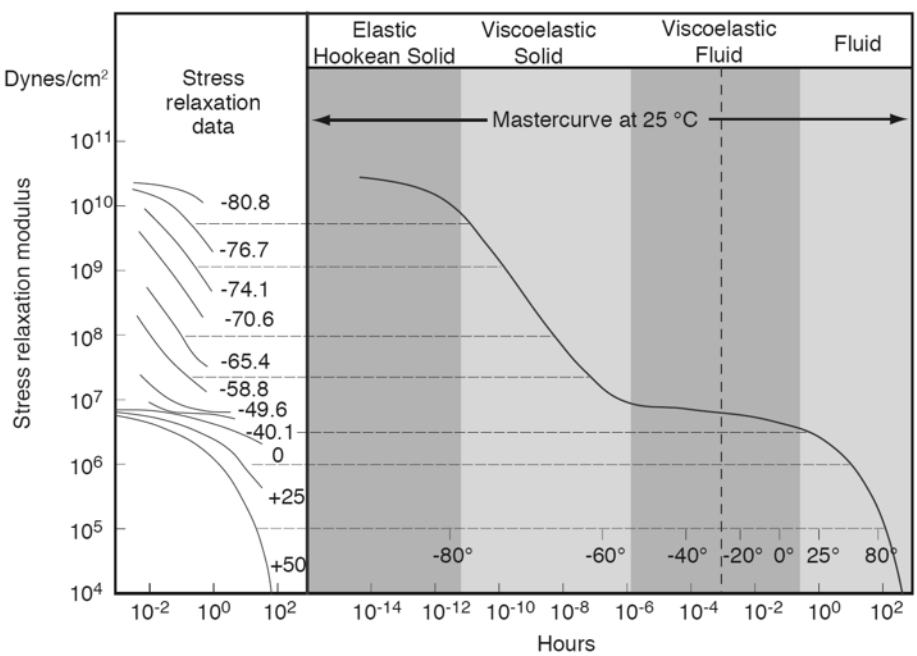

Figure 2.3.1: Relaxation modulus curves for polyisobuthylene and corresponding master curve at 25 ºC. Adapted from [7]

To build a master curve at a reference temperature the data at other temperatures must be shifted. For an amorphous polymer, the data at a higher temperature shifts to the right, representing a longer time required to achieve the same relaxation modulus at the reference temperature. The data at lower temperatures shifts to the left representing the short time scale measurement. Low temperatures restrict the movement of molecules, slowing them down. At a high temperature, molecules can move more easily. Accordingly, the shape of relaxation, or the viscoelastic property measured, does not change when shifted [7].

The appeal of TTSP is the possibility of changing time testing by changes in temperature. This allows carrying out mechanical tests that are not time consuming and determine viscoelastic properties that span many decades of time. By testing below the reference temperature, a researcher has access to a time scale that may not be reasonable to measure. Testing above the reference temperature, a researcher has access to a time scale for which testing may not be practical [38].

2.3.1 TTSP Shifting

Consider $H(\tau, T)$ as the relaxation spectrum of a viscoelastic material. It depends on temperature T, and a characteristic time for the material τ, which is also a function of temperature. Consider $F(\tau(T), T)$ to be any viscoelastic function of interest. An appropriate intensity function $g\big(t/\tau(T)\big)$ allows one to define any viscoelastic function of interest $F(t, T)$ from the relaxation spectrum as:

$$F(t,T) = \int H\,(\tau,T)g(t/\tau)\mathrm{d}\tau \tag{2.3.1}$$

The explicit dependence of $H(\tau(T), T)$ is relatively negligible, so the temperature dependence of the relaxation spectrum comes implicitly through the characteristic relaxation times [43]. According

to kinetic polymer theory the function $H(\tau, T)$ may be separated as the product of functions of τ and T, see equation (2.3.2), which transforms equation (2.3.1) into equation (2.3.3).

$$H(t,T) = b'_T(T)\, h(\tau) \tag{2.3.2}$$

$$F(t,T) = b'_T(T) \int h\,(\tau) g(t/\tau) \mathrm{d}\tau \tag{2.3.3}$$

Equation (2.3.3) holds for any temperature T_0 and its time scale $\bar{t}$, so changes in temperature always affects the characteristic time in the same way, so equation (2.3.3) turns into equation (2.3.4):.

$$F(\bar{t}, T_0) = b'_T(T_0) \int h\,(\tau) g(\bar{t}/\tau) \mathrm{d}\tau \tag{2.3.4}$$

The shift factor a_T connects the time scale between a reference temperature T_0 and another given temperature as $a_T = \frac{\tau}{\tau_0}$. Taking $b_T = \frac{b'_T(T)}{b'_T(T_0)}$Equation (2.3.1) and (2.3.4) then create equation (2.3.5).

$$F(t,T) = b_T F\left(\bar{t} = \frac{t}{a_T}, T_0\right) \tag{2.3.5}$$

Equation (2.3.5) shows how a given viscoelastic property at one temperature is the same at some other temperature if the timescale is modified by a multiplication factor; the viscoelastic property shifts with a multiplication factor of $b_T(T)$. Equation (2.3.5) is the formal definition that allows one to construct a master curve from temperature data. On a log-log plot of the viscoelastic property vs time, a_T horizontally shifts the data, while b_T results in a vertical shift. The horizontal scale shift factor

is the most important of the two shifts [43]. Most times, temperature changes are small enabling the approximation $b_T \approx 1$, such that only a horizontal shift is necessary [44].

For amorphous polymers $b'_T(T) = \rho T$, such that $b_T(T) = \rho T/\rho_0 T_0$ [42]. In such a case, the vertical shifting required depends directly on density and temperature. For small changes in temperature and density it is reasonable that $b_T \approx 1$. This form is not applicable to semi-crystalline polymers like HDPE.

2.3.2 Double Shifting

The preceding section made the case for TTSP and why often only one shift factor is used in the construction of master curves. However, it is possible to incur in significant errors if the second, vertical shift is missing. Figure 2.3.2 illustrates how this could happen. Errors accumulate when a vertical shift is required but not included. Figure 2.3.2 shows a sample master curve at a given temperature and data measured at temperature T_1 higher than the reference temperature. No amount of horizontal shifting allows it to overlap completely with the master curve; there is always a compliance and time error. Adding vertical shifting results in complete overlap of the T_1 data with the true master curve at the reference temperature

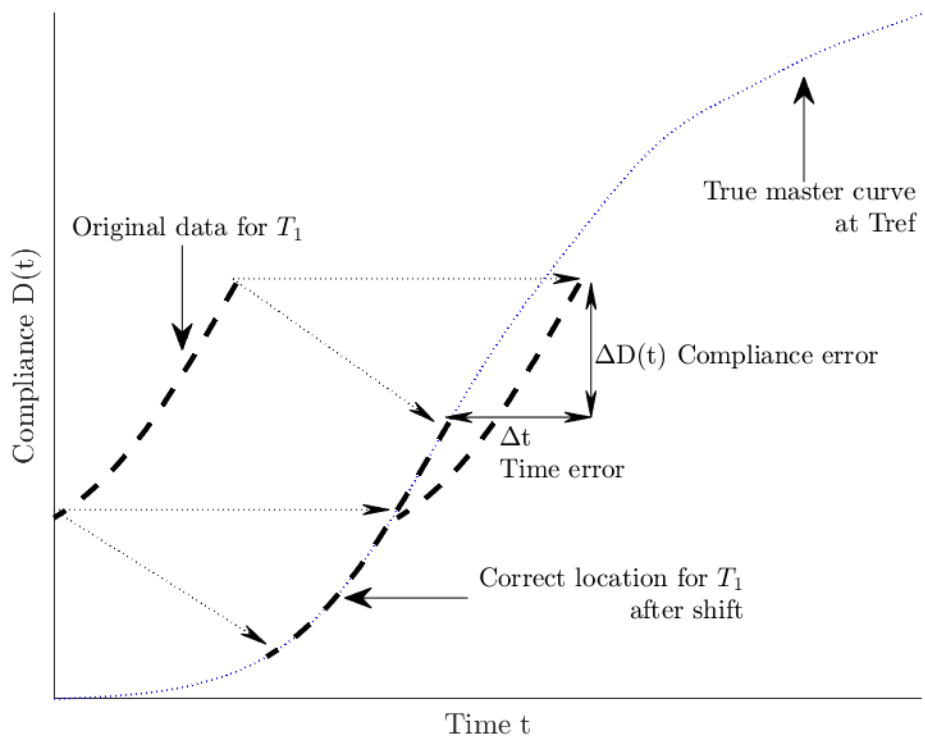

Figure 2.3.2: Qualitative plot showing how a lack of vertical shift can induce error. Adapted from [38]

Typical transient tests that measure creep compliance or relaxation mudulus at several temperatures do not provide a way to find the vertical and shift factors independently. DMA data enables a way to find if a vertical shift is required. Take $H(\tau, T)$ as the relaxation spectrum of a viscoelastic material. Some viscoelastic properties, such as storage and loss moduli, measured during DMA are in equations (2.3.6), (2.3.7), (2.3.8), and (2.3.9) [42].

$$G'(\omega, T) = \int_{-\infty}^{\infty} H(\tau, T) \frac{(\omega\tau)^2}{1 + (\omega\tau)^2} d\ln\tau \tag{2.3.6}$$

$$G''(\omega, T) = \int_{-\infty}^{\infty} H(\tau, T) \frac{(\omega\tau)}{1 + (\omega\tau)^2} d\ln\tau \tag{2.3.7}$$

$$G^*(\omega, T) = \sqrt{G'(\omega, T)^2 + G''(\omega, T)^2} \tag{2.3.8}$$

$$\tan\delta(\omega,T) = \frac{G''(\omega,T)}{G'(\omega,T)} \tag{2.3.9}$$

Let us call the vertical shift factor b_T. Note that for a thermos-rheologically simple material all viscoelastic properties will have the same shift factors [42], [45]. The horizontal shift, a_T, reveals the temperature dependence of the relaxation time. The vertical shift, b_T, reveals the temperature dependence of modulus [40], [45]. Note that the case of $b_T = 1$ gives conventional shifting back.

When building a master curve from DMA data, the storage modulus would then shift as $b_T G'(a_T\omega, T) = G'(\omega, T_0)$. This is not convenient, as it means that both modulus and frequency have to shift simultaneously giving the same case as creep compliance or relaxation modulus. However, tan δ, equation (2.3.9), has no vertical shifting when temperature changes: $\tan\delta(a_T\omega, T) = \tan\delta(\omega, T_0)$. We can redefine the viscoelastic properties as in equations (2.3.10), (2.3.11), (2.3.12) and (2.3.13).

$$G'(T,\tan\delta) = \frac{1}{b_T} G'(T_0,\tan\delta) \tag{2.3.10}$$

$$G''(T,\tan\delta) = \frac{1}{b_T} G''(T_0,\tan\delta) \tag{2.3.11}$$

$$G^*(T,\tan\delta) = \frac{1}{b_T} G^*(T_0,\tan\delta) \tag{2.3.12}$$

$$\omega(T,\tan\delta) = \frac{1}{a_T} \omega(T_0,\tan\delta) \tag{2.3.13}$$

A procedure to shift the data proposed by Mavridis [45] is that:

1. Graph the complex tan δ vs modulus for data at several temperatures. If the curves superimpose, there is no need for vertical shifting. The curves only require vertical shifting.
2. Graph frequency vs tan δ for data at several temperatures. The curves only require horizontal shifting.
3. If at any point the lines are not parallel and do not superimpose, the relaxation time may not have an uniform dependence on temperature, meaning the material is not thermo-rheologically simple

Below its melting temperature, classical TTSP will not produce continuous smooth master curves for all viscoelastic properties of HDPE. HDPE needs a vertical shift besides the classical horizontal shift [40], [41], [46], [47]. Some authors attribute this need to changes in crystallinity as a function of temperature [40] [48]. Others attribute it to the changed mobility of the chains, which results in uncoordinated motions of the crystalline lattice and deformation of the amorphous regions as a function of temperature [42], [46].

Several authors have needed to use vertical shifting to produce coherent master curves from HDPE. Popelar tested HDPE dog-bones for stress relaxation and established the vertical shifting required to get master curves [40]. He tested several conventional HDPE resins and found a TTS equivalence where one hour of testing at 80 °C was equivalent to 16 days at 25 °C. Another example comes from Fukui, who measured strain-optical coefficients of HDPE and developed master curves which required a vertical shift [47].

2.3.3 Shift Factor Models

When building a master curve, the viscoelastic data of interest allows one to find the shift factors by making sure that the curves superimpose on each other at the reference temperature. It is of interest to able to represent and know the temperature dependence of the shift factors, to shift data to intermediate temperatures with no data. In general, a span of 100 ºC will have shift factors that spans the order of 8 decades [43] so models usually include the logarithm of the shift factor and will always explicitly depend on the reference temperature chosen. Models for shift factors come from phenomenological arguments and do not come from fundamental laws of physics [23].

The WLF model, shown in equation (2.3.14), is commonly used for amorphous polymers with the glass transition temperature (T_g) chosen as the reference temperature. This model is ubiquitous in the polymer viscoelasticity literature. Even though its authors found the equation empirically after analyzing numerous polymers, it has a foundation in free volume concepts. The WLF model is valid between the temperatures T_g and T_g +100 ºC [49].

$$\log_{10} a_t = \frac{-C_1(T - T_g)}{C_2 + (T - T_g)} \tag{2.3.14}$$

However, the WLF does not work well for polyethylene. The model does not hold for semi-crystalline polymers. Finding the T_g of HDPE carries its own difficulties, as its crystallinity is high. Authors report values from -130 ºC to -40 ºC [50]. The testing temperatures for pipes fall outside the preferred range being above T_g + 100 ºC.

The Arrhenius shift factor model, shown in equation (2.3.15), also allows shifting viscoelastic data and enjoys widespread use. It is used over the WLF model, for example, for shifting viscosity data in polymer melts [51]; below the Tg where WLF does not apply anymore [38]; or when there are

localized motions in the crystalline regions of polymers so it does a better job of representing the shift factor [23], [52]. Another advantage is that it only needs two constants, an activation energy (E_a) and a reference temperature (T_0), vs the WLF model that needs three (C_1, C_2 and T_{ref}). Ward derives the Arrhenius temperature dependence of viscosity. Then he connects two temperatures to give the Arrhenius shift factor model [53]. Both models do a good job representing the shift factors, and a condition for TTSP holding is that a_T has a reasonable form such as WLF or Arrhenius behavior [54].

$$\ln a_T = \frac{E_a}{R}\left(\frac{1}{T} - \frac{1}{T_0}\right) \tag{2.3.15}$$

Popelar and coworkers [41] found that their shift factors for HDPE empirically fit a model of the form of equation (2.3.16). Chudnovsky [8] used an Arrhenius like model to fit his shift factor data and compared his results to those of Popelar, finding that the models produced similar shift factors in the temperature range considered.

$$\ln a_T = A(T - T_0) \tag{2.3.16}$$

2.4 Impact of Rheology

HDPE is a shear thinning resin. Its viscosity decreases when shear rate increases. At low shears, the polymer's molecules approximate entangled random coils, however, as shear increases, and the entanglements become undone, molecules can more easily slide past each other decreasing the resistance to flow. In this sense, HDPE melts acts conventionally.

Rheology allows one to get information on the molecular features of the polymer. Viscosity directly depends on MW, as the length and branching of the chains determines the concentration of entanglements. Shear thinning, or how much viscosity drops when shear rates increase, depends on branching and MWD. Shear thinning sets in at higher shear rates for resins with a broad MWD, but

then viscosity reduces more as a function of shear rate compared to otherwise similar resins with narrow MWD [55]. The more compact nature of branched polyethylene molecules makes them shear thin more easily as a compact molecule is not as likely to form entanglements as a linear one [24] .

Knowing the shear viscosity is key to understanding the processing of the polymer itself. Most polymer processing is shear dominated [56] and viscosity is one the basic parameters that allow determining the operating conditions that will govern shear stresses, shear rates, and pressure drops among others during processing. However, shear viscosity gives no information of what happens under shear-free flow conditions.

2.4.1 Parallel Plate Fixtures for High MW Polymers

Rotational devices, with parallel plates or cone and plate, allow measuring the rheological properties of molten polymers. The selection of these fixtures is because of the small amount of sample required to make measurements and their ability to generate viscometric flows. Viscometric flows are unidirectional shearing flows in which all material elements are shearing steadily. They allow a simple shear rate tensor, which allows a straightforward determination of viscosity [44].

Parallel plate fixtures, see Figure 2.4.1, are especially useful when dealing with highly viscous materials like pipe HDPE resins [57]. It is easier to prepare a flat sample and squeeze it with the fixtures, compared to the sample needed in cone and plate, which the instrument needs to squeeze to a tiny truncation gap. Equation (2.4.1) allows getting the steady shear viscosity from the measured torque $\mathcal{T}$, the imposed strain rate $\dot{\gamma}_R$ and the dimension of the fixture. Equation (2.4.2) allows getting the normal stress differences. Equations (2.4.1) and (2.4.2) have no assumptions about viscosity, which is why they include derivative terms. Analytical expressions for the derivative terms are determined explicitly for known viscosity functions . The derivative terms correct the non-homogeneous shear that the parallel plates impose on the melt, meaning several steady shear measurements are necessary

to determine viscosity [44], [58]. Such corrections are unnecessary in cone and plate fixtures as they generate a homogenous shear field.

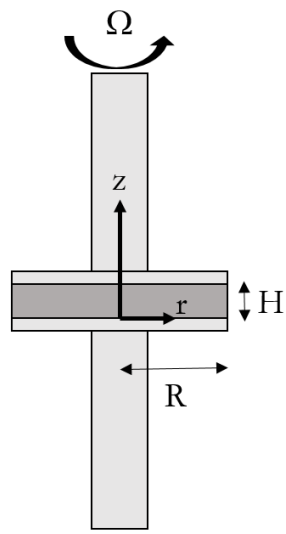

Figure 2.4.1: Cross section view of parallel plate fixtures.

$$\eta(\dot{\gamma}_R) = \frac{\mathcal{T}}{2\pi R^3 \dot{\gamma}_R}\left[3 + \frac{d\ln(\mathcal{T}/2\pi R^3)}{d\ln\dot{\gamma}_R}\right] \tag{2.4.1}$$

$$\Psi_1(\dot{\gamma}_R) - \Psi_2(\dot{\gamma}_R) = \frac{\mathcal{F}}{\pi R^2 {\dot{\gamma}_R}^2}\left[2 + \frac{d\ln(\mathcal{F}/\pi R^2)}{d\ln\dot{\gamma}_R}\right] \tag{2.4.2}$$

Because of inertia effects, the polymer melt comes out of the fixtures even at relatively low shear rates; around > 1 1/s. Small amplitude oscillatory shear (SAOS) allows one to get viscosity measurements at high frequencies. The Cox-Merz rule relates frequency to shear rate, see section 2.4.2. The SAOS experiment is equivalent to the DMA explained in section 2.2.1 measured on a polymer melt.

The non-Newtonian nature of HDPE also results in normal stresses appearing during simple shear flow. In equation (2.4.2) the term $\mathcal{F}$ represents the force required to keep the parallel plate separation constant. However, measuring normal stresses is more challenging than measuring viscosity since small changes in temperature lead to enough expansion or contraction of the sample to affect the force measured, unless the instrument is highly stiff [59], [60].

2.4.2 Cox-Merz Rule

The Cox-Merz rule states that shear viscosity at a shear rate $\dot{\gamma}$ is equal to the magnitude of the complex viscosity when $\omega = \dot{\gamma}$. This rule holds for linear polymers with simple structures [51], [58], which is the case for HDPE. Rheological studies of HDPE have shown good agreement between viscosities measured in steady state compared to oscillatory shear [27].

It is often easier to measure viscosity in an oscillatory test compared to steady shear. For example, inertia becomes an issue at very high shear rates, so the sample does not come out of the fixtures as easily. Frequency sweeps allow getting the viscosity data from one sample quickly and sequentially, with no need to of being mindful of accumulated deformation to the sample [58], [61].

2.4.3 Laun's Rule

Measuring the normal stress differences of polymers comes with the same set of difficulties as measuring shear viscosities at high shear rates. At low shear rates, changes in temperature as low as 0.01ºC cause enough contraction orexpansion of a sample to interfere with the measurement even for a highly stiff instrument [59], [60]. A convenient empiricism proposed by Laun [62], see equation (2.4.3), allows one to estimate the normal stress difference from small amplitude oscillatory shear data. The term $\eta' = \omega G''$ is the dynamic viscosity and $\eta'' = \omega G'$ associates to the elastic energy stored during deformation [51].

$$N_1(\dot{\gamma}) = 2\omega\eta'' \left[1 + \left(\frac{\eta''}{\eta'}\right)^2\right]^{0.7}\Bigg|_{\omega=\dot{\gamma}} \tag{2.4.3}$$

2.4.4 Viscous Flow Models

Several empirical models describe the relation between shear rate and viscosity. This section presents two of the most commonly used viscosity empiricisms. Equation (2.4.4) is the power law model and is one of the simplest models for representing viscosity as a function of shear rate. It is useful as it allows some analytical solutions to the equation of motion. It has only two parameters m and n, which are a consistency index and a power law index that represents the slope of the viscosity curve at high shear rates in a logarithmic plot. The downside to the power law model is that it does not represent the viscosity plateau that exists at low shear rates, but predicts that viscosity approaches infinity as shear rate approaches zero [51], [56].

$$\eta = m|\dot{\gamma}|^{n-1} \tag{2.4.4}$$

Equation (2.4.5) is the Bird-Carreau-Yasuda Model. It accurately represents a polymer's viscosity over the complete shear rate change. There are downsides to this empiricism; for one, it does not allow for analytical solutions to the equation of motion. It also needs five parameters to represent viscosity: η_0 represents the zero shear rate viscosity, η_∞ the terminal viscosity, λ is a relaxation time that shows where the zero shear rate region ends, a represents how sharp the viscosity transitions to the power law region after the zero shear rate viscosity region, and n represents the slope in the power law index region [58], [63].

$$\frac{\eta - \eta_\infty}{\eta_0 - \eta_\infty} = [1 + (\lambda|\dot{\gamma}|)^a]^{\frac{n-1}{a}} \tag{2.4.5}$$

2.5 Pipe Extrusion Process

Extrusion is the process of pumping a polymer melt through a shaping die. The single screw extruder is the most commonly used extruder in the polymer industry. Resin granules flow from a hopper and feed a screw whereby the action of heating elements and viscous dissipation from the rotation of the screw and the high viscosity of the polymer result in the gradual melting of the polymer. Most of the heat comes from the mechanical action of the screw and the heating elements provide fine control over temperature. An extruder heats, melts, mixes and conveys material to a die which shapes it into a final product. The extruder acts as a pump generating the pressure necessary to force the melt through the die. The diameter and length of the screw usually describe the dimensions of an extruder. Standard sizes for pipe extruder screws range from 50 to 200 mm, with length-to-diameter ratios of 20 to 30 depending on the application [56].

A pipe extrusion line comprises an extruder, die, sizing, cooling, puller, printer, saw, and haul-off equipment. Figure 2.5.1 shows a typical HDPE extrusion line. After the melt exits the die, it enters a vacuum sizing sleeve. For more detail on the die, see section 2.5.1. Vacuum sizing is versatile as it allows the pipe to maintain its round shape without clamping or using internal air pressure, which is only available to large diameter pipes. The sleeve is a tube with an adequate wall opening that lets the vacuum to draw the molten polymer into contact with the sleeve bore. The ratio between die diameter and sizing sleeve diameter should be big enough to make sure that the seal between the extrudate and the sleeve is airtight. Typical values are between 1.25:1 and 2:1. See Figure 2.5.2. The sizing sleeve should be around 3% larger than the desired outer diameter to account for shrinking. The sizing sleeve

sits in a vacuum tank with cooling water circulating around it. A vacuum pump supplies vacuum to the tank [64], [65].

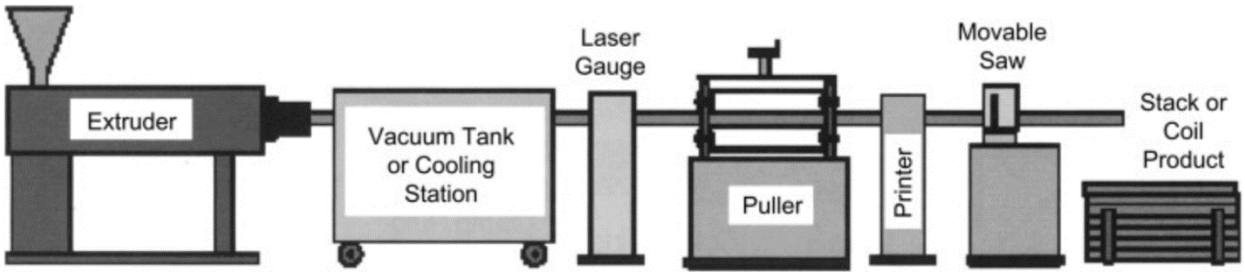

Figure 2.5.1: Typical HDPE Extrusion line. Reproduced with permission from [64]

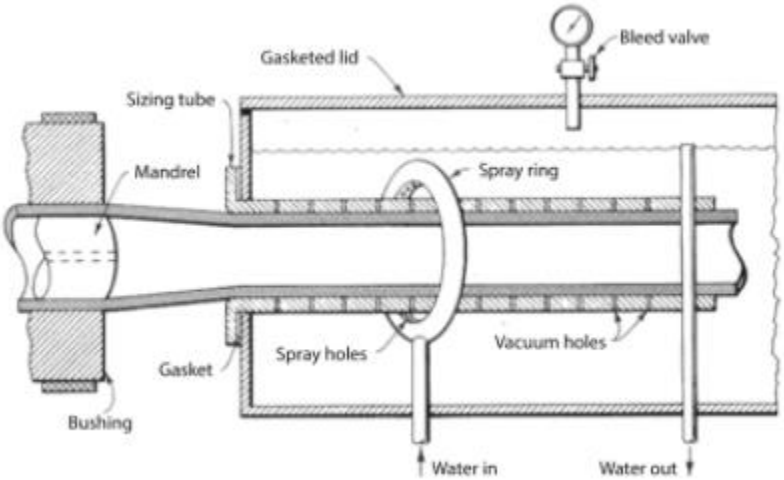

Figure 2.5.2: Vacuum sizing sleeve close up. Reproduced with permission from [65]

At least one auxiliary cooling water bath is necessary after the vacuum tank. As production rate and/or diameter increases, the need for cooling does too, requiring longer or multiple water baths. A small annealing effect occurs when multiple water baths are in a row since the air gap between them allows for a small increase of temperature in the pipe wall. It is typical to use closed water systems where water is recirculates, keeping a constant temperature so that shrinkage is the same regardless of changes in ambient temperature [66].

After the cooling section comes the haul-off device. The haul-off device's role is to string the pipe across the line and deliver the product to a moving saw that cuts it. If not cooled properly, the pipe is liable to flatten by the compressive force of the haul-off device. The haul-off includes a variable speed roll, which allows control of the line speed and the thickness of the pipe [67].

2.5.1 Flow Through the Pipe Die

The output from an extruder goes into an annular extrusion die, which is usually straight/co-axial with the extruder screw. Figure 2.5.3 shows a typical die for producing pipes. The die comprises an outer casing and an inner mandrel, secured by ties called spiders. Spiders are narrow, streamlined radial fins. The polymer melt flows between the outer barrel and the mandrel towards the end of the die, assuming an annular shape. The presence of the spiders causes the melt to separate and forms weld-lines when they recombine [24], [68]. The length of the die must be long enough to allow weld-lines to heal, or the polymer to re-entangle, and to allow the melt to relax some deformation imposed by the production process, but still short enough that it does not increase the pressure drop required for the desired flow too much [69]. Guidelines for die design suggest that the gap should be progressively smaller such that velocity steadily increases along the direction of flow [70]. The last part of the die, with the thinnest gap and a constant cross-sectional area, referred to as the die land, consumes most of the pressure generated by the extruder.

Dies often have adjustment capabilities by which the flow distribution can be changed externally while the extruder is running. Dies have their own heater bands, controlled independently from the extruder, that influence the flow profile. Screws called restrictors or choker bands, can change the relative position of the outer and inner casing of the die and physically alter the flow path the melt must flow through [70].

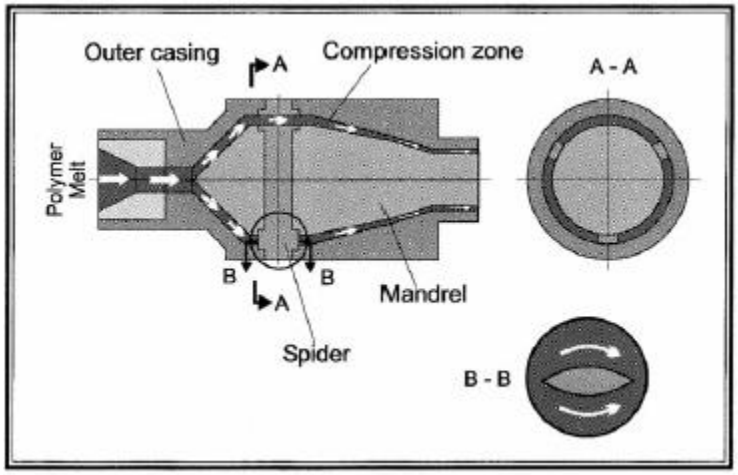

Figure 2.5.3: Spider die for the production of pipe. Reproduced with permission from [68]

The screws that change the relative positioning of the casing are employed during the startup phase of the extrusion process, to correct drift that happens due to the normal stresses arising from the viscoelastic nature of the fluid pushing the mandrel, and to compensate sagging. Sagging occurs when the polymer has insufficient melt strength to keep its shape while molten without deforming. The molten annulus has enough time to deform due to the low thermal conductivity of HDPE, which combined with thick walls, forces pipes to have long cooling times. According to Pittman, a pipe with a wall thickness of 30 mm will take over two hours to cool [71].

Since it is desirable to have a uniform thickness in the wall, it is common to purposefully decenter the mandrel downwards to compensate for the sag that naturally occurs during the cooling stage. The outer surface solidifies first and cooling progresses radially towards the center because there is no cooling on the inside of the pipe, only quiescent air. This allows the molten material on the inside of the tube enough time to flow downward due to its own weight [72]. Some researchers have analytically solved the problem of flow between eccentric cylinders for power law fluids by assuming that no secondary flows develop with an off-center die [73]–[76].

Shear rates in the die during pipe extrusion are low, around 10 – 100 s^{-1}, because the annulus are thick [24], [77]. This enables using the high MW resins desirable for the application, which have better mechanical properties. High MW resins are characterized in industry by having fractional melt flow index value [78]. The melt flow index is a standard industry test that shows how viscous a polymer is by melting it and having it flow through a hole of a small diameter under a constant weight. Even though the processing shear rates are low, the high viscosity of pipe HDPE resins ends up in high outer wall shear stresses [15]. This is a concern because of the shear stresses providing an upper bound for the value of residual stresses [79], [80] on the pipe and for being close to the critical values where surface defects are a concern for HDPE products [77], [81]

2.5.2 Morphology from Cooling and Draw Down

The slow cooling during pipe manufacturing allows HDPE to develop most of its crystallinity. Krishnaswamy [80] reports that the outside diameter region, which cools rapidly, shows lower crystallinity than the other regions and a narrower distribution of lamellar thickness too. This is because of the inside of the pipe remaining at a high temperature for a longer time than the outside. The polymer has then the opportunity to continue the crystallization process at a favorable high temperature [82]. However, Taherzadehboroujeni [83] reports that the crystallinity is even between the different layers of the pipe.

Figure 2.5.4 shows lamellae in the pipes. Figure 2.5.4 (A) shows no preferred direction for the spherulites at the pipe's interior surface; while Figure 2.5.4 (B) shows an external surface with a more ordered structure. The low draw down in pipe manufacturing gives a little molecular orientation to the pipes in the axial direction, especially in the pipes outer wall [80], [82]. Figure 2.5.5 (A) shows

Wide-Angle X-ray Diffraction (WAXD) results for a pipe, which suggests that the lamellar morphology of the overall pipe is weakly oriented, being mostly random in the core and inner regions [15]. Figure 2.5.4 (B) shows quantitative results for crystallinity in different sections of the pipe.

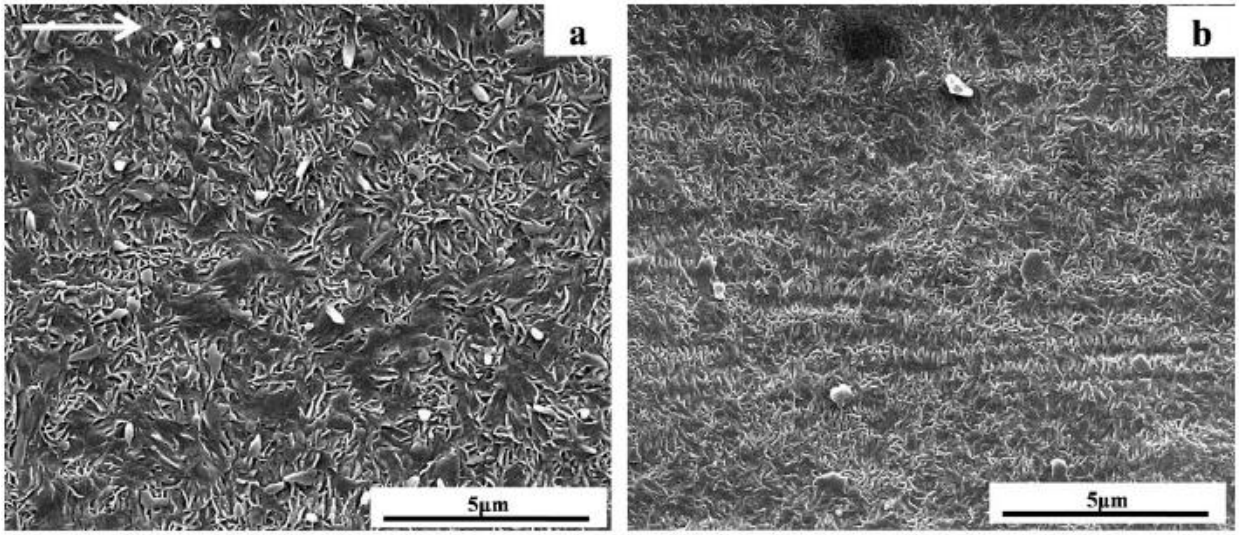

Figure 2.5.4: SEM of extruded pipe (a) Interior surface. (b) External Surface. Reproduced with permission from [82]

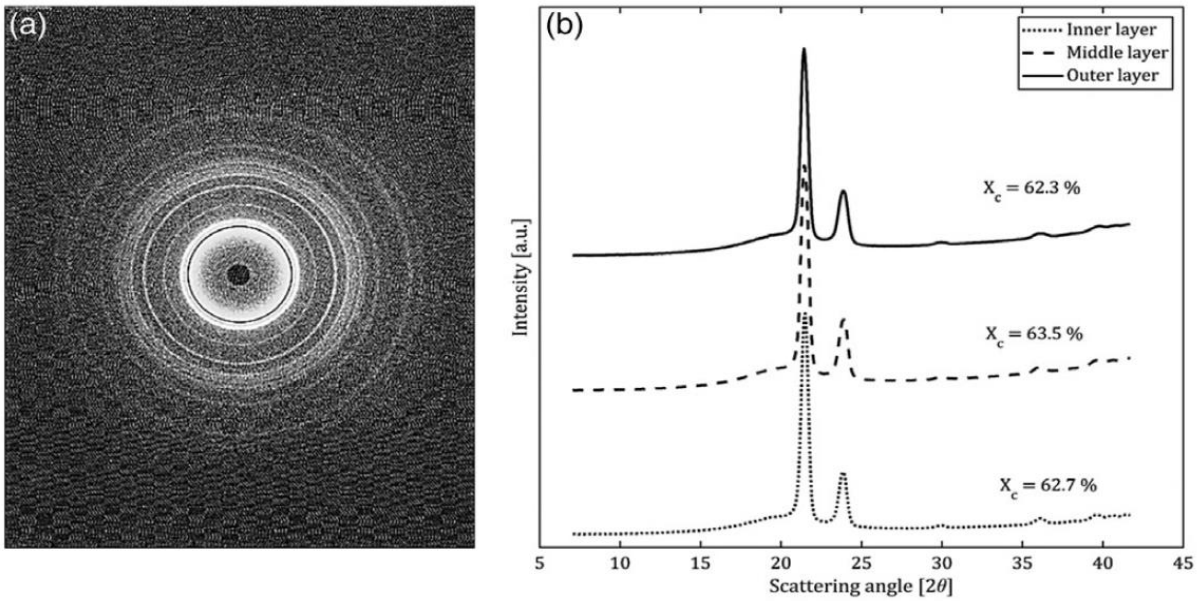

Figure 2.5.5: WAXD results (A) WAXD patterns (B) WAXD profiles. Reproduced with permission from [83]

Some authors [84], [85] argue that it is proper to consider the morphology of HDPE as having three phases, considering the interphase of the crystalline and amorphous region as separate. Nuclear magnetic resonance (NMR) measurements detect this, whereas other techniques such as differential scanning calorimetry (DSC) or infrared spectroscopy (FTIR) cannot. Sun [84] studied the evolution of the morphological properties of HDPE pipes during hydrostatic pressure tests, finding that the crystallinity increased at the expense of the interphase region. The morphological changes are mostly because of creep and small stresses slowly inducing crystallization.

To get a more favorable morphology for the pipe, several authors have worked on adapting the die-mandrel setup to rotate and induce the HDPE molecules to orient circumferentially [82], [86]–[88]. The aim is to produce orientation in the hoop direction, which has to endure the highest stresses during hydrostatic pressure, and could improve the performance of the pipe. However, such setups are still not common in commercial pipe extrusion lines.

References

[1] E. M. Hoàng and D. Lowe, "Lifetime prediction of a blue PE100 water pipe," *Polym. Degrad. Stab.*, vol. 93, no. 8, pp. 1496–1503, Aug. 2008.

[2] A. Frank, G. Pinter, and R. W. Lang, "Prediction of the remaining lifetime of polyethylene pipes after up to 30 years in use," *Polym. Test.*, vol. 28, no. 7, pp. 737–745, Oct. 2009.

[3] A. Adib, C. Domínguez, R. A. García, M. A. Garrido, and J. Rodríguez, "Influence of specimen geometry on the slow crack growth testing of HDPE for pipe applications," *Polym. Test.*, vol. 48, pp. 104–110, Dec. 2015.

[4] N. Robledo, C. Domínguez, and R. A. García-Muñoz, "Alternative accelerated and short-term methods for evaluating slow crack growth in polyethylene resins with high crack resistance," *Polym. Test.*, vol. 62, pp. 366–372, Sep. 2017.

[5] M. J. W. Kanters, K. Remerie, and L. E. Govaert, "A new protocol for accelerated screening of long-term plasticity-controlled failure of polyethylene pipe grades," *Polym. Eng. Sci.*, vol. 56, no. 6, pp. 676–688, Jun. 2016.

[6] ISO 9080:2003, *Plastics piping and ducting systems — Determination of the long-term hydrostatic strength of thermoplastics materials in pipe form by extrapolation*. ISO, Geneva, Switzerland.

[7] T. A. Osswald and G. Menges, *Materials Science of Polymers for Engineers*. Carl Hanser Verlag GmbH & Company KG, 2012.

[8] A. Chudnovsky, Y. Shulkin, D. Baron, and K. P. Lin, "New method of lifetime prediction for brittle fracture of polyethylene," *J. Appl. Polym. Sci.*, vol. 56, no. 11, pp. 1465–1478, Jun. 1995.

[9] ASTM D2837-13e1, "Standard Test Method for Obtaining Hydrostatic Design Basis for Thermoplastic Pipe Materials or Pressure Design Basis for Thermoplastic Pipe Products," ASTM International, 2013.
[10] T. J. McGrath and S. A. Mruk, "Thermoplastics Piping," in *Piping Handbook*, McGraw Hill Professional, 1999, pp. D3–D78.
[11] T. E. Nowlin, "Global Polyethylene Business Overview," in *Business and Technology of the Global Polyethylene Industry*, John Wiley & Sons, Inc., 2014, pp. 1–45.
[12] AWWA, *Pe Pipe-design and Installation (M55)*. American Water Works Association, 2011.
[13] D. B. Malpass, "Introduction to Polymers of Ethylene," in *Introduction to Industrial Polyethylene*, John Wiley & Sons, Inc., 2010, pp. 1–22.
[14] R. K. Krishnaswamy, Q. Yang, D. C. Rohlfing, M. P. McDaniel, K. C. Jayaratne, and J. E. French, "Polyethylene compositions and pipe made from same," US7589162 B2, 15-Sep-2009.
[15] R. K. Krishnaswamy, "Analysis of ductile and brittle failures from creep rupture testing of high-density polyethylene (HDPE) pipes," *Polymer*, vol. 46, no. 25, pp. 11664–11672, Nov. 2005.
[16] V. Rohatgi, Y. Inn, A. M. Sukhadia, Q. Yang, and P. J. DesLauriers, "Polymers with Improved Processability for Pipe Applications," US20160115264 A1, 28-Apr-2016.
[17] C. Li Pi Shan, J. B. P. Soares, and A. Penlidis, "HDPE/LLDPE reactor blends with bimodal microstructures—part I: mechanical properties," *Polymer*, vol. 43, no. 26, pp. 7345–7365, Dec. 2002.
[18] H.-T. Liu, C. R. Davey, and P. P. Shirodkar, "Bimodal polyethylene products from UNIPOLTM single gas phase reactor using engineered catalysts," *Macromol. Symp.*, vol. 195, no. 1, pp. 309–316, Jul. 2003.
[19] P. J. DesLauriers *et al.*, "A comparative study of multimodal vs. bimodal polyethylene pipe resins for PE-100 applications," *Polym. Eng. Sci.*, vol. 45, no. 9, pp. 1203–1213, Sep. 2005.
[20] S. Song, P. Wu, M. Ye, J. Feng, and Y. Yang, "Effect of small amount of ultra high molecular weight component on the crystallization behaviors of bimodal high density polyethylene," *Polymer*, vol. 49, no. 12, pp. 2964–2973, Jun. 2008.
[21] A. Lustiger and R. L. Markham, "Importance of tie molecules in preventing polyethylene fracture under long-term loading conditions," *Polymer*, vol. 24, no. 12, pp. 1647–1654, Dec. 1983.
[22] D. Covas, I. Stoianov, H. Ramos, N. Graham, and C. Maksimovic, "The dynamic effect of pipe-wall viscoelasticity in hydraulic transients. Part I—experimental analysis and creep characterization," *J. Hydraul. Res.*, vol. 42, no. 5, pp. 517–532, Jan. 2004.
[23] K. S. Cho, *Viscoelasticity of Polymers: Theory and Numerical Algorithms*. Springer, 2016.
[24] A. Peacock, *Handbook of Polyethylene: Structures: Properties, and Applications*. CRC Press, 2000.
[25] R. G. Matthews, A. P. Unwin, I. M. Ward, and G. Capaccio, "A comparison of the dynamic mechanical relaxation behavior of linear low- and high-density polyethylenes," *J. Macromol. Sci. Part B*, vol. 38, no. 1–2, pp. 123–143, Jan. 1999.
[26] G. M. Odegard, T. S. Gates, and H. M. Herring, "Characterization of viscoelastic properties of polymeric materials through nanoindentation," *Exp. Mech.*, vol. 45, no. 2, pp. 130–136, Apr. 2005.
[27] P. M. Wood-Adams, J. M. Dealy, A. W. deGroot, and O. D. Redwine, "Effect of Molecular Structure on the Linear Viscoelastic Behavior of Polyethylene," *Macromolecules*, vol. 33, no. 20, pp. 7489–7499, Oct. 2000.
[28] R. K. Krishnaswamy, Q. Yang, L. Fernandez-Ballester, and J. A. Kornfield, "Effect of the Distribution of Short-Chain Branches on Crystallization Kinetics and Mechanical Properties of High-Density Polyethylene," *Macromolecules*, vol. 41, no. 5, pp. 1693–1704, Mar. 2008.
[29] F. J. Stadler, J. Kaschta, and H. Münstedt, "Dynamic-mechanical behavior of polyethylenes and ethene-/α-olefin-copolymers. Part I. α'-Relaxation," *Polymer*, vol. 46, no. 23, pp. 10311–10320, Nov. 2005.

[30] N. Dusunceli and O. U. Colak, "Modelling effects of degree of crystallinity on mechanical behavior of semicrystalline polymers," *Int. J. Plast.*, vol. 24, no. 7, pp. 1224–1242, Jul. 2008.
[31] N. Dusunceli and O. U. Colak, "The effects of manufacturing techniques on viscoelastic and viscoplastic behavior of high density polyethylene (HDPE)," *Mater. Des.*, vol. 29, no. 6, pp. 1117–1124, Jan. 2008.
[32] N. Dusunceli and O. U. Colak, "High density polyethylene (HDPE): Experiments and modeling," *Mech. Time-Depend. Mater.*, vol. 10, no. 4, pp. 331–345, Dec. 2006.
[33] F. Vakili-Tahami and M. R. Adibeig, "Using developed creep constitutive model for optimum design of HDPE pipes," *Polym. Test.*, vol. 63, no. Supplement C, pp. 392–397, Oct. 2017.
[34] K. P. Menard, *Dynamic Mechanical Analysis: A Practical Introduction, Second Edition*. CRC Press, 2008.
[35] Y. P. Khanna, E. A. Turi, T. J. Taylor, V. V. Vickroy, and R. F. Abbott, "Dynamic mechanical relaxations in polyethylene," *Macromolecules*, vol. 18, no. 6, pp. 1302–1309, 1985.
[36] E. Laredo, N. Suarez, A. Bello, B. Rojas de Gáscue, M. A. Gomez, and J. M. G. Fatou, "α, β and γ relaxations of functionalized HD polyethylene: a TSDC and a mechanical study," *Polymer*, vol. 40, no. 23, pp. 6405–6416, Nov. 1999.
[37] R. Popli, M. Glotin, L. Mandelkern, and R. S. Benson, "Dynamic mechanical studies of α and β relaxations of polyethylenes," *J. Polym. Sci. Polym. Phys. Ed.*, vol. 22, no. 3, pp. 407–448, Mar. 1984.
[38] H. F. Brinson and L. C. Brinson, *Polymer Engineering Science and Viscoelasticity: An Introduction*. Springer, 2015.
[39] K. Nitta and H. Maeda, "Creep behavior of high density polyethylene under a constant true stress," *Polym. Test.*, vol. 29, no. 1, pp. 60–65, Feb. 2010.
[40] C. F. Popelar, C. H. Popelar, and V. H. Kenner, "Viscoelastic material characterization and modeling for polyethylene," *Polym. Eng. Sci.*, vol. 30, no. 10, pp. 577–586, May 1990.
[41] C. H. Popelar, V. H. Kenner, and J. P. Wooster, "An accelerated method for establishing the long term performance of polyethylene gas pipe materials," *Polym. Eng. Sci.*, vol. 31, no. 24, pp. 1693–1700, Dec. 1991.
[42] J. D. Ferry, *Viscoelastic Properties of Polymers*. John Wiley & Sons, 1980.
[43] E. Passaglia and J. R. Knox, "Viscoelastic Behavior and Time-Temperature Relationships," in *Engineering Design For Plastics*, E. Baer, Ed. 1964, pp. 143–174.
[44] R. B. Bird and O. Hassager, *Dynamics of Polymeric Liquids: Fluid mechanics*. Wiley, 1987.
[45] H. Mavridis and R. N. Shroff, "Temperature dependence of polyolefin melt rheology," *Polym. Eng. Sci.*, vol. 32, no. 23, pp. 1778–1791, Dec. 1992.
[46] S. Onogi, T. Sato, T. Asada, and Y. Fukui, "Rheo-optical studies of high polymers. XVIII. Significance of the vertical shift in the time-temperature superposition of rheo-optical and viscoelastic properties," *J. Polym. Sci. Part -2 Polym. Phys.*, vol. 8, no. 7, pp. 1211–1225, 1970.
[47] Y. Fukui, T. Sato, M. Ushirokawa, T. Asada, and S. Onogi, "Rheo-optical studies of high polymers. XVII. Time-temperature superposition of time-dependent birefringence for high-density polyethylene," *J. Polym. Sci. Part -2 Polym. Phys.*, vol. 8, no. 7, pp. 1195–1209, 1970.
[48] A. V. Tobolsky and J. R. McLoughlin, "Viscoelastic properties of crystalline polymers: polytrifluorochloroethylene," *J. Phys. Chem.*, vol. 59, no. 9, pp. 989–990, 1955.
[49] J. Wang and R. S. Porter, "On the viscosity-temperature behavior of polymer melts," *Rheol. Acta*, vol. 34, no. 5, pp. 496–503, Sep. 1995.
[50] U. Gaur and B. Wunderlich, "The glass transition temperature of polyethylene," *Macromolecules*, vol. 13, no. 2, pp. 445–446, 1980.
[51] D. G. Baird and D. I. Collias, *Polymer Processing: Principles and Design*. Wiley, 2014.
[52] I. M. Ward and J. Sweeney, *An Introduction to the Mechanical Properties of Solid Polymers*. John Wiley & Sons, 2005.
[53] R. B. Bird, W. E. Stewart, and E. N. Lightfoot, *Transport Phenomena*. John Wiley & Sons, 2007.

[54] M. Tajvidi, R. H. Falk, and J. C. Hermanson, "Time–temperature superposition principle applied to a kenaf-fiber/high-density polyethylene composite," *J. Appl. Polym. Sci.*, vol. 97, no. 5, pp. 1995–2004, Sep. 2005.
[55] N. Rudolph and T. A. Osswald, *Polymer Rheology: Fundamentals and Applications*. Carl Hanser Verlag GmbH & Company KG, 2014.
[56] T. A. Osswald and J. P. Hernández-Ortiz, *Polymer Processing: Modeling and Simulation*. Hanser Publishers, 2006.
[57] C. W. Macosko, *Rheology: principles, measurements, and applications*. VCH, 1994.
[58] F. A. Morrison, *Understanding Rheology*. Oxford University Press, 2001.
[59] J. Meissner, R. W. Garbella, and J. Hostettler, "Measuring Normal Stress Differences in Polymer Melt Shear Flow," *J. Rheol.*, vol. 33, no. 6, pp. 843–864, Aug. 1989.
[60] J. Meissner, "Experimental problems and recent results in polymer melt rheometry," *Makromol. Chem. Macromol. Symp.*, vol. 56, no. 1, pp. 25–42, Apr. 1992.
[61] K. Walters, *Rheometry*. Chapman and Hall, 1975.
[62] H. M. Laun, "Prediction of Elastic Strains of Polymer Melts in Shear and Elongation," *J. Rheol.*, vol. 30, no. 3, pp. 459–501, Jun. 1986.
[63] Z. Tadmor and C. G. Gogos, *Principles of Polymer Processing*. John Wiley & Sons, 2013.
[64] J. R. Wagner, E. M. Mount, and H. F. Giles, "50 - Pipe and Tubing Extrusion," in *Extrusion (Second Edition)*, J. R. Wagner, E. M. Mount, and H. F. Giles, Eds. Oxford: William Andrew Publishing, 2014, pp. 573–583.
[65] P. L. Maeger, V. Rohatgi, D. Hukill, N. Koganti, and B. Martinez, "Polyethylene Pipe Extrusion," in *Handbook of Industrial Polyethylene and Technology: Definitive Guide to Manufacturing, Properties, Processing, Applications and Markets*, M. A. Spalding and A. Chatterjee, Eds. John Wiley & Sons, 2017, pp. 592–602.
[66] K. Saul, G. Hiesgen, M. Moellenbeck, and C. Rauwendaal, "Automated design and optimization of cooling lines for extrusion using chillWARE cooling simulation," *AIP Conf. Proc.*, vol. 1779, no. 1, p. 030006, Oct. 2016.
[67] K. Cantor, *Blown Film Extrusion*. Hanser Publications, 2011.
[68] Y. Huang, C. R. Gentle, M. Lacey, and P. Prentice, "Analysis and improvement of die design for the processing of extruded plastic pipes," *Mater. Des.*, vol. 21, no. 5, pp. 465–475, Oct. 2000.
[69] W. Michaeli, *Extrusion dies: design and engineering computations*. Hanser, 1984.
[70] C. Rauwendaal, *Polymer Extrusion*. Carl Hanser Verlag GmbH & Company KG, 2014.
[71] J. F. T. Pittman, G. P. Whitham, and I. A. Farah, "Wall thickness uniformity in plastic pipes: Computer simulations of the effectiveness of die mandrel offsetting and pipe rotation in combatting sag," *Polym. Eng. Sci.*, vol. 35, no. 11, pp. 921–928, Jun. 1995.
[72] D. N. Githuku and A. J. Giacomin, "Simulation of Slump in Plastic Pipe Extrusion," *J. Eng. Mater. Technol.*, vol. 114, no. 1, pp. 81–83, Jan. 1992.
[73] C. Saengow, A. J. Giacomin, and C. Kolitawong, "Extruding plastic pipe from eccentric dies," *J. Non-Newton. Fluid Mech.*, vol. 223, pp. 176–199, Sep. 2015.
[74] C. Kolitawong, A. J. Giacomin, and U. Nontakaew, "Viscous dissipation in plastic pipe extrusion," *Polym. Eng. Sci.*, vol. 53, no. 10, pp. 2205–2218, Oct. 2013.
[75] C. Kolitawong and A. J. Giacomin, "Axial Flow Between Eccentric Cylinders," *Polym.-Plast. Technol. Eng.*, vol. 40, no. 3, pp. 363–384, May 2001.
[76] C. Kolitawong, N. Kananai, A. J. Giacomin, and U. Nontakaew, "Viscous dissipation of a power law fluid in axial flow between isothermal eccentric cylinders," *J. Non-Newton. Fluid Mech.*, vol. 166, no. 1–2, pp. 133–144, Jan. 2011.
[77] Y. Inn, P. J. DesLauriers, Q. Yang, A. M. Sukhadia, and D. C. Rohlfing, "Controlling Melt Fracture in Bimodal Resin Pipe," US20130319131 A1, 05-Dec-2013.

[78] M. G. Harris, "High density polyethylene melt blends for improved stress crack resistance in pipe," US6822051 B2, 23-Nov-2004.
[79] X. Guo and A. I. Isayev, "Thermal residual stresses in freely quenched slabs of semicrystalline polymers: Simulation and experiment," *J. Appl. Polym. Sci.*, vol. 75, no. 11, pp. 1404–1415, Mar. 2000.
[80] R. K. Krishnaswamy and M. J. Lamborn, "The influence of process history on the ductile failure of polyethylene pipes subject to continuous hydrostatic pressure," *Adv. Polym. Technol.*, vol. 24, no. 3, pp. 226–232, Sep. 2005.
[81] S. G. Hatzikiriakos and J. M. Dealy, "Role of slip and fracture in the oscillating flow of HDPE in a capillary," *J. Rheol.*, vol. 36, no. 5, pp. 845–884, Jul. 1992.
[82] M. Nie, Q. Wang, and S. Bai, "Morphology and property of polyethylene pipe extruded at the low mandrel rotation," *Polym. Eng. Sci.*, vol. 50, no. 9, pp. 1743–1750, Sep. 2010.
[83] M. Taherzadehboroujeni, R. Kalhor, G. B. Fahs, R. B. Moore, and S. W. Case, "Accelerated testing method to estimate the long-term hydrostatic strength of semi-crystalline plastic pipes," *Polym. Eng. Sci.*, vol. 0, no. 0.
[84] N. Sun, M. Wenzel, and A. Adams, "Morphology of high-density polyethylene pipes stored under hydrostatic pressure at elevated temperature," *Polymer*, vol. 55, no. 16, pp. 3792–3800, Aug. 2014.
[85] R. Kitamaru, F. Horii, and K. Murayama, "Phase structure of lamellar crystalline polyethylene by solid-state high-resolution carbon-13 NMR detection of the crystalline-amorphous interphase," *Macromolecules*, vol. 19, no. 3, pp. 636–643, Mar. 1986.
[86] L. Pi, X. Hu, M. Nie, and Q. Wang, "Role of Ultrahigh Molecular Weight Polyethylene during Rotation Extrusion of Polyethylene Pipe," *Ind. Eng. Chem. Res.*, vol. 53, no. 35, pp. 13828–13832, Sep. 2014.
[87] M. Nie and Q. Wang, "Control of rotation extrusion over shish-kebab crystal alignment in polyethylene pipe and its effect on the pipe's crack resistance," *J. Appl. Polym. Sci.*, vol. 128, no. 5, pp. 3149–3155, Jun. 2013.
[88] C. Kaiyuan, Z. Nanqiao, L. Bin, and W. Shengping, "Effect of vibration extrusion on the structure and properties of high-density polyethylene pipes," *Polym. Int.*, vol. 58, no. 2, pp. 117–123, Feb. 2009.

Chapter 3. Effect of High Molecular Weight Tails on the Rheology of High-Density Polyethylene for Pipes

3.1 Abstract

It is desired to understand the rheological behavior of pipe High Density Polyethylene resins, specifically when they are of bimodal molecular weight distributions but differ in the proportion of high molecular weight tails present. This is a common difference between resin grades for pipe applications and is information of interest to those who extrude these types of resins. Using the cone-and-plate and parallel-plate geometries in a rheometer allowed characterizing the rheological behavior of the materials. Through dynamic shear, steady shear, startup and cessation of flow, and jump strain tests, rheological material functions were measured for the resins to reveal the distinct differences between such materials. A higher proportion of a high molecular weight tail results in an increased zero shear-rate viscosity, a much slower relaxation of stresses and a resin that more readily deviates from linear viscoelastic behavior. The possibility of superior mechanical properties, which may come from using a resin with a higher molecular weight, needs to be balanced against more difficult processing and the possibility of higher residual stresses.

3.2 Introduction

The features of a high-density polyethylene (HDPE) resin that will determine its performance in a pipe application are density, molecular weight (MW), and molecular weight distribution (MWD). These need to strike a certain balance of good mechanical properties and ease of processing [1]. High-density polyethylene (HDPE) resins for pipes have high MWs, which make extrusion difficult compared to standard HDPE resins. For HDPE pipe resins, MWs are usually over 100,000 g/mol compared to 30,000-50,000 g/mol for HDPE resins intended for uses such as bottles or film [2], [3].

High average MWs give superior mechanical properties to manufactured parts. Longer molecules entangle with each other more readily than short molecules, creating a stronger structure with more tie-in molecules. This network allows the mechanical properties of a part like stiffness, strength and impact, to increase with the MW of the resin; however, they eventually reach an asymptote and further increases in MW do not significantly affect mechanical properties [4].

High MWs also improve melt strength. Melt strength measures the resistance of a polymer to deformation during extension [5]. Pipes are a significantly thick product and during the cooling stage, the melt may deform or sag under its own weight as it slowly cools down [6]. A high melt strength is desirable since it helps assure the dimensional stability of the pipe through manufacturing.

However, increasing MW also increases viscosity. Viscosity is proportional to the 3.4 power of MW [7], [8], and too high of a viscosity may make an extrusion process more difficult or costly in the form of excessive pressure drops and high shear stresses that compromise the equipment. The tradeoff of working with a high viscosity resin may come without a significant improvement of the mechanical properties of the finished part [4].

The challenge of resin manufacturers is to balance the high viscosity of the resin with the high mechanical properties pipe need. The current strategy adopted by HDPE resin manufacturers to improve processability in pipe extrusion without sacrificing a great deal in mechanical properties, has been to give resins a bimodal MWD [9]. Resin manufacturers can tailor the proportion between the peaks in said bimodal distributions, by modifying the reaction conditions, along the use of novel catalysts or reactor design. Figure 3.1 explains the reason for this approach. Having high MW molecules gives good mechanical properties while keeping some low MW molecules will allow for overall lower viscosity of the resin [10], [11].

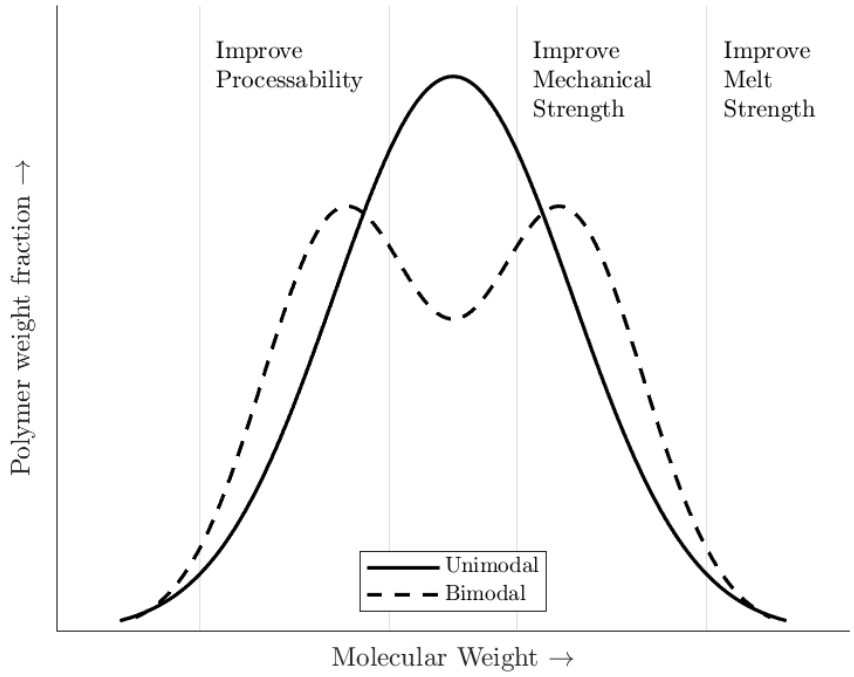

Figure 3.1. Concept of the role played by the chain lengths in a given HDPE MWD. Adapted from Liu et al [9]

The resins chosen for this study, resin A and resin B from LyondellBasell, both have bimodal MWD but differ between the proportions of each MW peak. This enables isolating the effect of the peaks in the MWD. MW peaks in a bimodal MWD affect the rheology of the resins and this paper studies them because they will directly influence resin performance in the extrusion process.

Both resins also meet the same specification for pipe performance, so they have similar mechanical properties. The relevant classification comes from ASTM D2837, which classifies pipes made from certain materials according to their resistance to failure at classified levels of hoop stresses [12]. This test standardizes the maximum allowable pressure or flow rate that a pipe can handle if not disturbed by external events such as an impact. Meeting a high classification in this standard allows pipe manufacturers to produce a thinner pipe, compared to a lower-rated resin for the same application, saving weight and allowing for faster processing [13].

For two resins made in the same reactor and with the same catalyst, this study tries to find distinct differences in the rheology of the resins. Measurements in dynamic shear, steady shear, startup of shear and cessation of shear flow, and jump strain allow characterizing the resins. The influence of properties like zero shear-rate viscosity (η_0), the first normal stress difference (N_1) and stress relaxation will reveal if the melt rheology differences influence the extrusion process itself, or the finished product, for instance, via residual stresses.

3.3 Experimental

3.3.1 Resins

Two HDPE resins made available by LyondellBasell, resin A and resin B, were used. To produce them, polymerization took place in a slurry process in the presence of a Ziegler Catalyst. Two polymerization reactors produce the resins, employing a process in series where product from the first reactor goes into the second reactor. Each resin is the intimate mixture of the product of two reactors in series and are bimodal because each reactor produces a material with different MW and MWD [14], [15].

3.3.2 MW Characteristics

A PolymerChar GPC-IR instrument measured the MW and MWD of the HDPE resins. A narrow MWD polystyrene provided a known MWD for calibration purposes. The samples were dissolved in 1,2,4-trichlorobenzene and continuously mixed until injected in the GPC equipment.

3.3.3 Melt Properties

An ARES G2 rheometer, with either parallel-plate fixtures or cone-and-plate fixtures, 25 mm in diameter, was used to carry out the rheological tests. Namely, small amplitude oscillatory shear (SAOS), simple shear in the steady mode, startup of flow or cessation of flow, and the jump strain

characterization. For SAOS and simple shear in the steady mode, the temperatures analyzed were 200, 220, and 240 °C as these are common processing temperatures for pipe manufacturing [6], [16], [17]. The frequency sweeps ran from 0.1 to 100 rad/s at a strain of 5%. Simple steady shear ran from 10^{-3} to 0.1 s^{-1} in order to have some overlap with the oscillatory frequencies. Startup and cessation of flow, and jump strain, were analyzed at 200 °C as the authors received and studied pipes produced at this temperature. For startup of flow, the shear rate was 0.1 s^{-1}. For jump strain, strains were 20, 40, 80, 160, 320 and 640%.

Rheological testing is used to characterize the melt response of both resins. Frequency sweeps provide complex viscosity information, which gives shear viscosity according to the Cox-Merz rule [7]. To determine the applicability of the Cox-Merz rule, steady simple shear tests at low shear rates allow direct measurement of shear viscosity at an equivalent frequency. The small amplitude oscillatory shear tests will also allow determining the shifting behavior for the rheological properties of the melt.

All samples were compression-molded disks made directly from resin pellets. For the case of a high viscosity resin, it is disadvantageous to mold the disks directly in the fixtures of the ARES G2. The ARES G2 maximum squeezing force compresses the pellets slowly and may not remove all the air between the pellets getting to the desired gap. If it reaches the desired gap, it is likely to leave weld marks at the boundaries of the molten pellets if it can compress the disk.

For the startup and cessation of flow, the rheometer measures the samples' shear and normal stresses for pre-defined periods, alternating between simple shear and having no flow. The test reveals the development of stresses in the resin as a function of time. Specifically, it lets us know how easily the resins de-entangle when they flow and how long it takes to re-entangle after the flow has stopped. This reveals their tendency to keep residual stresses.

For jump strain, the rheometer instantaneously deforms the sample a set amount and measures the relaxation of stresses as a function of time. With a low enough deformation, the polymer stays within the linear viscoelastic region (LVR) and its molecules tend to return to their initial position, always with the same modulus. With increasing strain, the deformation becomes permanent, but the resin recovers from the strained state more rapidly, compared to low deformations, causing the relaxation modulus to be lower than the LVR modulus [8].

3.4 Results and Discussion

3.4.1 MW Results

Figure 3.2 shows the MWD of resin A and resin B. The bimodal nature of both resins is clear. A summary of key results is in Table 1. The number average (M_n) and weight average (M_w) MW reflect that the distribution for Resin A skews towards having more high MW molecules than Resin B. The polidispersity index or the ratio between Mw and Mn is similar for both resins.

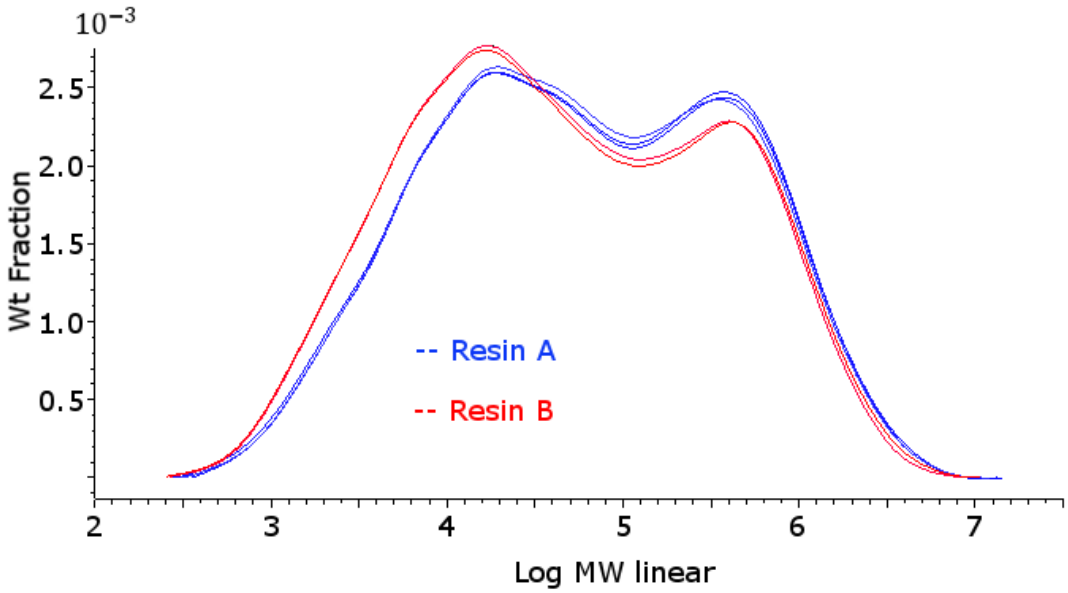

Figure 3.2. GPC results with conventional MWD plots for resin A and resin B.

	Resin A	Resin B
$\overline{M_n}$ (g/mol)	$11.5 \cdot 10^3$	$9.51 \cdot 10^3$
$\overline{M_w}$ (g/mol)	$2.96 \cdot 10^5$	$2.51 \cdot 10^5$
$\overline{M_w/M_n}$	25.7	26.4

Table 1. Qualitative results for the molecular weight of Resin A and Resin B

3.4.2 Shear Viscosity and Models

Figure 3.3 shows the viscosity master curves for both resins characterized in this study. The Bird-Carreau-Yasuda model, shown in eq. (6), fits the viscosity of the resins. Parameters were obtained using the Excel solver and the results for the model parameters are in Table 2. Figure 3.3 shows how both resins tend towards a constant zero shear-rate viscosity (η_0) in the low shear-rate regions. The main difference between the parameters of the Bird-Carreau-Yasuda model for both resins is their η_0 value. This was expected from the difference in the molecular weight of the resins. The other parameters (λ, n and a), do not show much difference. All error bars in this paper represent 95% t-student confidence intervals. For viscosity, the error bars do not overlap, so the values are statistically different.

$$\eta = \eta_0[1 + (\lambda\dot{\gamma})^a]^{(n-1)/a} \tag{6}$$

Table 2. Bird-Carreau-Yasuda parameters for Resin A and Resin B

Parameter	Resin A	Resin B
η_0	303400	217690
λ	6.29	5.03
n	0.27	0.26
a	0.41	0.40

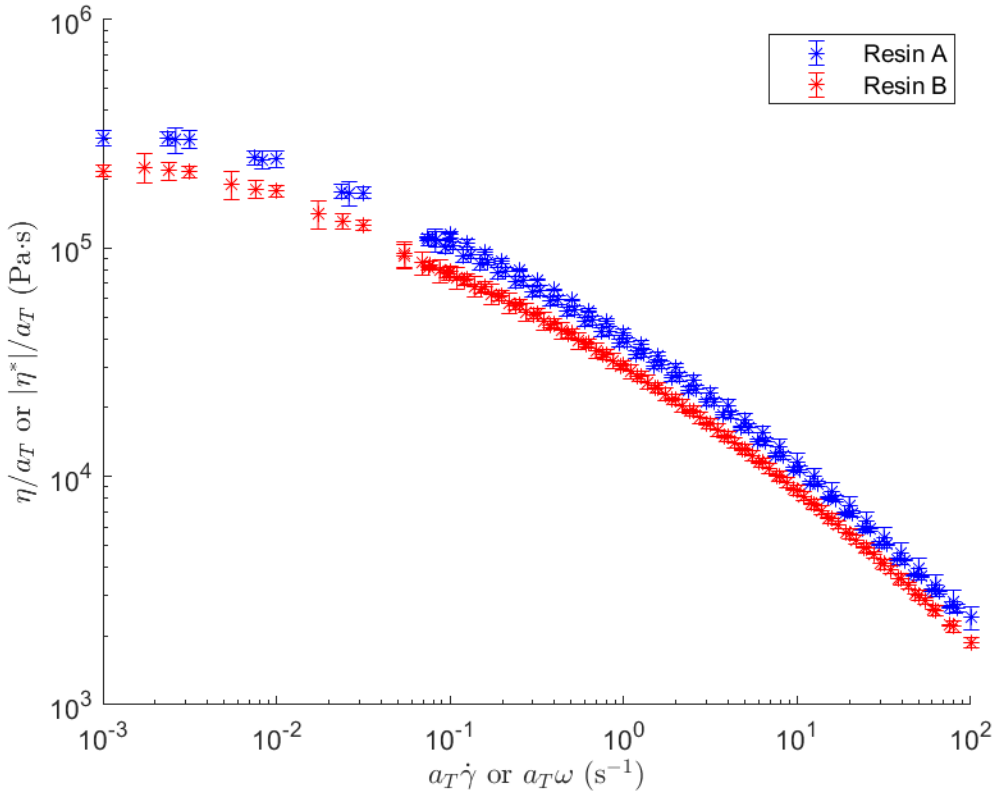

Figure 3.3. Viscosity master curves at T = 200 °C for Resin A and Resin B.

An Arrhenius model allowed modeling of the shift factor, a_T, values as a function of temperature. Eq. (7) shows a_T as an Arrhenius model and the definition of a_T as the ratio of η_0 values. The a_T values allow shifting viscoelastic data from one temperature to another. The values of ($\Delta H/R$) are 1837 and 3538 K^{-1} for Resin A and Resin B respectively, which unexpectedly means the activation energy for Resin A is much lower than that of Resin B. This makes processing Resin A different from Resin B as increasing temperature in the extruder and die will not give a significantly less viscous polymer, while viscosity may affect sagging during the cooling portion of the process. Both values are within the usual order of magnitude expected for an HDPE resin [7].

$$a_T = \frac{\eta_0(T)}{\eta_0(T_0)} = \exp\left[\frac{\Delta H}{R}\left(\frac{1}{T} - \frac{1}{T_0}\right)\right] \tag{7}$$

3.4.3 First Normal Stress Difference

In Figure 3.4 is shown the results of estimating the first normal stress difference, N_1, using SAOS data and Laun's rule. Resin A shows a higher N_1 than Resin B, a reasonable result, considering its higher MW. However, the difference between both resins is not as large as expected from the difference in the viscosity of the resins. Because η_0 is proportional to the 3.4 power of MW and N_1 with the 6.8 power [7], the difference should be about double, but it is about the same.

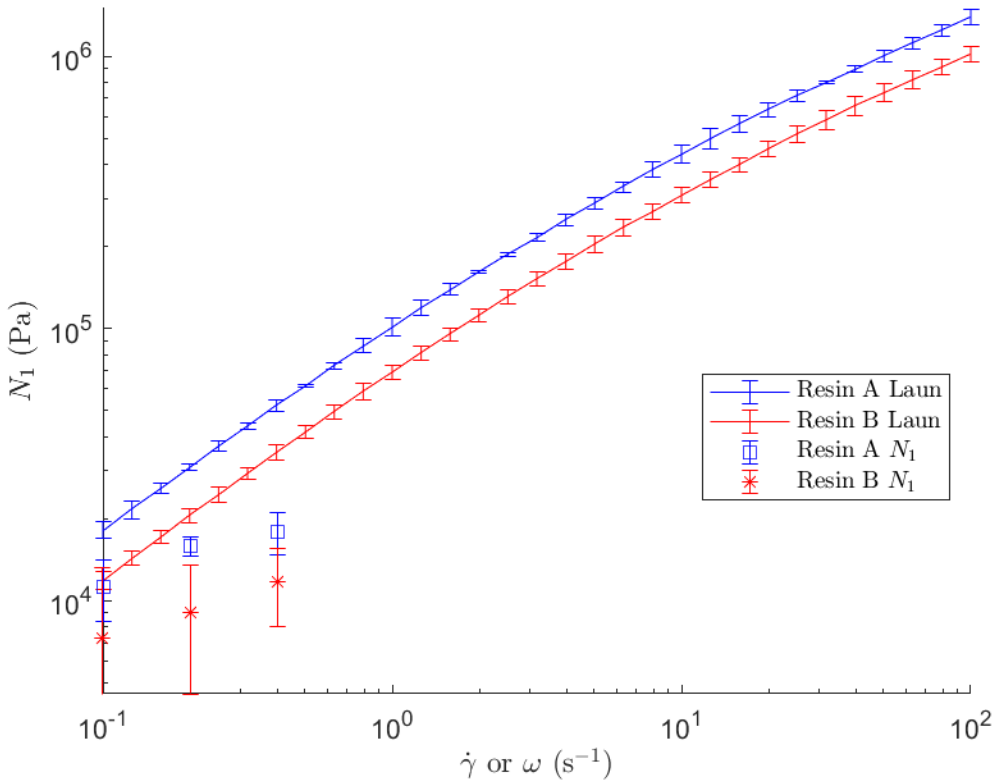

Figure 3.4. N1 from Laun's rule and from steady shear measurements. Temperature 200 °C

To measure the normal stress values in the shear mode, resin disks were subjected to steady shear, and then an average of the measurement was taken after the overshoot hump in normal stress occurs. However, the measurements showed lots of noise. See section 3.4.4 for more details. At higher

shear rates, inertia took over and the resin would exit the fixtures, giving an artificially lower value for N_1. At lower shear rates, the normal force signal was low and had significant noise. This may have happened as well to the measurements in the plot, however, in a small quantity not readily clear to the naked eye.

Resin A showed a higher N_1 Resin B in the direct shear measurements, but the values are consistently lower than predicted by Laun's rule from SAOS data. The values for both resins follow the same trend, and unlike the viscosity master curves in the previous section, did not merge and become more similar when shear rate increases or decreases.

3.4.4 Stress Relaxation

Figure 3.5 shows the results from a startup and cessation of flow test. The samples alternate between flowing and staying stationary. Flow would last 150 seconds and the stationary mode for decreasing amounts of time starting with 120 seconds. The flow portions of Figure 3.5 have a shear-rate of 0.1 s^{-1}. Similar behavior was observed for shear-rates of 0.05 and 0.2 s^{-1} and are reported in the appendix.

Shear stress is higher for Resin A than Resin B. After an initial overshoot, it stabilizes,, but over the whole experiment it slowly trends downwards. This is may be due to edge fracture. Edge fracture is a product of high normal stress differences [18], [19]. According to Tanner and Keentok [20], the critical normal stress value for polyethylene is $N_{1,c} = 4000$ Pa, which are below the values for this study. As the edge of the sample fractures inwards, the flow lines in the geometry change ending in a lower measured torque.

There is overshoot in all the startup of flow parts of the test, but the downward trend continues after the overshoot is over and picks up where it left off. During the cessation of flow portions,

shear stresses relax, but they do not fully dissipate after two minutes. In extended cessation of flow tests, over 10 minutes, the shear stresses did not dissipate fully. Among other reasons, this contributes to the pipes keeping residual stresses during the cooling portion of manufacturing [21], [22].

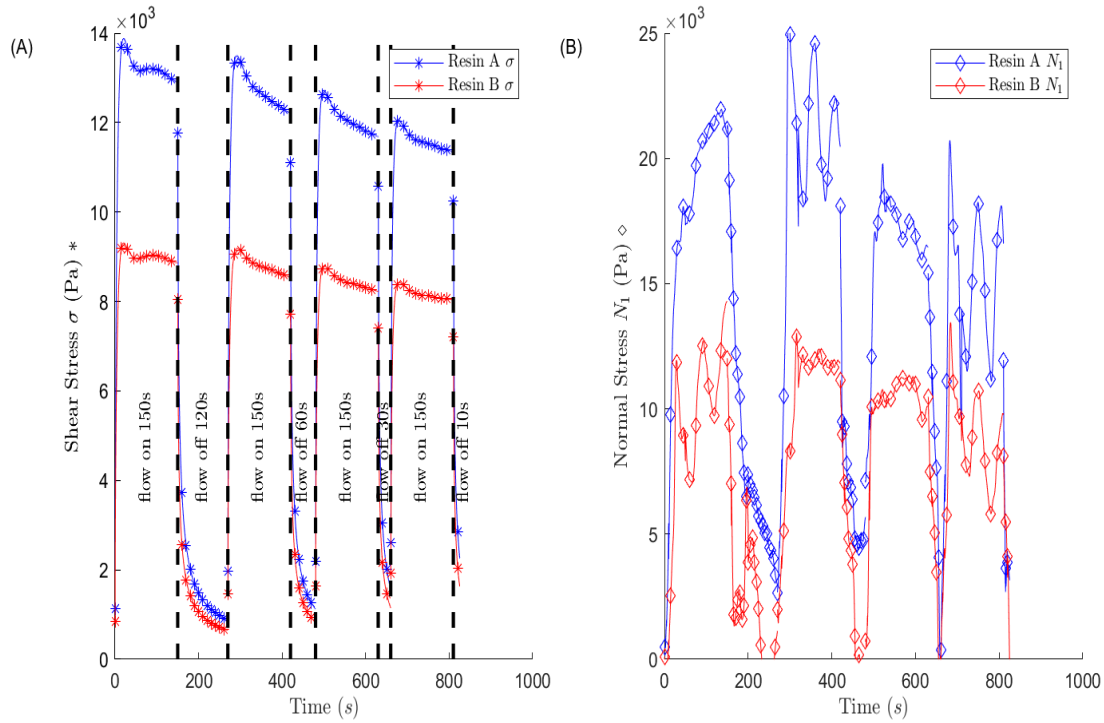

Figure 3.5. Startup and cessation of flow. (A) Shear stress vs time. Vertical lines divide time intervals between flow and no-flow. (B) Normal stress vs time. Flow was on for 150 seconds and then off for decreasing amounts of time. Temperature 200 °C and shear rate 0.1 s^{-1}

A more pronounced overshoot occurs when cessation of flow is longer. With longer cessation of flow times, molecules have more opportunities to re-entangle and stress to relax. The overshoot in shear stress comes from the initial de-entanglement needed for the molecules to flow, and after an initial barrier breaks, flow continues without needing as much stress.

N_1 measurements show significant noise for both resins. However, this shear rate shows no overshoot. Walters reports that in general, overshoot in N1 shows up after the one in shear stress, with a less pronounced peak [23]. Still, Resin A displays higher values of N_1 than Resin B. Despite the

noise, and similar to shear stress measurements, after an initial increase in N1 values with the startup of flow, N_1 trends towards lower values. After cessation of flow has taken place, N_1 values recover their trend downwards. During cessation of flow, N1values do not dissipate to zero, but significant residual normal stresses remain, similar to shear stress. In an extrusion case, this would also contribute to frozen in residual stresses.

3.4.5 Jump Strain

Figure 3.6 shows the stress relaxation modulus of Resin A and Resin B. In this test, the rheometer measures relaxation modulus as a function of time and strain ($G(t,\gamma_0)$). At infinitesimal values of strain, the relaxation modulus is independent of strain ($G(t)$). The SAOS measurements allow obtaining $G(t)$ after fitting the data to a Prony series following the procedure from Brinson [24]. $G(t)$ is higher for the higher MW resin.

The functions $G(t,\gamma_0)$ in Figure 3.6 show different behavior at low and high strains. At low deformations, the relaxation modulus is equivalent to $G(t)$. At high strains, after 80%, the deviations from $G(t)$ become more significant and the linear viscoelastic relaxation modulus is no longer a good approximation. The stress relaxation modulus can be factored as a function of only time and only strain as $G(t,\gamma_0) = G(t)\ \phi_1(\gamma_0)$.

The memory function, or the derivative of $-G(t,\gamma_0)$ respect time, behaves similar to the relaxation modulus. When strains are low, the memory function of Resin A is higher than Resin B, but that reverses when strains are high. This suggests that the memory function is also separable from strain. The resins display different behavior as Resin A has higher modulus than Resin B when strains are low. But Resin A has lower modulus than Resin B when strains are high.

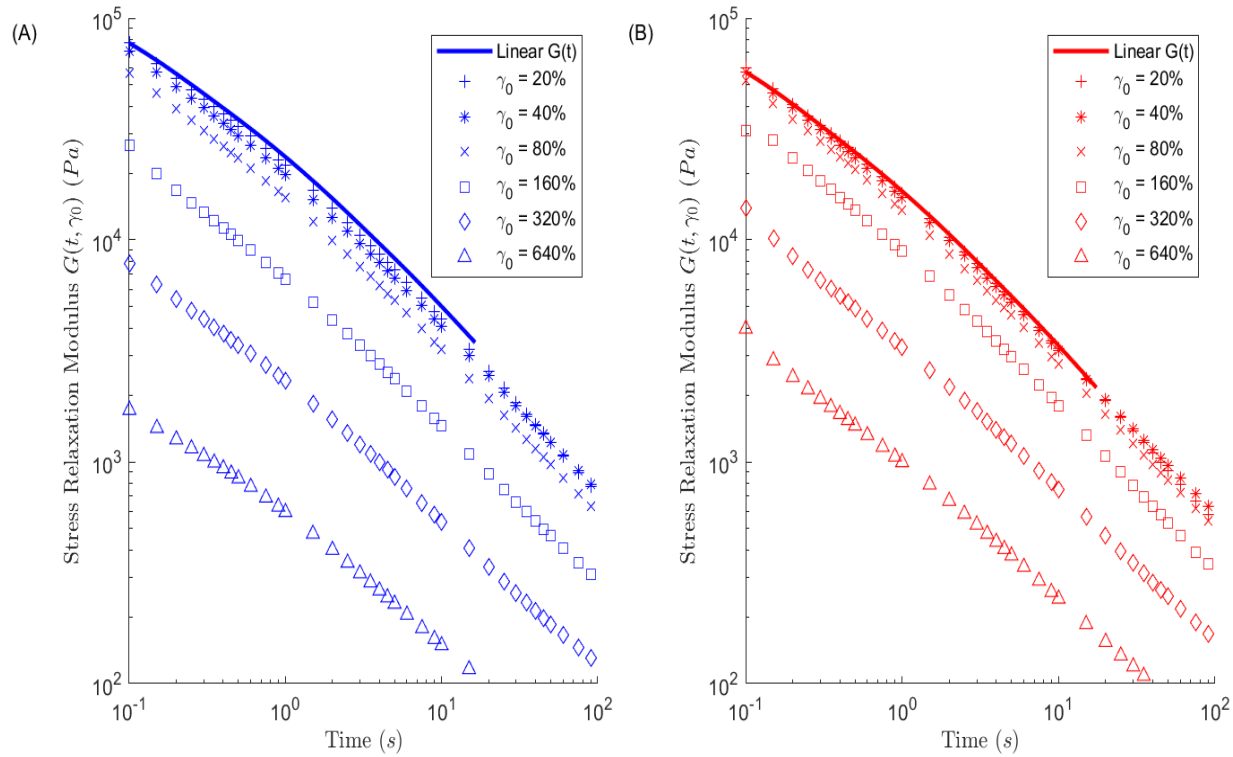

Figure 3.6. Stress relaxation modulus for (A) Resin A and (B) Resin B at a temperature of 200 °C

The Wagner Model allows comparing the strain dependence of both resins. It can also be used to predict the behavior of melts when strains are significant and no longer in the linear viscoelastic region [25]. The Wagner model relates the ratio between the relaxation modulus as a function of time and strain to the linear viscoelastic relaxation modulus. This is the damping function ϕ_1, shown in eq. (8), which states the evolution of fluid's memory due to past events [8]. A high beta parameter is a sign of a polymer that will quickly deviate from ideal linear viscoelastic behavior.

$$\phi_1(I_1, I_2) = e^{-\beta|\gamma_{yx}|} \tag{8}$$

Figure 3.7 shows the damping function for both resins. Given that the damping values are linear in a semi-log plot, the Wagner model fits the data well. The beta values are 0.617 and 0.415 for Resin A and Resin B, respectively. Resin A dampens much more readily than Resin B, and it departs

the linear viscoelastic region more readily. This may balance some of the difficulty in extrusion, as large deformations readily end in a melt that does not have a high modulus for the high MW material.

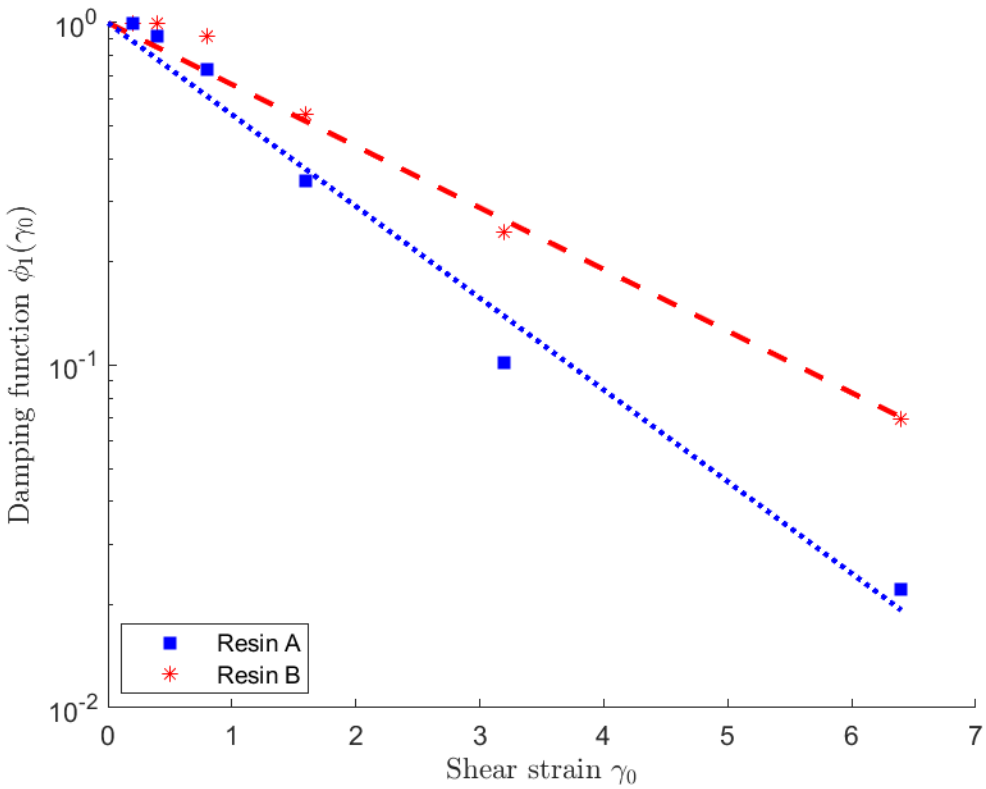

Figure 3.7. Damping function for Resin A and Resin B at a temperature of 200 °C

3.5 Conclusions

The more pronounced high MW tail of resin A compared to resin Baffects the rheological properties of the resin. It affects properties in the low shear-rate regions, as the relatively low probing that occurs at low shear rates reveals more about the molecular characteristics of a particular resin, where the long range motion of the molecules is not important.

The higher MW resin has various distinct rheological properties. As expected, a higher η_0. N_1 values are higher, both those predicted by Laun's rule and from direct steady shear measurements. Jump strain showed that the strain dependence of the relaxation modulus and memory function are

separable from time. The damping function of the higher MW decreases from a value of one more rapidly when strain increases, which means it deviates more readily from ideal linear viscoelastic behavior.

The startup and cessation of flow reveals that significant stresses, both shear and normal, remain in both resins after a few minutes at high temperatures. 200 °C is typical of pipe processing conditions and those significant remaining stresses cannot dissipate during the cooling process, which will freeze significant residual stresses into the finished product.

3.6 Acknowledgments

The authors gratefully acknowledge the materials and financial support provided by Lyondell-Basell.

References

[1] AWWA, *Pe Pipe-design and Installation (M55)*. American Water Works Association, 2011.
[2] R. K. Krishnaswamy, "Analysis of ductile and brittle failures from creep rupture testing of high-density polyethylene (HDPE) pipes," *Polymer*, vol. 46, no. 25, pp. 11664–11672, Nov. 2005.
[3] T. J. McGrath and S. A. Mruk, "Thermoplastics Piping," in *Piping Handbook*, McGraw Hill Professional, 1999, pp. D3–D78.
[4] T. A. Osswald and G. Menges, *Materials Science of Polymers for Engineers*. Carl Hanser Verlag GmbH & Company KG, 2012.
[5] H. C. Lau, S. N. Bhattacharya, and G. J. Field, "Melt strength of polypropylene: Its relevance to thermoforming," *Polym. Eng. Sci.*, vol. 38, no. 11, pp. 1915–1923, 1998.
[6] P. Poungthong, C. Kolitawong, C. Saengow, and A. J. Giacomin, "Plastic pipe solidification in extrusion," *J. Polym. Eng.*, vol. 0, no. 0, 2018.
[7] D. G. Baird and D. I. Collias, *Polymer Processing: Principles and Design*. Wiley, 2014.
[8] R. B. Bird and O. Hassager, *Dynamics of Polymeric Liquids: Fluid mechanics*. Wiley, 1987.
[9] H.-T. Liu, C. R. Davey, and P. P. Shirodkar, "Bimodal polyethylene products from UNIPOLTM single gas phase reactor using engineered catalysts," *Macromol. Symp.*, vol. 195, no. 1, pp. 309–316, Jul. 2003.
[10] V. Rohatgi, Y. Inn, A. M. Sukhadia, Q. Yang, and P. J. DesLauriers, "Polymers with Improved Processability for Pipe Applications," US20160115264 A1, 28-Apr-2016.
[11] C. Li Pi Shan, J. B. P. Soares, and A. Penlidis, "HDPE/LLDPE reactor blends with bimodal microstructures—part I: mechanical properties," *Polymer*, vol. 43, no. 26, pp. 7345–7365, Dec. 2002.
[12] R. Kalhor, "Accelerated Testing Method to Estimate the Lifetime of Polyethylene Pipes," Thesis, Virginia Tech, 2017.

[13] R. Gard, C. Stamm, and H. Schmidt, "PP-RCT: a new material class for plumbing and heating applications," in *Proceedings of Plastics Pipes XIII, Washington DC, USA*, 2006.
[14] S. Joseph, "Multimodal polyethylene pipe resins and process," US9249286 B2, 02-Feb-2016.
[15] H. Mavridis, C. D. Lee, S. W. Horwatt, and S. D. Mehta, "Low-sag polyethylene pipes and methods thereof," US20180030252A1, 01-Feb-2018.
[16] J. M. Nóbrega, O. S. Carneiro, J. A. Covas, F. T. Pinho, and P. J. Oliveira, "Design of calibrators for extruded profiles. Part I: Modeling the thermal interchanges," *Polym. Eng. Sci.*, vol. 44, no. 12, pp. 2216–2228, Dec. 2004.
[17] D. Tátraaljai, M. Vámos, Á. Orbán-Mester, P. Staniek, E. Földes, and B. Pukánszky, "Performance of PE pipes under extractive conditions: Effect of the additive package and processing," *Polym. Degrad. Stab.*, vol. 99, pp. 196–203, Jan. 2014.
[18] Hutton J. F. and Sugden Theodore Morris, "The fracture of liquids in shear: the effects of size and shape," *Proc. R. Soc. Lond. Ser. Math. Phys. Sci.*, vol. 287, no. 1409, pp. 222–239, Aug. 1965.
[19] M. Keentok and S.-C. Xue, "Edge fracture in cone-plate and parallel plate flows," *Rheol. Acta*, vol. 38, no. 4, pp. 321–348, Oct. 1999.
[20] R. I. Tanner and M. Keentok, "Shear Fracture in Cone-Plate Rheometry," *J. Rheol.*, vol. 27, no. 1, pp. 47–57, Feb. 1983.
[21] J. Poduška *et al.*, "Residual stress in polyethylene pipes," *Polym. Test.*, vol. 54, pp. 288–295, Sep. 2016.
[22] J. Kim, J. Yoo, and Y. Oh, "A study on residual stress mitigation of the HDPE pipe for various annealing conditions," *J. Mech. Sci. Technol. Heidelb.*, vol. 29, no. 3, pp. 1065–1073, Mar. 2015.
[23] K. Walters, *Rheometry*. Chapman and Hall, 1975.
[24] H. F. Brinson and L. C. Brinson, *Polymer Engineering Science and Viscoelasticity: An Introduction*. Springer, 2015.
[25] A. J. Giacomin, R. S. Jeyaseelan, T. Samurkas, and J. M. Dealy, "Validity of separable BKZ model for large amplitude oscillatory shear," *J. Rheol.*, vol. 37, no. 5, pp. 811–826, Sep. 1993.

Chapter 4. Viscoelastic Characterization of High Density Polyethylene Pipes

4.1 Abstract

High density polyethylene pipes are expected to last 50 or more years once they are in use. The flow of a fluid through a pipe causes constant hoop stress, which eventually makes the pipe fail. Tests that characterize the service lifetime of pipes take long times and are expensive. The present work studies the linear viscoelastic response of pipes under different loading geometries: torsion and three-point bending. Dynamical mechanical analysis allows characterizing the viscoelastic properties of the pipe and creep testing confirms that shift factors work for independently measured viscoelastic properties. For the characterized pipes, one hour of testing at 80 °C is equivalent to four months of testing at 25 °C. This work presents first steps into shifting short-term test data of high density polyethylene pipes into predictions of their service lifetime.

4.2 Introduction

High density polyethylene (HDPE) pipes usually have to last 50 years or more after installation. The failure of plastic pipes under constant stress is a time dependent event. Standards ASTM D2837 and ISO 9080 provide a means towards estimating the maximum allowable stresses for a pipe. During testing, pipes undergo constant pressure over one year to gather failure data at multiple temperatures. This allows predicting failure by extrapolating from the time range tested, but strictly interpolating between the temperatures used [1], [2]. These tests are expensive and time consuming.

It is the goal of this study to find the degree of time shifting from changing the temperature of HDPE pipes. The authors received pipes made from two resins and two different processing conditions, so it is of interest to compare their viscoelastic properties and check whether DMA and creep

data allows one to distinguish between them. Furthermore, it is of interest to measure their viscoelastic properties under different loading geometries, torsion and three point bending, to compare if they require the same degree of shifting.

It is of interest to test the pipes directly to account for any effects that come from the extrusion process. This allows comparing materials as well. Dynamic mechanical analysis (DMA) and creep testing allow measuring their relevant viscoelastic properties. DMA gives the storage and loss modulus (G' and G") of a material as a function of frequency for an input sinusoidal strain. Creep gives deformation as a function of time for constant stress. With strips cut out along the length of the pipe, a three point bending configuration tests the crystalline structure strictly along the length of the pipe, while a torsional configuration probes along the tangential direction and the axial direction of the pipe [3].

High temperatures speed up the creep failure of viscoelastic materials. The challenge is to relate the results from high temperature testing to a reference temperature. For thermo-rheological simple materials, the solution is to use the classical time-temperature superposition (TTS) principle, where data shifts along the time axis (horizontal shifting) to produce smooth master curves. The amount of shifting gives a shifting function. Every viscoelastic property must shift with the same shifting function [4].

Below its melting temperature, classical TTS will not produce continuous smooth master curves for all viscoelastic properties of HDPE. HDPE needs a vertical shift besides the classical horizontal shift [5]–[8]. Some authors attribute this need to changes in crystallinity as a function of temperature [5] [9]. Others attribute it to the changed mobility of the chains, which results in uncoordinated motions of the crystalline lattice and deformation of the amorphous regions as a function of temperature [4], [8].

Errors accumulate when a vertical shift is required but not included. Figure 4.1 shows a sample master curve at a given temperature and data measured at temperature T_1 higher than the reference temperature. No amount of horizontal shifting allows it to overlap completely with the master curve; there is always a compliance and time error. Adding vertical shifting results in complete overlap of the T_1 data with the true master curve at the reference temperature.

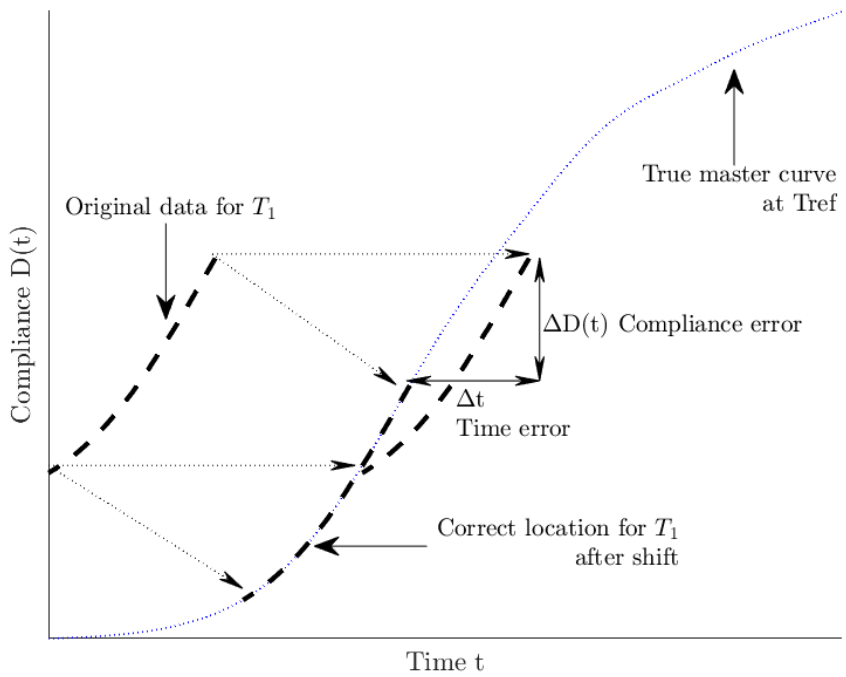

Figure 4.1. Potential error in a master curve from not including vertical shifting. Adapted from Brinson et al [10]

Several authors have needed to use vertical shifting to produce coherent master curves from thermoplastics. Popelar tested HDPE dog-bones for stress relaxation and established the vertical shifting required to get master curves [5]. He tested several conventional HDPE resins and found a TTS equivalence where one hour of testing at 80 °C was equivalent to 16 days at 25 °C. Another example comes from Fukui, who measured strain-optical coefficients of HDPE and developed master curves which required a vertical shift [7]. Mavridis found that LDPE melts required vertical shifting to produce master curves from viscosity data [11].

4.3 Temperature Dependence and Double Shifting

Transient tests that measure creep compliance or relaxation modulus at several temperatures do not provide a way to find vertical and shift factors independently. DMA data enables a way to determine whether a polymer requires vertical shifting. Let $H(\tau, T)$ be the relaxation spectrum of a viscoelastic material. Some viscoelastic properties such as G' and G" (equations (4.3.1) and (4.3.2)), measured during DMA, are by definition a function of $H(\tau, T)$ [4]:

$$G'(\omega, T) = \int_{-\infty}^{\infty} H(\tau, T) \frac{(\omega\tau)^2}{1 + (\omega\tau)^2} d\ln\tau \tag{4.3.1}$$

$$G''(\omega, T) = \int_{-\infty}^{\infty} H(\tau, T) \frac{(\omega\tau)}{1 + (\omega\tau)^2} d\ln\tau \tag{4.3.2}$$

The main assumption to shift viscoelastic data is that the relaxation spectrum shifts according to equation (4.3.3). The shift factor, a_T, reflects the temperature dependence of relaxation times and b_T reflects the temperature dependence of the viscoelastic property itself [5], [11]. Note that all visco-elastic properties will have the same shift factors [4], [11] and the case $b_T = 1$ gives conventional TTS shifting back. A common DMA plot of G' as a function of frequency would have to shift then as equation (4.3.4):

$$b_T H(\tau / a_T, T) = H(\tau_0, T_0) \tag{4.3.3}$$

$$b_T G'(a_T \omega, T) = G'(\omega, T_0) \tag{4.3.4}$$

It is inconvenient to shift any viscoelastic property horizontally and vertically simultaneously. However, the ratio between G" and G', tan δ, would require only horizontal shifting with temperature

changes. A convenient way to present DMA data for shifting is as presented in equations (4.3.5) and (4.3.6) as this allows getting the horizontal and vertical shift factors independently:

$$G'(T, \tan\delta) = \frac{1}{b_T} G'(T_0, \tan\delta) \tag{4.3.5}$$

$$\omega(T, \tan\delta) = \frac{1}{a_T} \omega(T_0, \tan\delta) \tag{4.3.6}$$

4.4 Experimental

4.4.1 Materials

Strips of dimensions 50x12x3.5 mm were cut out of pipes manufactured by LyondellBasell. The pipes had an outer diameter of 33 mm and a standard dimension ratio of 11. The extrusion process used two different dies for the production of the pipes: die "OD" had an inner diameter of 1.2" and an outer diameter of 1.43"; die "ND" had an inner diameter of 1.32" and an outer diameter of 1.75". It was of interest whether the change in die dimensions influenced the properties of the finished product.

All pipes received were produced using Resin A and Resin B. The resins were produced in a slurry process using a Ziegler catalyst, had a bimodal molecular weight distribution, and are designed for the production of pipe [12], [13]. Resin A has a higher molecular weight than Resin B, though both have similar polydispersity indices. For more details, see section 4.4.1. Pipes made from these resins resist hoops stresses of 1600 psi at 23 °C for 50 years according to ASTM D2837. Taherzadehbor-oujeni et al studied the morphology of these pipes, finding no significant orientation or gradients of crystallinity in the radial direction [14].

Flat samples were compression molded from resin pellets. The mold's dimensions were 50x200 mm and filled to a thickness of 3.5mm. A temperature of 250 °C melted the pellets for 5 minutes and then cooled to room temperature before cutting to dimensions similar to the strips cut out of pipe.

4.4.2 DMA Data

To produce master curves, an ARES G2 rheometer measured DMA data using torsional and three point bending fixtures. See Figure 4.2 for the torsional geometry setup. The frequencies examined ranged from 1.0 to 100 rad/s, at a strain of 5%, with temperatures from 25 to 80 °C in increments of 5 °C for the torsional fixture. The tree point bending fixture imposed a deformation of 0.5%. The data collected was G', G" and tan δ for each frequency sweep. The selected maximum of 80 °C was because of the occurrence of significant changes in the crystalline structure above this temperature [8]. All tests were run three times, the results averaged, and all error bars represent 95 % t-student confidence intervals.

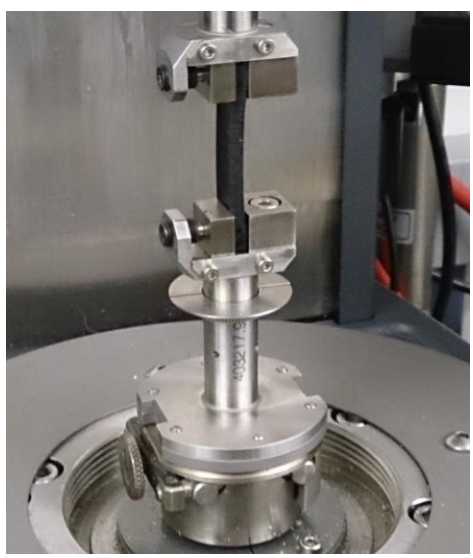

Figure 4.2. Torsional geometry used for DMA and Creep

4.4.3 Creep

An ARES G2 rheometer measured creep using torsional and three point bending fixtures. The rheometer held a constant stress of 1MPa at 25, 40, 60 and 80 °C for one hour. This stress produced modulus values within the linear viscoelastic region of the pipes, as sample tests were also run at 0.5 MPa finding that the creep compliance was the same as 1.0 MPa, a result expected within the linear viscoelastic region.

4.5 Results and Discussion

4.5.1 Shifting Procedure

The plots in Figure 4.3 illustrate the shifting performed on the collected DMA data using the torsional fixtures. Figure 4.3 (A) shows that tan δ requires only horizontal shifting to produce a master curve as a function frequency. An appropriate set of shift factors allowed producing a smooth master curve at 25 °C of tan δ vs frequency as shown in Figure 4.3 (B). Figure 4.3 (C) shows that G' requires only vertical shifting to produce a master curve as a function of tan δ. A different set of shift factors allowed shifting the data to a smooth master curve at 25 °C of G' vs tan δ as shown in Figure 4.3 (D). The associated shift factor plots are in section 4.5.5.

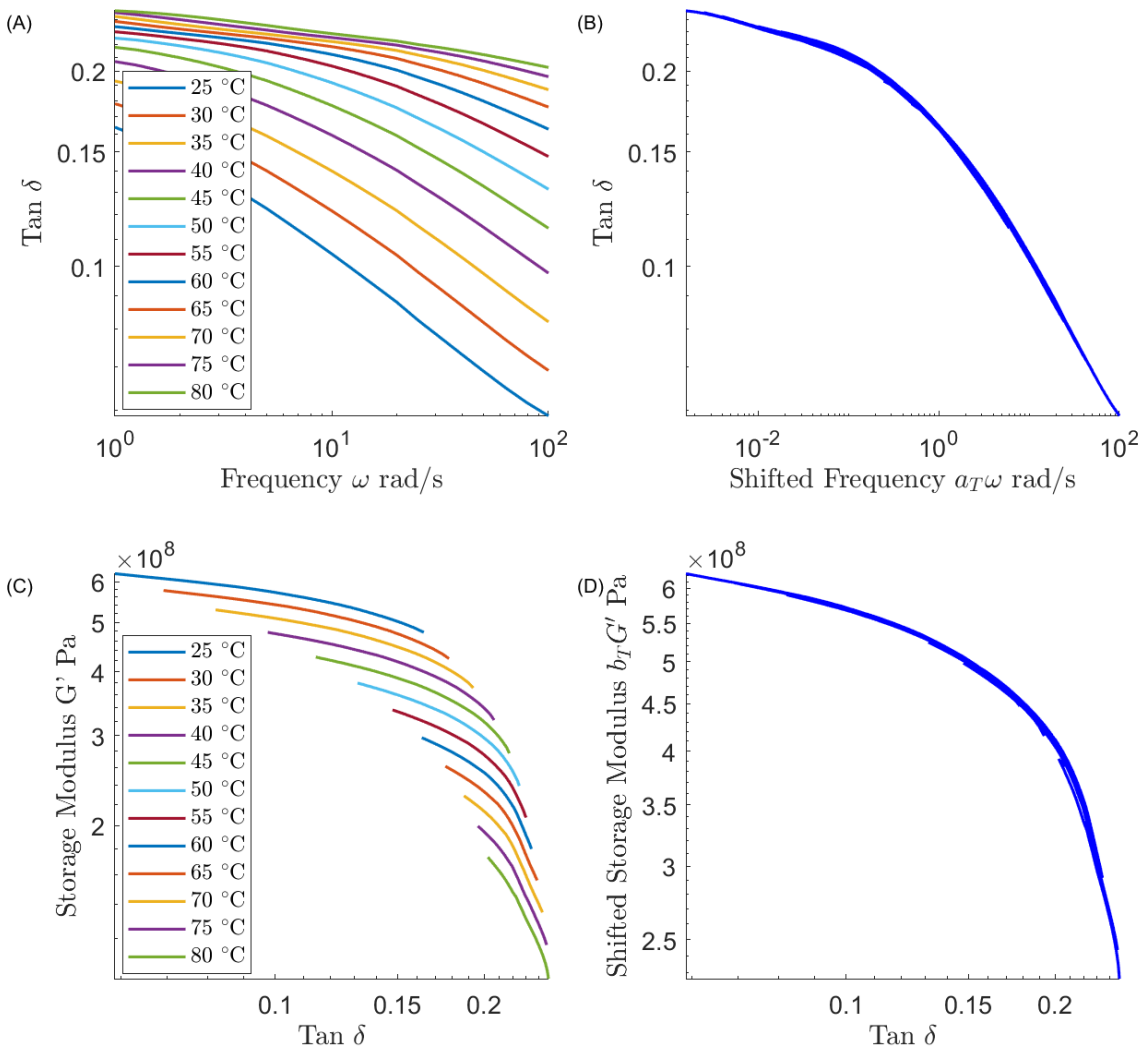

Figure 4.3. DMA Data for Resin B-OD (A) Tan δ vs Frequency before Horizontal Shifting (B) Tan δ vs Frequency Master Curve at 25 °C (C) G' vs Tan δ Before Vertical Shifting (D) G' vs Tan δ Master Curve at 25 °C

All the plots in Figure 4.3 are for pipes from Resin B extruded from the die OD. For all the other resin, die, and fixture combinations, the same procedure allowed producing their master curve plots. All the results were for smooth continuous master curves, similar to the ones shown here and are in the appendix.

4.5.2 Modulus Master Curves

Figure 4.4 shows G' master-curves as a function of frequency for both resins and dies using a torsional fixture. The horizontal and vertical shift factors from section 4.5.1 allow showing master curves of reduced G' as a function of reduced frequency, as is customary for TTS master curves [15]. Figure 4.4 (A) compares the pipes made from the two different resins but extruded from the same die. The master curves comparing the two resins lie within the error bars of each other, and so they do not produce pipes with different master curves. Figure 4.4 (B) compares the pipes made from Resin B but extruded from two different dies. The two dies do not change the properties of the pipes, which would have resulted in different master curves.

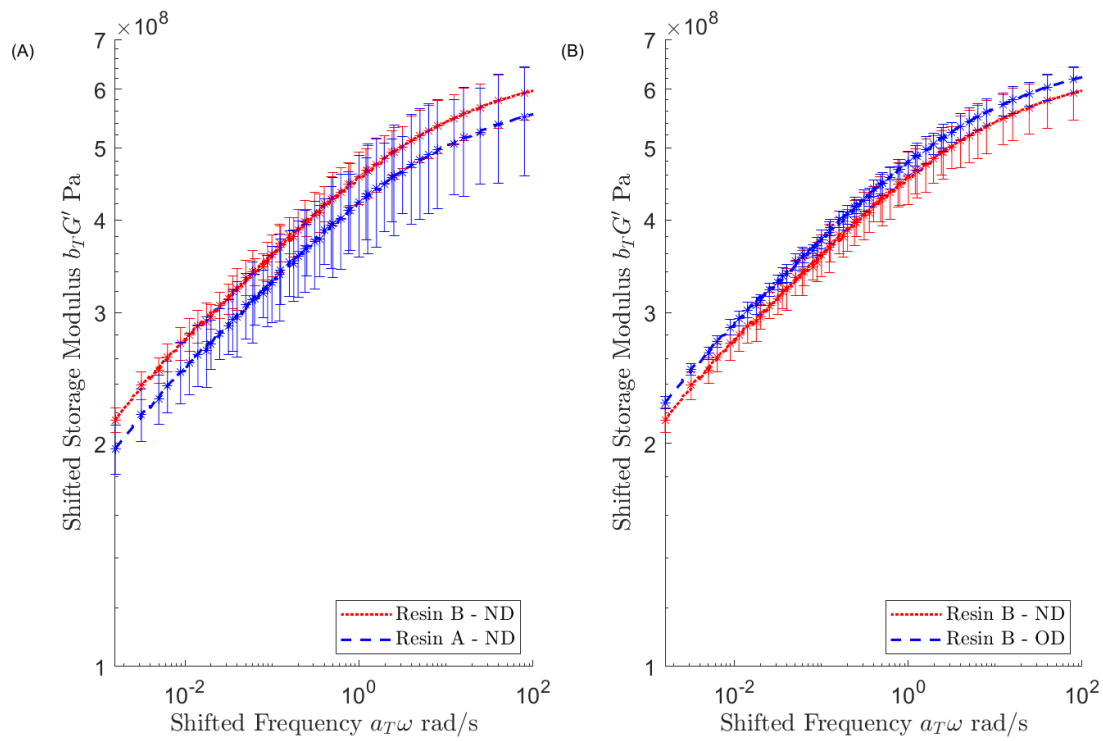

Figure 4.4 G' Master Curves at 25 °C. (A) Comparing the dies ND and OD. (B) Comparing Resin A and Resin B.

4.5.3 Creep

Figure 4.5 (A) shows the results of measuring creep at several temperatures using a torsional fixture. With a constant stress, the samples undergo continued increasing strain. Strain also increases with temperature when stresses are constant. Figure 4.5 (B) shows a creep master curve after shifting the creep data taken at several temperatures. When shifting to a reference temperature of 25C, the strain curves at higher temperatures shift to the right with time and down with strain.

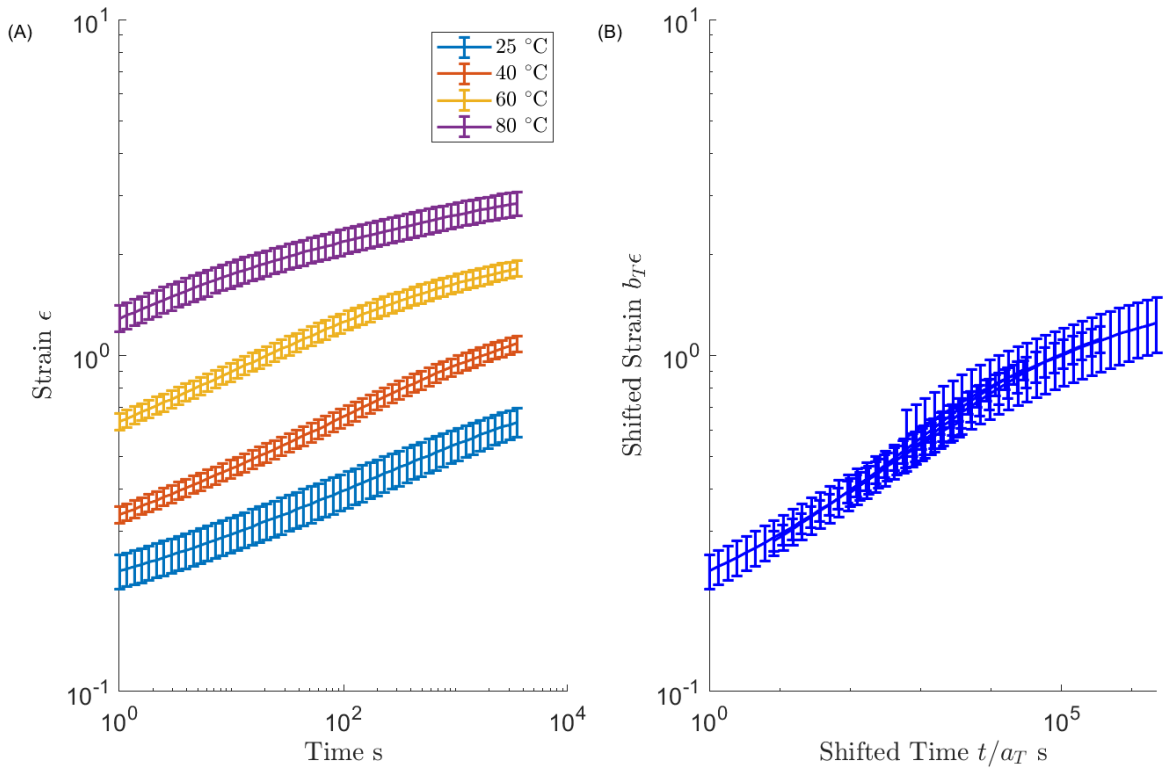

Figure 4.5. Results from creep measurements. Stress was constant at 1.0 MPa (A) Creep at several temperatures for Resin A extruded in the die OD (B) Master Curve at 25C for creep data of Resin A – OD

Creep tests on their own do not determine if vertical shifting is necessary. At first glance, it seems as if horizontal shifting is enough to produce a master curve. However, all viscoelastic properties must use the same set of shift factors for TTS to be valid [4], [16]. The same shift factors used in section 4.5.1 produce a smooth and continuous master curve for the creep data of Resin A

extruded from the OD. Comparing the creep master curves from the different dies and resins, gives similar creep master curves that fall within the error bars of each other. Creep master curve results for the other resins, dies, and fixtures were similar and are in the appendix.

4.5.4 Effect of Loading Geometry

Flat rectangular samples compression molded from resin pellets allowed measuring master curves of the resin with controlled processing. A flat sample would have none of the effects from the slight curvature of a strip cut out directly from the pipe. Figure 4.6 shows a comparison between the master curves of a pipe sample versus a prepared compression molded flat sample. The master curves for both resins are similar. The shifting required for both samples was not different, which suggests that the results are the same for testing strips cut out directly from the pipe versus compression molded flat samples. The cures differ at low frequencies by as much as the Resin A vs Resin B difference.

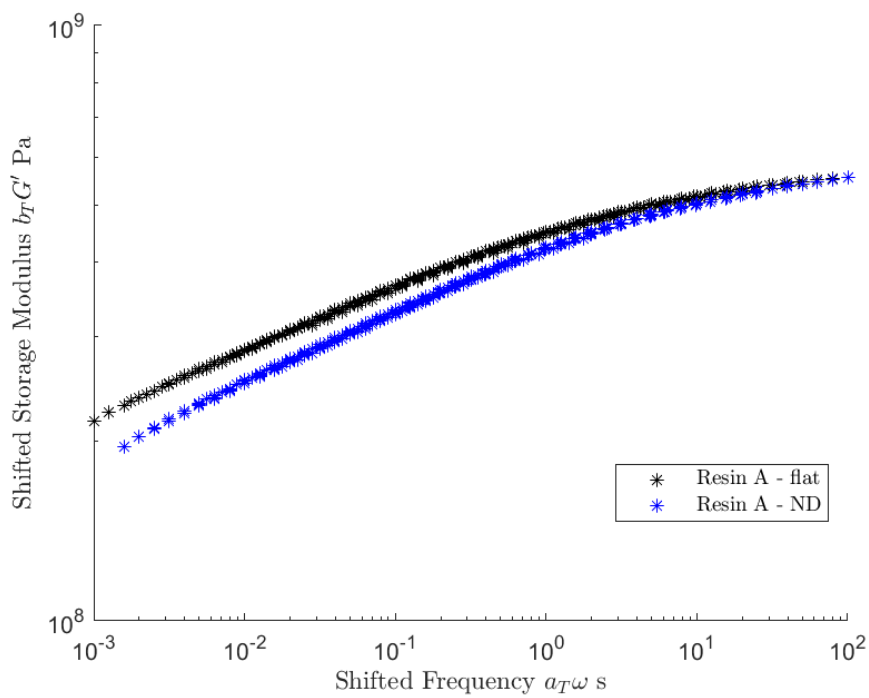

Figure 4.6. G' master curves at 25C of a strip of pipe vs a compression molded flat sample.

Results were different when loading under a three point bending geometry. Figure 4.7 compares the E' master curves of the two resins extruded from the same die. Once again, there was no statistically significant difference between the master curves of both resins. The modulus values are higher than the torsional values presented in section 4.5.2, as E' is always higher than G'. However, notice that the shifted frequency range is not as broad as that of G'. This indicates a different temperature dependence, which will be discussed in section 4.5.5.

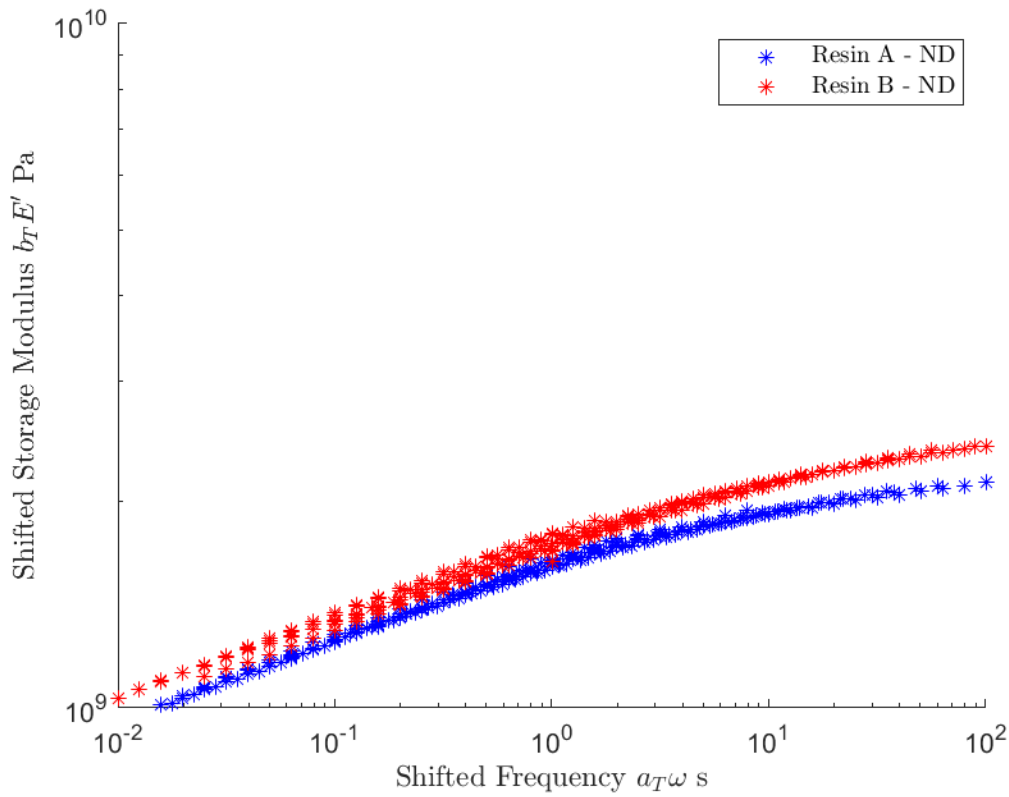

Figure 4.7. E' master curves at 25C for three point bending of Resin A and Resin B made from the die ND.

4.5.5 Shift Factors

The different resins and die combinations for each geometry used the same set of shift factors from sections 4.5.1 and 4.5.4. As the resins have similar polymeric architectures [12], [13] and the dies are not very different, see Rauwendaal for effect of die size on draw down ratio [17], it is not surprising

that the shift factors are not different [4]. Figure 4.8 shows an Arrhenius plot of the a_T and b_T values used to get the different master curves at 25 °C. The linear trend exhibited by the shift functions using natural logarithm versus inverse temperature axis suggests that an Arrhenius model fits the data well. The activation energies divided by the universal gas constant values are in Table 4.1, and the values are in the order of magnitude typical for thermoplastics [18]. The positive activation energy values for a_T in the Arrhenius models means that reference times will be longer when shifting from high temperatures. The negative activation energy values for b_T decrease modulus when shifting from high temperatures.

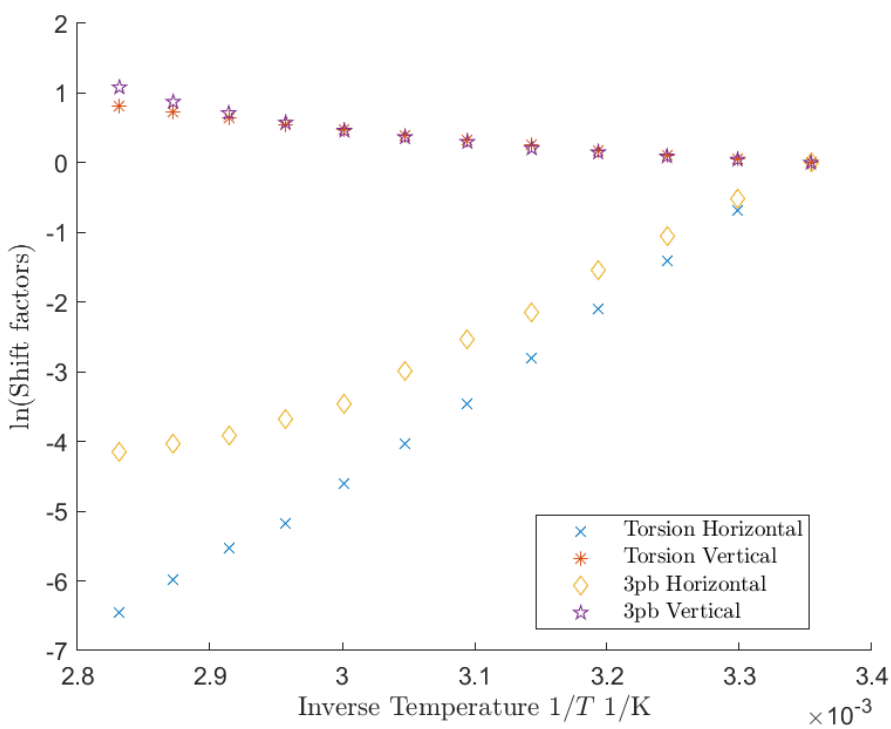

Figure 4.8. Arrhenius Plot for a_T and b_T for the pipes.

Table 4.1. Activation energies for horizontal and vertical shift factors of an Arrhenius model fit.

Activation Energy	Torsion (K)	3PB(K)
ΔE_H	12730	8909
ΔE_V	-1432	-1596

The horizontal activation energies obtained allow relating the results from one temperature to another. In the case of torsion, testing for one hour at 80 °C is equivalent to a month of testing at 25 °C. About two weeks at 80 °C would be equivalent to 50 years at room temperature. The corresponding b_T value corrects shifts the viscoelastic property too with temperature.

Interestingly, the shift factors got when shifting the DMA data from the torsional fixture differ significantly from those of the three point bending fixture. This may be because of the polymer having a different structure in the tangential versus axial direction, changing the mobility of the crystallites as the DMA probing occurs. As pipe extrusion is a slow process and does not impart much orientation to the finished product [14], it was originally hypothesized that the same shift factors would apply regardless of the testing geometry.

4.6 Conclusions

The DMA data allowed establishing the temperature dependence for the viscoelastic properties of the resins. The temperature dependence was the same for the viscoelastic properties measured, as the shift factors from DMA produced smooth master curves from the creep data. The shift factors produced reasonable shift functions that fit to an Arrhenius model well. Times and stresses from a given temperature translated well to other temperatures of interest. DMA, compared to stress relaxation and other transient tests, allowed for fast and simple testing.

However, one could not observe differences between the two resins and dies. The master curves for G', E' and creep for them lie within the error bars of each other. This suggests similar

performance from the resins and dies used in the pipes. Additionally, consider that pipes from both resins have the same classification under ASTM D2837, with those pipes failing from creep.

The degree of shifting was different when loading under different geometries. This is possibly because they probe the structure along different directions, and the polymer morphology may not be uniform in the axial direction compared to the tangential direction. However, using a flat sample compression molded from pellets yielded similar results to strips cut out from the pipe.

4.7 Acknowledgments

The authors gratefully acknowledge the materials and financial support provided by LyondellBasell.

References

[1] ISO 9080:2003, Plastics piping and ducting systems — Determination of the long-term hydrostatic strength of thermoplastics materials in pipe form by extrapolation. ISO, Geneva, Switzerland.
[2] ASTM D2837-13e1, "Standard Test Method for Obtaining Hydrostatic Design Basis for Thermoplastic Pipe Materials or Pressure Design Basis for Thermoplastic Pipe Products," ASTM International, 2013.
[3] K. P. Menard, Dynamic Mechanical Analysis: A Practical Introduction, Second Edition. CRC Press, 2008.
[4] J. D. Ferry, Viscoelastic Properties of Polymers. John Wiley & Sons, 1980.
[5] C. F. Popelar, C. H. Popelar, and V. H. Kenner, "Viscoelastic material characterization and modeling for polyethylene," Polym. Eng. Sci., vol. 30, no. 10, pp. 577–586, May 1990.
[6] C. H. Popelar, V. H. Kenner, and J. P. Wooster, "An accelerated method for establishing the long term performance of polyethylene gas pipe materials," Polym. Eng. Sci., vol. 31, no. 24, pp. 1693–1700, Dec. 1991.
[7] Y. Fukui, T. Sato, M. Ushirokawa, T. Asada, and S. Onogi, "Rheo-optical studies of high polymers. XVII. Time-temperature superposition of time-dependent birefringence for high-density polyethylene," J. Polym. Sci. Part -2 Polym. Phys., vol. 8, no. 7, pp. 1195–1209, 1970.
[8] S. Onogi, T. Sato, T. Asada, and Y. Fukui, "Rheo-optical studies of high polymers. XVIII. Significance of the vertical shift in the time-temperature superposition of rheo-optical and viscoelastic properties," J. Polym. Sci. Part -2 Polym. Phys., vol. 8, no. 7, pp. 1211–1225, 1970.
[9] A. V. Tobolsky and J. R. McLoughlin, "Viscoelastic properties of crystalline polymers: polytrifluorochloroethylene," J. Phys. Chem., vol. 59, no. 9, pp. 989–990, 1955.
[10] H. F. Brinson and L. C. Brinson, Polymer Engineering Science and Viscoelasticity: An Introduction. Springer, 2015.

[11] H. Mavridis and R. N. Shroff, "Temperature dependence of polyolefin melt rheology," Polym. Eng. Sci., vol. 32, no. 23, pp. 1778–1791, Dec. 1992.
[12] S. Joseph, "Multimodal polyethylene pipe resins and process," US9249286 B2, 02-Feb-2016.
[13] H. Mavridis, C. D. Lee, S. W. Horwatt, and S. D. Mehta, "Low-sag polyethylene pipes and methods thereof," US20180030252A1, 01-Feb-2018.
[14] M. Taherzadehboroujeni, R. Kalhor, G. B. Fahs, R. B. Moore, and S. W. Case, "Accelerated testing method to estimate the long-term hydrostatic strength of semi-crystalline plastic pipes," Polym. Eng. Sci., vol. 0, no. 0.
[15] T. A. Osswald and G. Menges, Materials Science of Polymers for Engineers. Carl Hanser Verlag GmbH & Company KG, 2012.
[16] M. Van Gurp and J. Palmen, "Time-temperature superposition for polymeric blends," Rheol Bull, vol. 67, no. 1, pp. 5–8, 1998.
[17] C. Rauwendaal, Polymer Extrusion. Carl Hanser Verlag GmbH & Company KG, 2014.
[18] D. G. Baird and D. I. Collias, Polymer Processing: Principles and Design. Wiley, 2014.

Chapter 5. Conclusions and Recommendations for Future Work

5.1 Conclusions

The work presented in this dissertation investigating the objectives stated in chapter 1 leads to the conclusions that:

1. The higher MW of Resin A compared to Resin B distinctly affects the rheological properties of the resin. Most of the effects are clear in the low shear-rate ranges. The higher MW resin has various distinct rheological properties: higher viscosity and normal stress differences. For both HDPE resins, the relaxation modulus and memory function are separable into individual functions of time and strain. The higher MW resin also deviates more readily from ideal linear viscoelastic behavior. Significant stresses remain in the molten resin even after a few minutes at typical processing temperatures. The residual stresses cannot dissipate during the cooling process and most likely freeze into the finished product.
2. Time-temperature superposition allowed establishing the temperature dependence of the viscoelastic properties of pipes. Shifting yielded that one hour of testing at 80 °C is equivalent to about one month at 25 °C. It was not possible to use temperatures higher than 80 °C as the crystalline structure of HDPE changes above this value [1], [2]. The semi-crystalline nature of HDPE forced a time temperature superposition that required vertical shifting combined with horizontal shifting. Not only time but also the viscoelastic property measured at a different temperature must shift when going to the reference temperature. The shift factors were independent of the viscoelastic property measured as confirmed by creep and the dynamic data. The shift factors produced reasonable shift functions that fit an Arrhenius model well. Times and stresses translated well to the reference temperatures.

DMA, compared to stress relaxation and other transient tests, allowed for fast and simple testing.

3. Creep and dynamic mechanical testing did not reveal differences in the pipes studied. Using Resin A or Resin B, or changing the dies resulted in pipes with similar viscoelastic properties. This occurred even when the rheology of both resins showed differences. Testing the pipes or samples compression molded from pellets gave similar results. Pipes from both resins exhibit creep failure and the two resins have the same classification under ASTM D2837, the industrial standard for assessing the failure of pipes. The "New Die" had gentler processing than the "Old Die", but the draw down ratios for both resins were low. With similar burst behavior, it was reasonable that the pipes would show similar viscoelastic behavior and properties.

5.2 Recommendations for Future Work

It would be interesting to have other HDPE pipe resins to compare their respective rheologies. The ones studied are both BMW and made with Ziegler catalysts and of very high MW. For relevant contrasts, the comparisons would be against unimodal MWD, or resins made with different catalysts, like a Phillips catalyst. One challenge to compare that scenario properly is to have similar variables such as Mn, Mw, or Mw/Mn. If selecting among commercial resins, it is difficult to find resins to compare keeping certain variables. The production conditions of HDPE make it very challenging to carry out at the laboratory scales, so the resins for the study would probably have to be obtained commercially. The relevant MW would be those used in HDPE pipe manufacturing.

Some long-term testing would allow further confirmation of the shift factors. Testing creep around two weeks at 25 °C should be comparable to results obtained using short-term DMA measurements at 80 °C. The creep values tested here are much lower than those that make pipes fail. It

would be interesting to find how time-stress superposition might make the results more general, even though the testing and mathematical framework to do so would be more complicated. Additionally, directly testing pipes for two weeks at 80 °C would be equivalent to 50 years at room temperature, so this is a reasonable test. Because the failure stresses are not known beforehand, a handful of pressures could be tested with pipes to categorize the failure hoop stresses.

References

[1] Y. Fukui, T. Sato, M. Ushirokawa, T. Asada, and S. Onogi, "Rheo-optical studies of high polymers. XVII. Time-temperature superposition of time-dependent birefringence for high-density polyethylene," *J. Polym. Sci. Part -2 Polym. Phys.*, vol. 8, no. 7, pp. 1195–1209, 1970.

[2] S. Onogi, T. Sato, T. Asada, and Y. Fukui, "Rheo-optical studies of high polymers. XVIII. Significance of the vertical shift in the time-temperature superposition of rheo-optical and viscoelastic properties," *J. Polym. Sci. Part -2 Polym. Phys.*, vol. 8, no. 7, pp. 1211–1225, 1970.

Appendix A

A1. Extensional Rheology

The transient extensional viscosity of Resin A was measured at T = 200, 220 and 240 °C between Henky strain rates of 0.01 and 3 s^{-1}. The samples would break above Henky strains of 2.5. Figure A.1 shows pictures of the measurements in the Sentmanat Extensional Rheology (SER) fixture. Figure A.2 shows no special features such as strain hardening are present in the resins. The elongational viscosity increases steadily with time until the sample fails at all the strain rates tested. Figure A.3 shows that elongational viscosity decreases with increasing temperature. Figure A.4 shows that both resins have similar elongational viscosities.

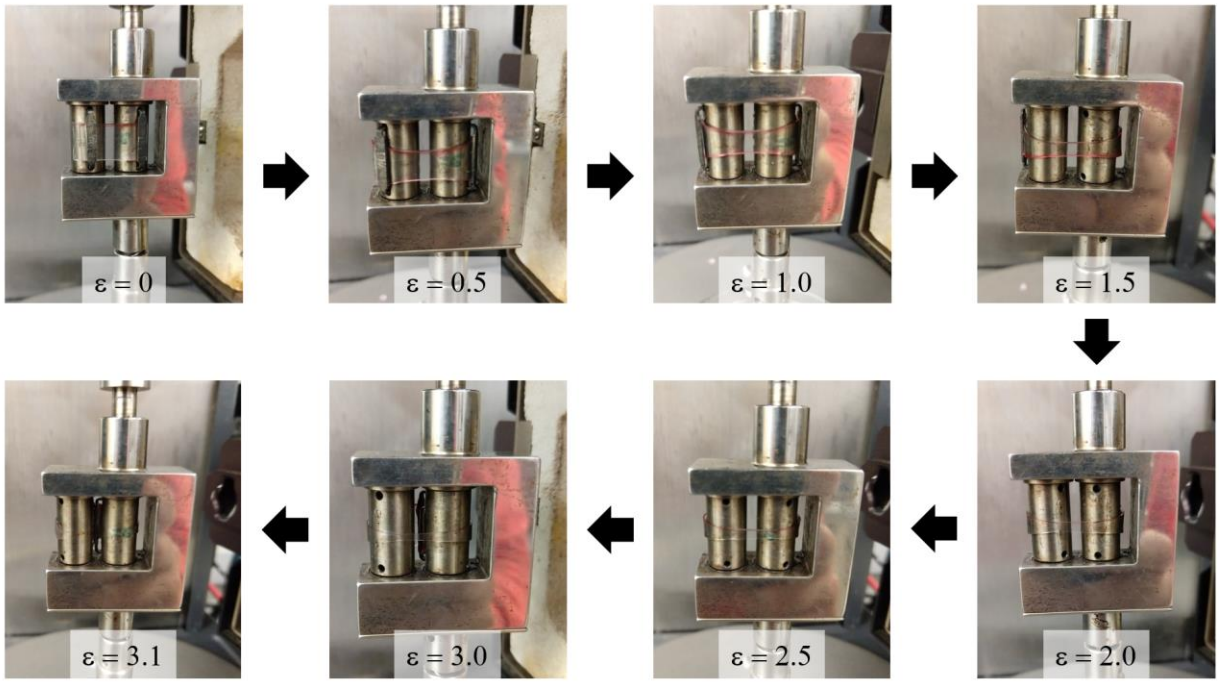

Figure A.1. Photos of SER fixture while running measurements.

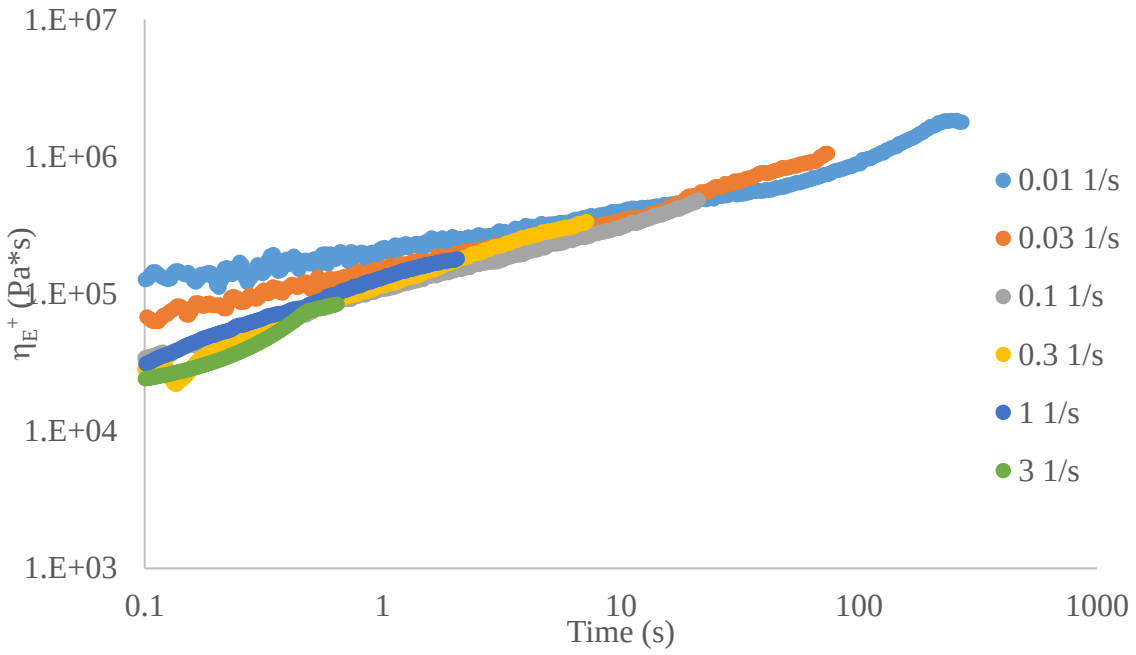

Figure A.2. Extensional viscosity as a function of time for Resin B at 200 °C – Comparing different Henky strain rates

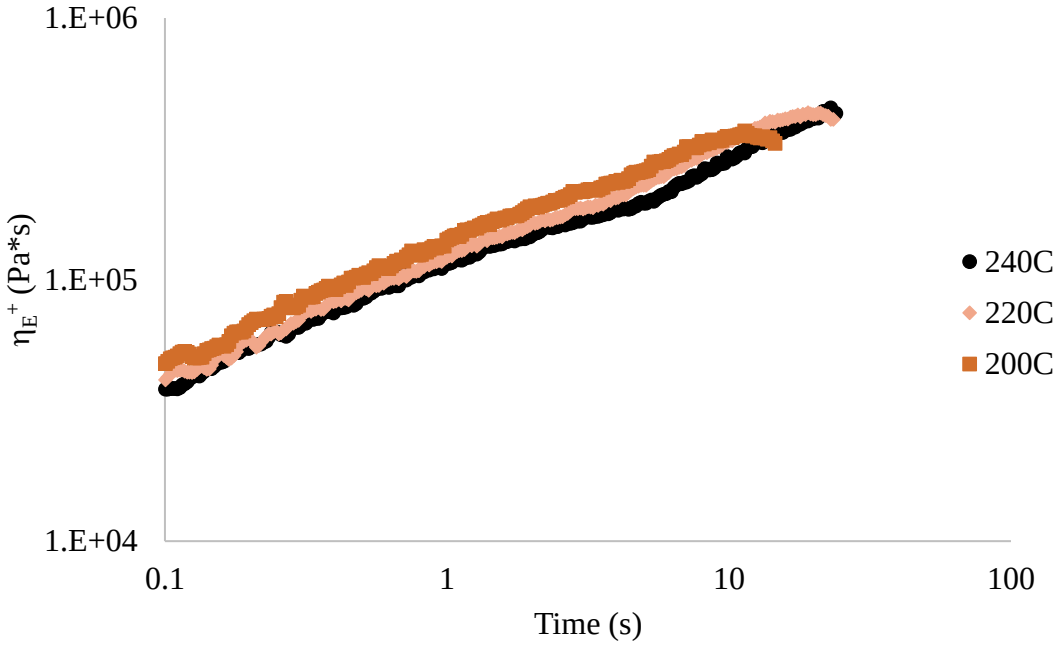

Figure A.3. Extensional viscosity as a function of time for Resin B at a Henky strain rate of 0.1 s^{-1} – Comparing different temperatures

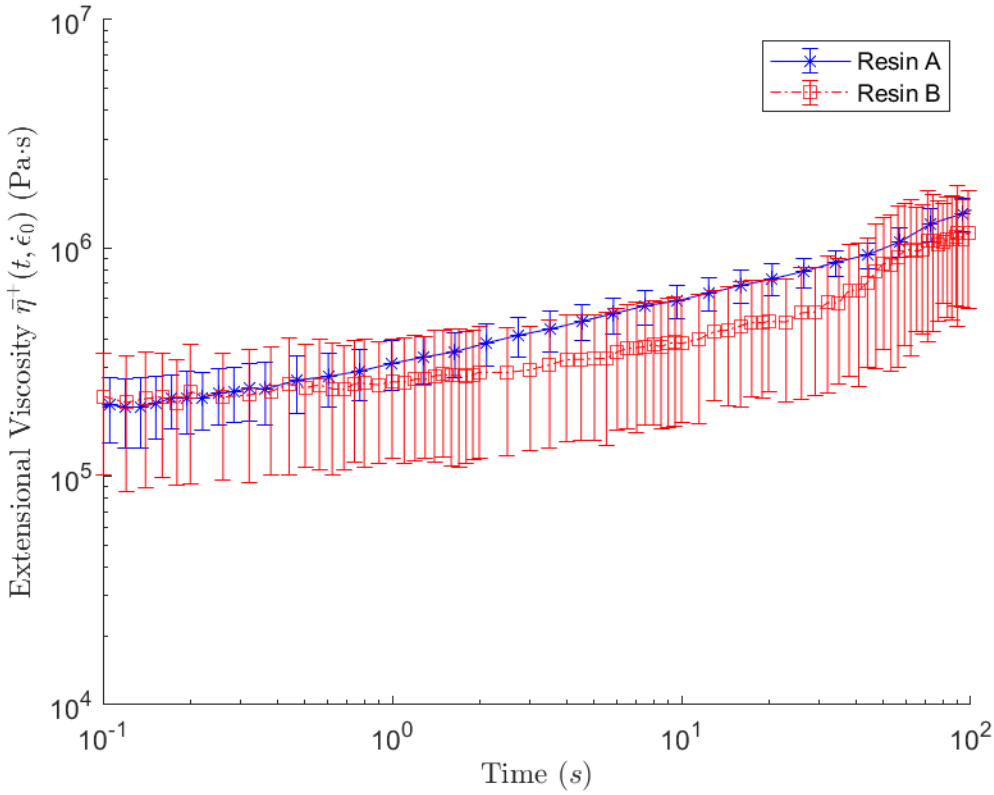

Figure A.4. Comparison of the extensional viscosity of Resin A and Resin B at T = 200 °C and Henky strain rate 0.1 s^{-1}

A2. Additional Shear Rheology Results

Figure A.5 and Figure A.6 show viscosity curves as a function of temperature for Resin A and Resin B respectively. The behavior was as expected. Viscosity decreases when either shear rate or temperature increase.

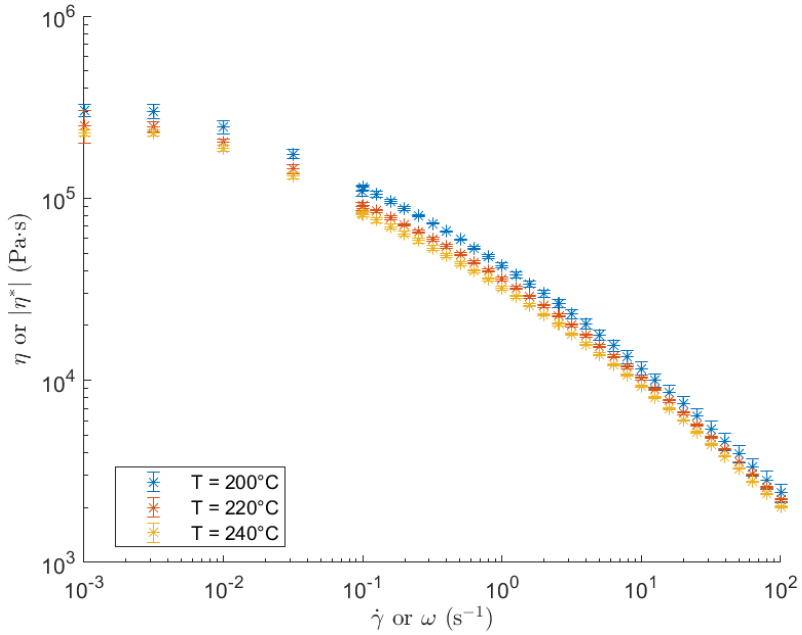

Figure A.5. Viscosity results for Resin A

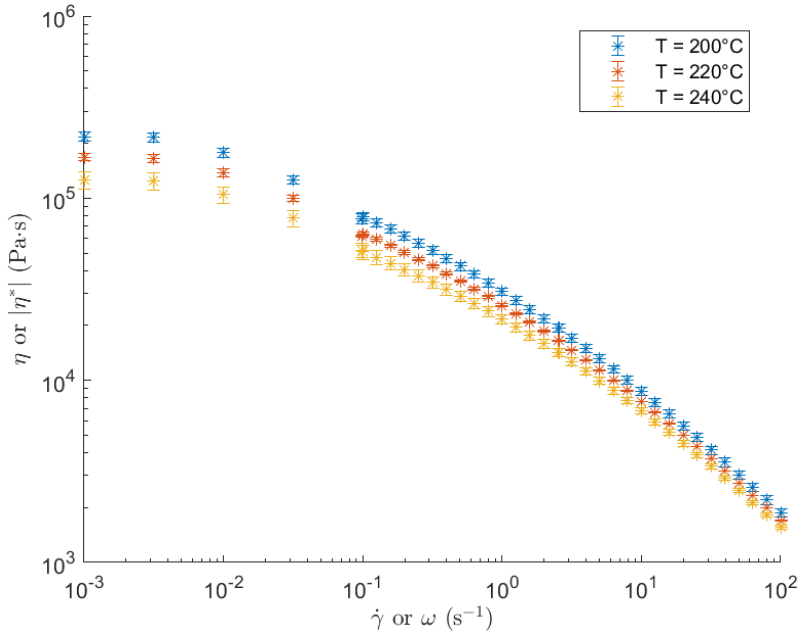

Figure A.6. Viscosity results for Resin B

Figure A.7 and Figure A.8 show sample results of transient simple steady shear at a temperature of 240 °C for Resin A and Resin B respectively. When flow begins shear stresses build and overshoot to then decrease and stabilize around a steady value. The first normal stress difference N_1 steadily builds until it reaches a steady value. However, it does it with more noise and no overshoot.

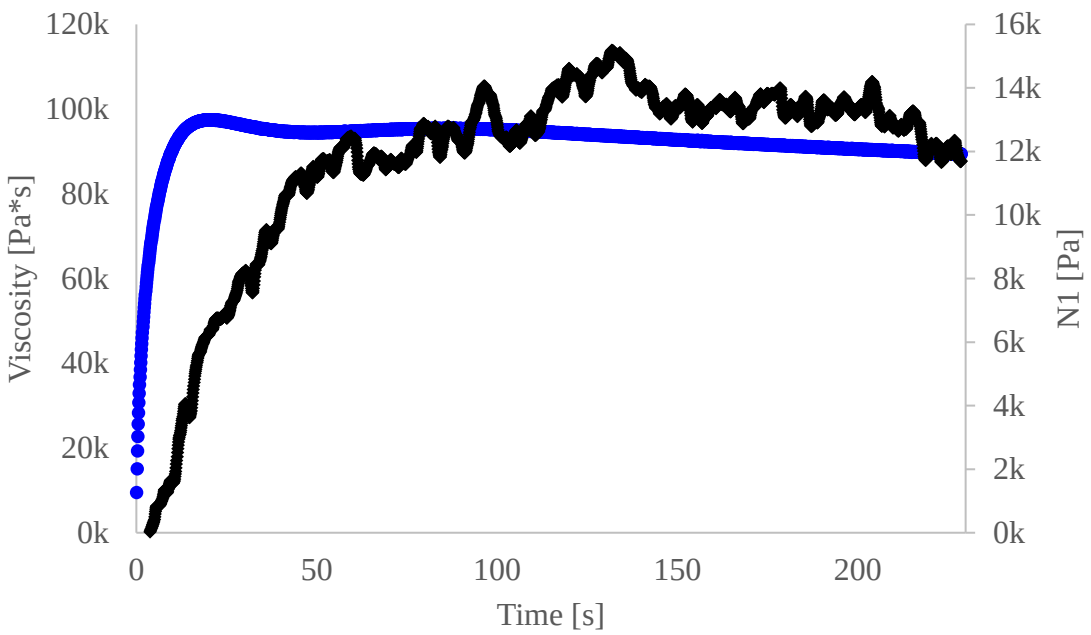

Figure A.7. Resin A - Cone and Plate - T = 240C - γ = 0.1 1/s

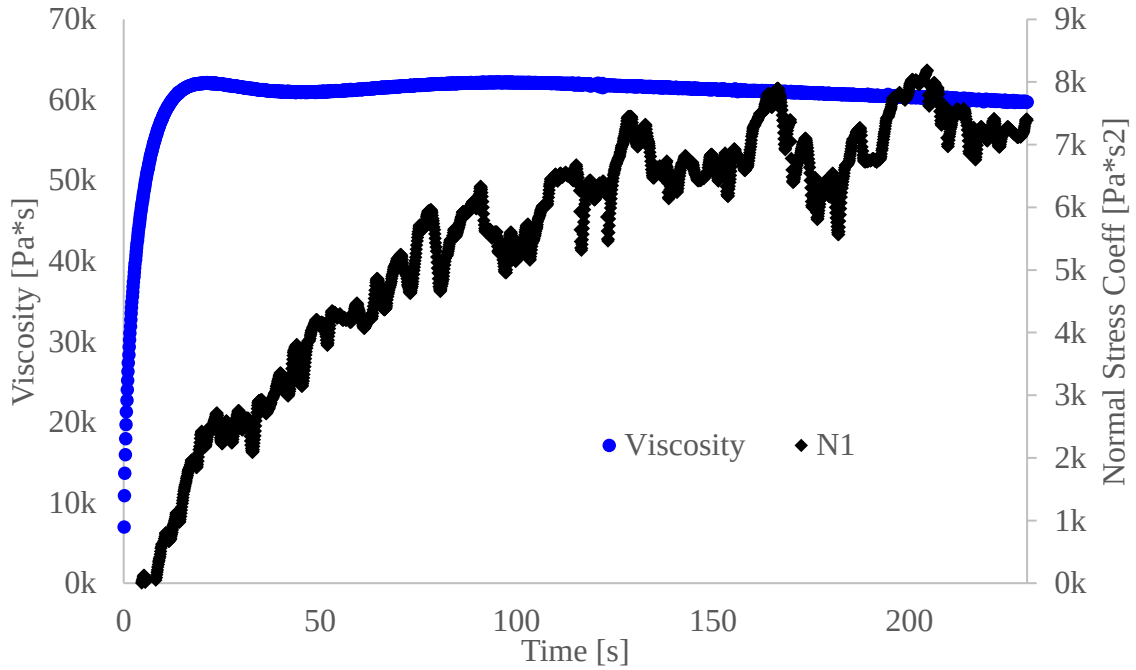

Figure A.8. Resin B - Cone and Plate - T = 240C - γ = 0.1 1/s

Figure A.9 and Figure A.10 show results for startup and cessation of flow at 200 °C and a shear rate of 0.05 s^{-1}. Figure A.11 and Figure A.12 show results for startup and cessation of flow at 200 °C and a shear rate of 0.2 s^{-1}. All the N1 plots show significant noise.

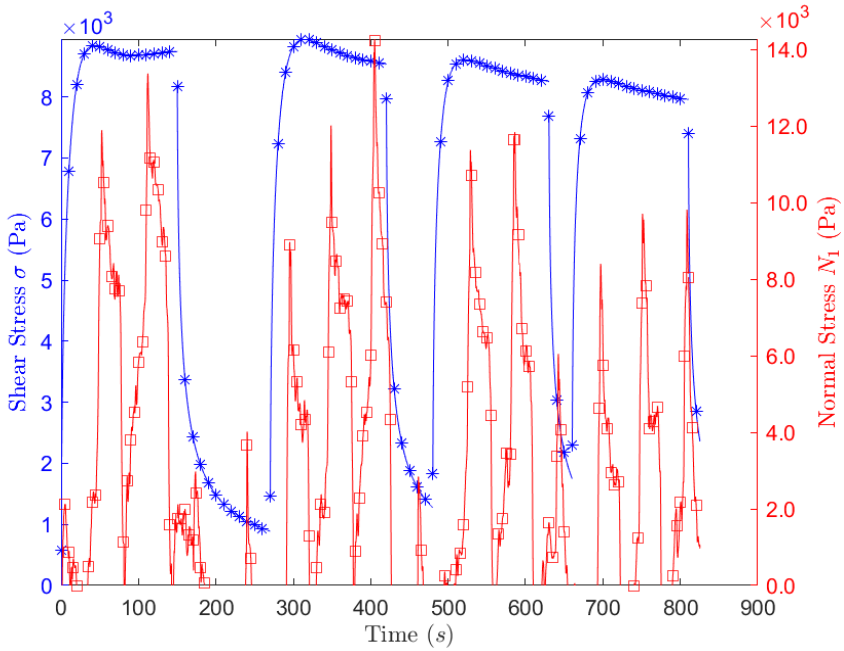

Figure A.9. Start up and cessation of flow for Resin A, T = 200 C, γ = 0.05 s^{-1}

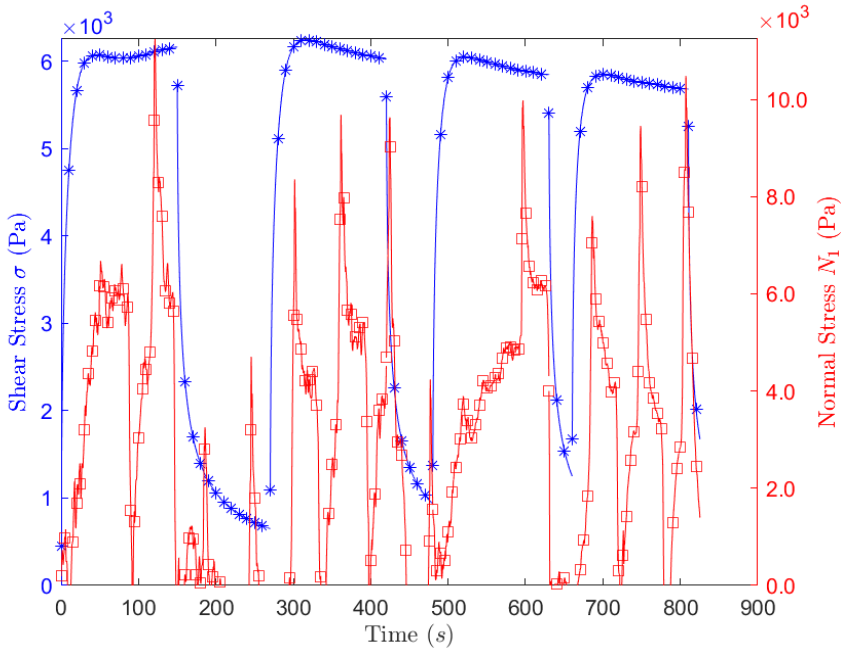

Figure A.10. Start up and cessation of flow for Resin B, T = 200 C, γ = 0.05 s^{-1}

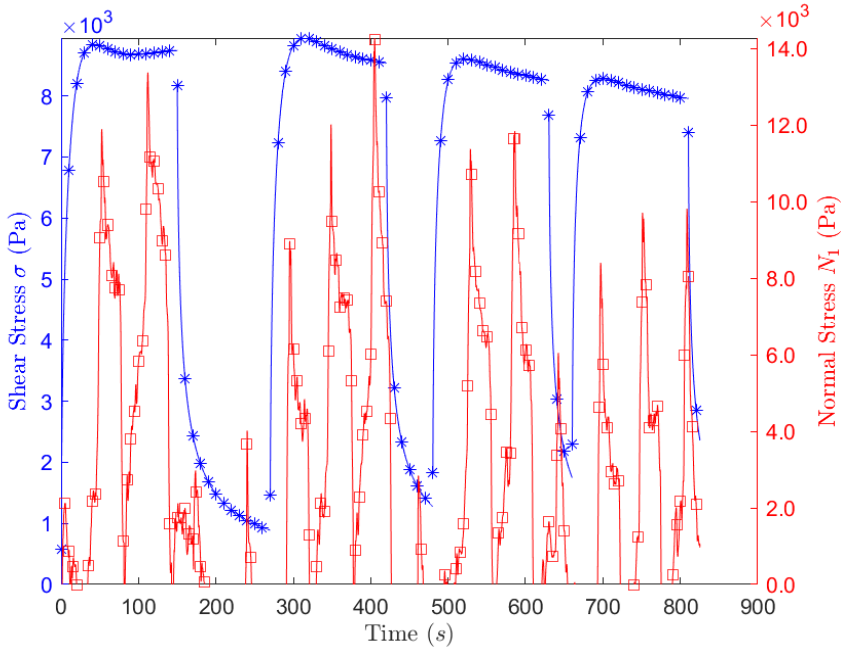

Figure A.11 Start up and cessation of flow for Resin A, T = 200 C, γ = 0.2 s^{-1}

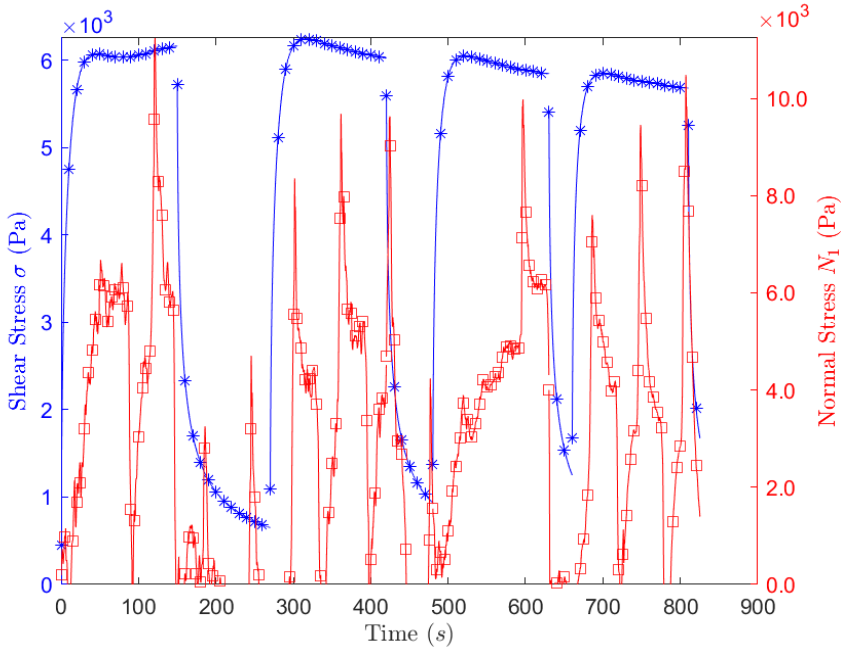

Figure A.12. Start up and cessation of flow for Resin B, T = 200 C, γ = 0.2 s^{-1}

A3. Modeling the flow of the resins in the processing dies

Pressure driven flow through concentric cylinders is a classic problem for Newtonian fluids. However, no analytical solutions are available when using viscosity models such as Bird-Carreau-Yasuda. The assumptions are no-slip boundary conditions, die temperatures of 190-200ºC, and a productivity of 22.7 kg/h. Figure A.13 shows drawings of the dies used in production.

The equation of motion is numerically solved in cylindrical coordinates in the z direction using finite differences. Of interest were the velocity, viscosity, shear rate, shear stress and normal stress distribution over the die gap opening. Two comparisons will be made, first both resins flowing through the same die; second, the same resins flowing through the different dies. Since both dies have different outer and inner radius, radius is made dimensionless as: $\xi = (r - R_i)/(R_o - R_i)$. This allows comparing the die gap on a scale of zero to one.

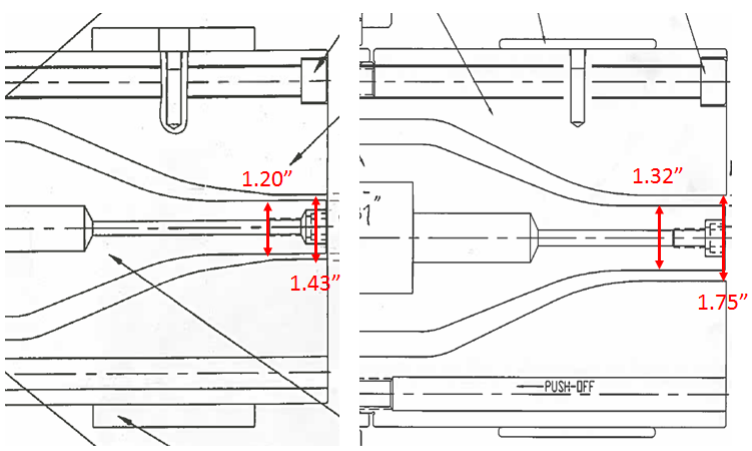

(a) Old Die (b) New Die

Figure A.13. Die drawings for the (a) Old Die and (b) New Die.

A3.1. Flow of Resin A

Figure A.14, Figure A.15 and Figure A.16 shows profiles for Resin A in the old die and the new die. Results for Resin B are similar. Since the new die has a wider gap than the old die, it allows

for slower velocities, lower shear rates and shear stresses. The new die also has a lower pressure drop along the length of die, so it allows for gentler processing during extrusion.

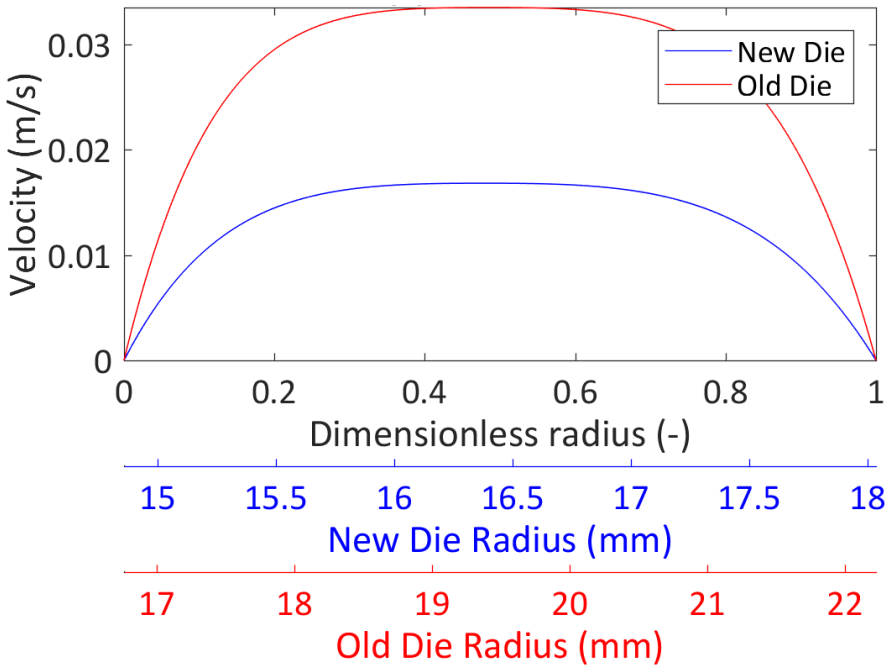

Figure A.14. Velocity profiles for Resin A.

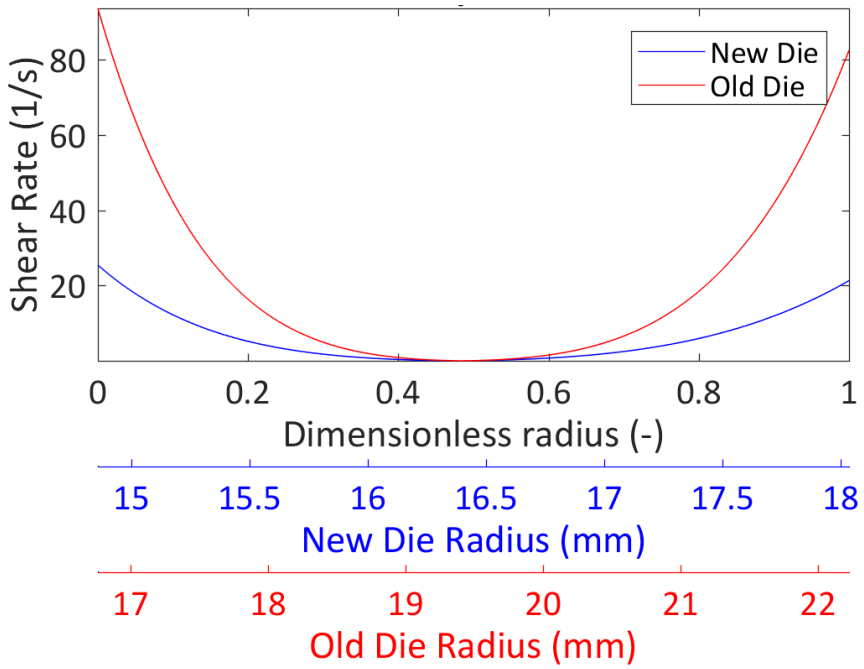

Figure A.15. Shear rate profiles for Resin A

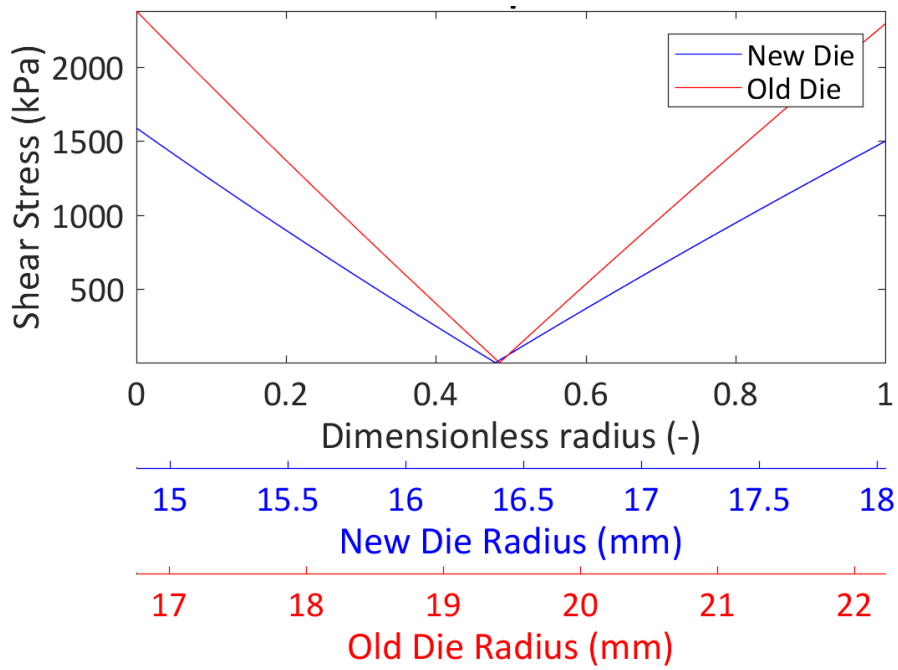

Figure A.16. Shear stress profiles for Resin A

A3.2. Flow in New Die

Figure A.17, Figure A.18 and Figure A.19 show the melt behavior in the new die. Results for the old die are similar. Since the productivity is the same for both resins, the velocity flow profile and the shear rate profile are the same for both resins. The higher viscosity of Resin A compared to Resin B results in higher shear stresses during processing of Resin A and in higher required pressure drop. While a shear rate of around 25-100 1/s at the walls may seem low for an extrusion process, shear stresses around 1500-2200 kPa are high.

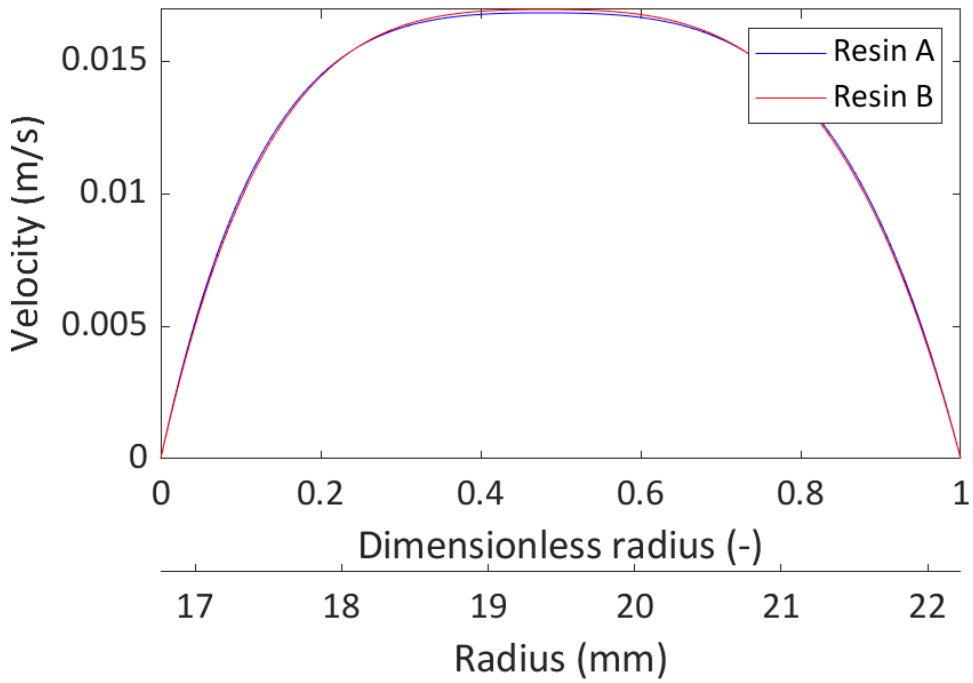

Figure A.17 Velocity profiles for Resin A and Resin B in the new die

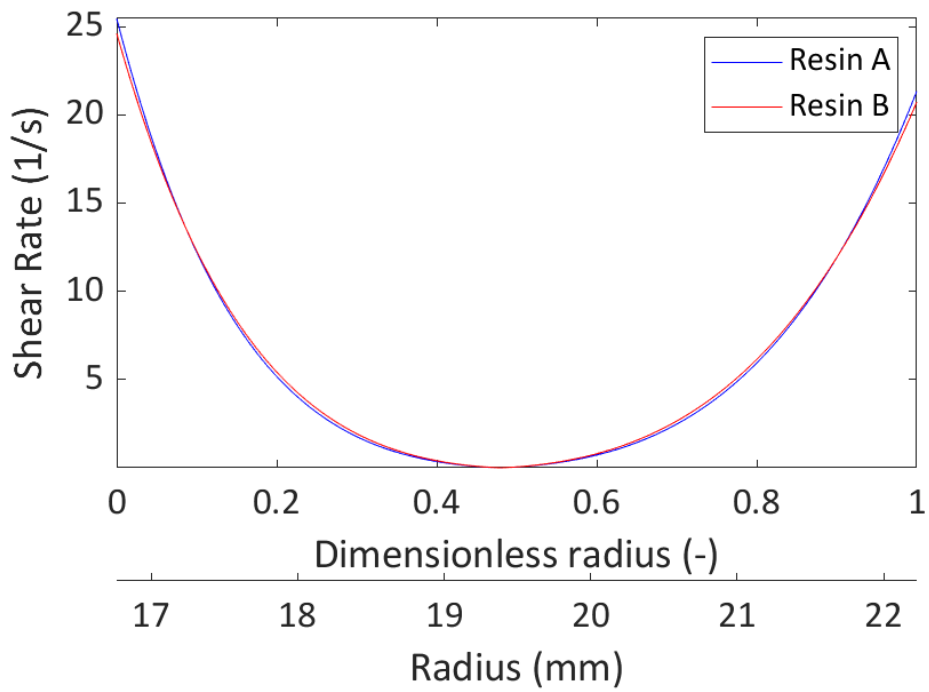

Figure A.18 Shear rate profiles for Resin A and Rein B in the new die

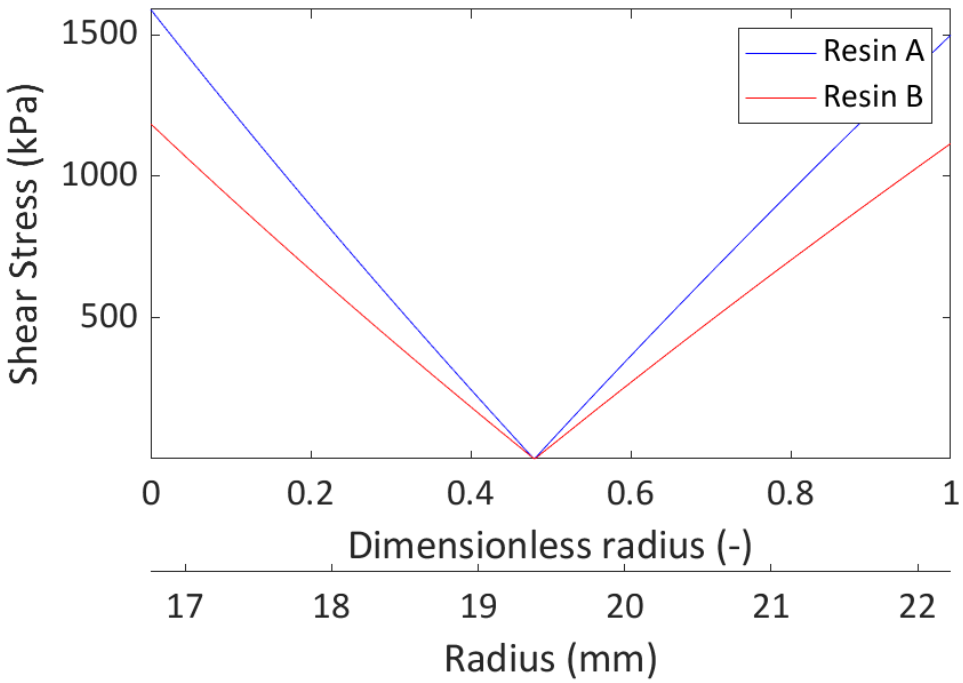

Figure A.19 Shear stress profiles for Resin A and Resin B in the new die

A4. Additional viscoelastic testing results

Figure A.20 shows creep master curves for pipes made of Resin A and Resin B with the "Old Die" the curves overlap, so the creep behavior is the same between these pipes.

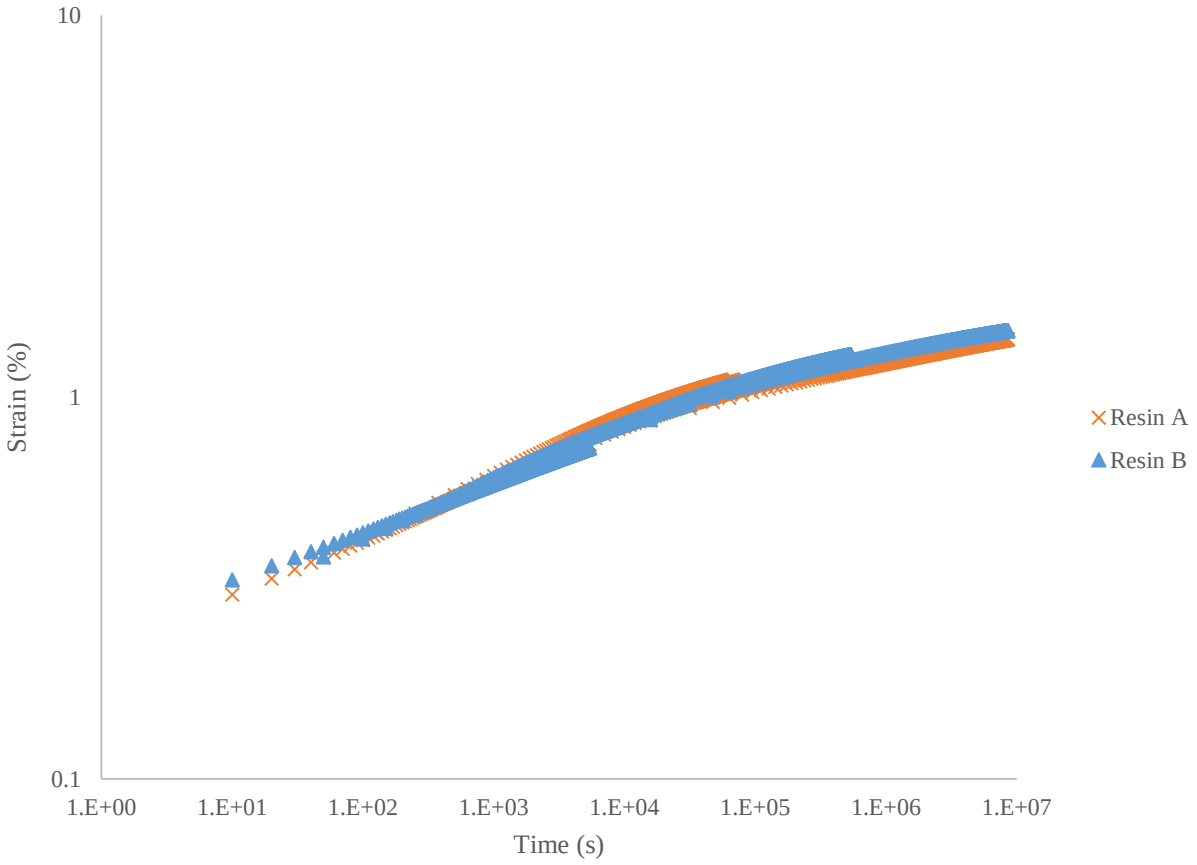

Figure A.20. Creep - OD - Master Curves at T=25ºC.